2004-07-30

Capillary Liquid Chromatography Using Micro Size Particles

Yanqiao Xiang
Brigham Young University - Provo

CAPILLARY LIQUID CHROMATOGRAPHY USING MICRO SIZE PARTICLES

by

Yanqiao Xiang

A dissertation submitted to the faculty of

Brigham Young University

In partial fulfillment of the requirements for the degree of

Doctor of Science

Department of Chemistry and Biochemistry

Brigham Young University

December 2004

BRIGHAM YOUNG UNIVERSITY

GRADUATE COMMITTEE APPROVAL

of a dissertation submitted by

Yanqiao Xiang

This dissertation has been read by each member of the following graduate committee and by a majority vote has been found to be satisfactory.

Date	Milton L. Lee, Committee Chair
Date	Steven W. Graves, Committee Member
Date	Steven R. Goates, Committee Member
Date	Adam T. Woolley, Committee Member
Date	David V. Dearden, Committee Member

BRIGHAM YOUNG UNIVERSITY

As chair of the candidate's graduate committee, I have read the dissertation of Yanqiao Xiang in its final form and have found that (1) its format, citation, and bibliographical style are consistent and acceptable and fulfill university and department style requirements; (2) its illustrative materials including figures, tables, and charts are in place; and (3) the final manuscript is satisfactory to the graduate committee and is ready for submission to the university library.

_____ _____

Date

Milton L. Lee
Chair, Graduate Committee

Accepted for the Department

_____

Paul B. Farnsworth
Department Chair

Accepted for the College

_____

G. Rex Bryce
Associate Dean, College of Physical and Mathematical Sciences

ABSTRACT

CAPILLARY LIQUID CHROMATOGRAPHY USING MICRON SIZE PARTICLES

Yanqiao Xiang

Department of Chemistry and Biochemistry

Doctor of Philosophy

High speed and/or high efficiency separations can be realized using small particles (~ 1 μm) in liquid chromatography (LC). However, due to the large pressure drop caused by small particles, conventional LC pumping systems cannot satisfy the pressure requirements needed to drive the mobile phase through the column. Use of ultrahigh pressure, elevated temperature, or both can overcome these pressure limitations and allow the use of very small particles for high speed and/or high efficiency separations.

In this dissertation, the use of ultrahigh pressures with and without elevated temperatures in capillary LC is described. Very fast separations of various samples on silica-based stationary phases were achieved using optimized equipment and conditions. Great reduction in separation time, while maintaining high efficiency, is the most significant result of this work.

Mechanically, chemically and thermally stable new packing materials were required for this research. Polybutadiene encapsulated nonporous zirconia particles, which are chemically and thermally more stable than silica, were evaluated for fast separations of pharmaceuticals and herbicides at temperatures and pressures as high as 100 °C and 30 kpsi, respectively.

Safety is a concern when extremely high pressures are used in LC. Column rupture and system component failure can lead to the creation of high speed liquid jets and capillary projectiles. The use of a plexiglass shroud to cover the initial section of the installed capillary column can eliminate any safety-related concerns about these liquid jets or capillary projectiles.

An ultrahigh pressure sample injector, with small dwell volume is critical for sample injection and gradient operation at high pressures. A novel injection assembly, composed of six small needle valves, withstood pressures as high as 30 kpsi. A new capillary connector was designed to hold the capillary by “two-point” holding forces under high pressures. With this new injector and capillary connector, gradient elution was easily achieved for the high resolution separation of a protein tryptic digest.

ACKNOWLEDGMENTS

I would like to give my greatest thanks to Dr. Milton L. Lee, my advisor, for his guidance, trust, encouragement, friendship, and unwavering support throughout my graduate studies. I can sincerely say that what I have learned from him is invaluable for my future career and daily life. I am very honored that he gave me this opportunity to work and study in his group.

I would like to extend my gratitude to my committee members, Dr. Steven W. Graves, Dr. Steven R. Goates, Dr. Adam T. Woolley and Dr. David V. Dearden for their professional advice, instruction, support and very resourceful discussions regarding my research. I would like to give sincere thanks to all of the professors who taught me during these five years.

Special thanks goes to my mother, Jinmei Rong and my husband, Zhengrong Zhao. Without their continual loving support and encouragement, this work would not have been possible. I also want to thank my sweet little baby boy, Tony Bohan Zhao, for his sweet smile. I would also like to acknowledge my family in China for their kind love and support.

I am very grateful to Dr. Naijun Wu, Dr. Qinglin Tang, Dr. David Collins, Dr. Edgar Lee, Binfang Yue, Dr. Binwen Yan, Dr. Yinhan Gong and Dr. Zlata Peterson for useful discussions about my research. I would also like to acknowledge all scientists, postdoctoral fellows, graduate students and undergraduate students in Dr. Lee's group for

their friendship and support during these five years here. They include Dr. Qirong Wu, Dr. Paul Humble, Shu-ling Lin, Yansheng Liu, Li Zhou, Jikun Liu, Lailiang Zhai, Jenny Armenta, Binghe Gu, and Nosa Agbonkonkon. I would like to give special thanks to our secretary, Susan Tachka, for her help and support. I owe particular thanks to Greg Henry for his generous help in my research during my pregnancy.

I sincerely appreciate the help from the people in the instrument shop. Keith Kling, Bart Whitehead, and Robert Hallock have always been available for assistance.

Finally, I gratefully acknowledge the department of Chemistry and Biochemistry at Brigham Young University for providing me this opportunity and financial support to pursue my Ph.D degree. Life here will be a great memory for me forever.

TABLE OF CONTENTS

LIST OF FIGURES

LIST OF TABLES

LIST OF ABBREVIATIONS, ACRONYMS, AND SYMBOLS

β-CD	β-cyclodextrin
C	carbon
CE	capillary electrophoresis
CEC	capillary electrochromatography
GC	gas chromatography
HP-β-CD	2-hydroxypropyl-β- cyclodextrin
PBD	polybutadiene
HPLC	high performance liquid chromatography
LC	liquid chromatography
m/z	mass to charge ratio
MS	mass spectrometry
TOFMS	time-of-flight mass spectrometry
UV	ultraviolet
i.d.	internal diameter
o.d.	outer diameter
ODS	*n*-octadecyl silica
PBS	phosphate buffer saline
PEEK	poly(etheretherketone)
NPS	nonporous silica
PS	polystyrene
PTFE	polytetrafluoroethylene
RSD	relative standard deviation

S/N	signal-to-noise ratio
SFC	supercritical fluid chromatgraphy
TAME	Nα-p-tosyl-L-arginine methyl ester
TFA	trifluoroacetic acid
TPCK	L-(tosylamido-2-phenyl) ethyl chloromethyl ketone
TLC	thin layer chromatography
UHPLC	ultrahigh pressure liquid chromatography
v/v	ratio of volume to volume
VHPLC	very high pressure liquid chromatography
w/v	ratio of weight to volume

k_f	isocratic retention factor of the most retained sample component at the final mobile phase composition
N_r	required plate number
k_f	retention factor
ϕ	flow resistance factor
η	viscosity of the mobile phase
λ	structural factor of the packing material
θ	tortuosity factor of the packing material
σ	fractional loss of the column plate number
ε	column porosity

φ	phase ratio of the column
μA	microampere
ΔH	enthalpy of transfer from the stationary phase to the mobile phase
δ_i	solubility parameter (polarity) for the analyte
μL	microliter
δ_m	solubility parameter (polarity) for the initial mobile phase
μm	micrometer
ΔP	pressure drop along the column
δ_s	solubility parameter (polarity) for the stationary phase
ΔS^o	entropy of transfer from the stationary phase to the mobile phase
δ_w,	solubility parameter (polarity) for water
A	dimensionless coefficient for multipath dispersion
B	dimensionless coefficient for longitudinal band dispersion
C	dimensionless coefficient for resistance to mass transfer
C_{18}	n-octadecylsilane group
C_6	isohexylsilane group
C_m	dimensionless coefficient for resistance to mass transfer in the mobile phase
d_c	inner diameter of the column
d_f	thickness of the stationary phase layer
d_p	particle diameter
r	column radius

D_m	diffusion coefficient of solute in the mobile phase
D_s	diffusion coefficient of solute in the stationary phase
R	resolution
α	selectivity
C_s	dimensionless coefficient for resistance to mass transfer in the stationary phase
C_{stag}	dimensionless coefficient for resistance to mass transfer in the stagnant mobile phase
g	gram
H	plate height
h	reduced plate height
h_{min}	minimum reduced plate height
k	solute retention factor
K	injection profile constant
k_0	isocratic retention factor of the most retained sample component at the initial mobile phase compositions
kpsi	kilopounds per square inch
m	meter
mg	miligram
mL	mililiter
mM	milimolar
mV	milivolt
N	plate number

nL	nanoliter
pL	picoliter
R	gas constant
T	absolute temperature
t_0	dead time
t_G	gradient time
t_R	solute retention time
u	linear velocity of the mobile phase
u_{opt}	optimum linear velocity of the mobile phase
v	reduced linear velocity of the mobile phase
V_i	molar volume of the analyte
V_{max}	maximum injection volume

CHAPTER I

INTRODUCTION

I.1 Theoretical Predictions Underlying Fast Separations Using Capillary Liquid Chromatography

High performance liquid chromatography (HPLC) has been widely used in routine analytical work, method development, process monitoring, and quality control. However, separation is often the slow step in any analytical method in which it is involved. This feature has limited the use of this technique for "in-process analysis," which is important in process monitoring, environmental analysis, biological screening, and drug discovery. The need for high speed chromatographic techniques and methods is obvious. Because of its high resolving power, HPLC is superior over other conventional on-line monitoring methods, such as spectroscopic or electrochemical measurements. When "high speed" separations are considered, "high efficiency" is also important to achieve sufficient resolution of analytes of interest.[1]

I.1.1 Separation Time

The chromatographic separation time can be defined as the retention time, t_R, of the most retained component in the sample. Under isocratic conditions in LC, the separation time can be expressed as[2]

$$t_R = \frac{L}{u}(1+k) \qquad \text{I. 1}$$

where k is the retention factor of the last eluting peak, L is the column length and u is the mobile phase linear velocity. The column efficiency expressed as plate number (N_{req})

depends on the column length, the reduced plate height (h), and the particle diameter of the packing (d_p) as

$$N_{req} = \frac{L}{d_p h} \qquad \text{I. 2}$$

The reduced linear velocity v can be expressed as

$$v = \frac{u d_p}{D_m} \qquad \text{I. 3}$$

where D_m is the solute diffusion coefficient in mobile phase. Combining equations I.1, I.2 and I.3 yields[3]

$$t_R = \frac{(1+k) N_{req} h}{D_m v} \cdot d_p^2 \qquad \text{I. 4}$$

From the above equation, it can be seen that separation time can be shortened obviously by reducing retention (k). However, this will compromise the resolution of the analytes. Increasing the flow rate, while decreasing the analysis time, can increase the plate height (discussed in the next section), yield lower resolution, and lead to prohibitive back pressure effects. The separation time can also be decreased by using short columns which decrease retention and cause a loss in efficiency. Also, it can be seen that the separation time is proportional to the square of the particle diameter. Therefore, reducing the diameter (d_p) of the chromatographic packing material is another way to decrease separation time, which actually is the most effective way to achieve high speed and retain high efficiency separations (this will be discussed in the next section). In addition, use of elevated temperature to decrease the mobile phase viscosity and increase analyte diffusion will assist in achieving high speed and high efficiency separations.

From the previous discussion, several parameters can be manipulated to shorten the separation time. However, achieving sufficient resolution of analytes of interest within the shortest possible time is dependent on the separation dispersion process (rate theory) and some practical factors such as the maximum pressure the LC instrument can supply. The rate theory and pressure limitation will be discussed in the followed sections.

I.1.2 Separation Efficiency

According to the rate theory, during a chromatographic run, three independent types of dispersion contribute to the total peak variance: eddy diffusion, longitudinal diffusion, and resistance to mass transfer. The van Deemter equation describes the relationship between peak variance (expressed as plate height) and these band broadening processes in chromatography as[4,5]

$$H = A + \frac{B}{u} + Cu \qquad \text{I. 5}$$

where u is the average linear velocity of the mobile phase. A, B, and C are constants accounting for the three causes of variance as described above. At the optimum linear velocity (u_{opt}), the minimum plate height (best column efficiency) can be reached. From the van Deemter equation, the minimum plate height ($H_{\min}$) can be obtained as

$$H_{\min} = A + 2\sqrt{BC} \qquad \text{I. 6}$$

Generally, for fast separations, the column is operated at a linear velocity much higher than optimum.

Eddy diffusion, the A term in the van Deemter equation, describes the non-uniformity of solute flow paths in the column. Individual molecules in a solute band will

travel along different flow paths. Due to a heterogeneous packing structure, some of these flow paths are less tortuous than others, and it takes less time for solute molecules to travel along these shorter flow paths than others experiencing longer flow paths. Therefore, these non-uniform solute flow paths cause band broadening. Eddy diffusion is defined as

$$A = 2\lambda d_p \qquad \text{I. 7}$$

where λ is a structural factor that is inherent to the packing, and d_p is the particle diameter. It can be seen that eddy diffusion is proportional to the particle diameter and, therefore, decreasing the particle size should decrease the contribution of eddy diffusion to band broadening.[6]

Longitudinal diffusion, the B term in the van Deemter equation, depicts band broadening caused by axial solute diffusion in the mobile phase. At high flow rate, the solute spends less time in the mobile phase, leading to less diffusion and, thus, less band broadening. In addition, if the solute has a small diffusion coefficient, the contribution of longitudinal diffusion to band broadening can be negligible. The B term is expressed as

$$\frac{B}{u} = \frac{2\gamma D_M}{u} \qquad \text{I. 8}$$

where γ is the tortuosity or obstruction factor and D_m is the diffusion coefficient of an analyte in the mobile phase.

The resistance to mass transfer, or C term in the van Deemter equation, represents band broadening caused by radial diffusion in and out of the mobile phase and stationary phase. The C term can be divided into three different components which account for contributions to band broadening from the resistance to mass transfer of the

solute in the stationary phase (C_s), the bulk mobile phase (C_m) and the stagnant mobile phase in the particles (C_{sm}):

$$C = C_s + C_m + C_{sm} \qquad \text{I. 9}$$

The resistance to mass transfer of the solute in the stationary phase (C_s) represents the relative time solute resides in the stationary phase. Solutes diffusing deeper into the stationary phase or diffusing slower in the stationary phase will reside longer before they re-enter the mobile phase. C_s is expressed as

$$C_s = \frac{2kd_f^2 u}{3D_s(1+k)^2} \qquad \text{I. 10}$$

where d_f is the stationary phase film thickness, k is the solute retention factor, and D_s is the analyte diffusion coefficient in the stationary phase. When bonded stationary phases or very thin stationary phase films (small d_f) are used in LC, the C_s term becomes a small part of the overall C term.[7]

Resistance to mass transfer of the solute in the bulk mobile phase (C_m) is partially related to the parabolic flow profile of pressure-driven flow.[8] Solutes in midstream travel faster than those near the column surface. These differences lead to broadening of the solute band in the bulk mobile phase. C_m is defined as

$$C_m = \frac{\chi(1+6k+11k^2)d_p^2 u}{24(1+k)^2 D_m} \qquad \text{I. 11}$$

where χ is a geometric factor and D_m is the analyte diffusion coefficient in the mobile phase.

The resistance to mass transfer of the solute in the stagnant mobile phase (C_{sm}) arises from the existence of stagnant mobile phase in the intraparticle void volume of the packing particles. Solutes that diffuse slower or deeper into the pores of the particles will lag behind those that enter and exit the pores more rapidly. C_{sm} can be expressed as

$$C_{sm} = \frac{(1 - \phi' + k)^2 d_p^2 u}{30(1 - \phi')(1 + k)^2 \gamma D_m} \qquad \text{I. 12}$$

where ϕ' is the fraction of the total mobile phase in the pores and γ is the tortuosity or obstruction factor. It is obvious that C_{sm} becomes negligible when nonporous particles are used.

From the above equations, it can be seen that all three C terms are proportional to the linear velocity. Therefore, band broadening due to the C term becomes worse as the linear velocity increases. The C_m and C_{sm} terms are proportional to the square of the particle diameter. Furthermore, the A term is also directly proportional to the particle diameter. Therefore, decreasing the particle size will greatly reduce the band broadening caused by mass transfer resistance in the mobile phase and, to a lesser extent, eddy diffusion. In addition, all three C terms are inversely proportional to the diffusion coefficients (D_m and D_s), which increase with an increase in temperature. Therefore, band broadening due to the C term decreases at elevated temperature. It can be seen, from rate theory, that use of small particles and elevated temperature in liquid chromatography are the most effective ways to achieve high speed and high efficiency separations.

I.1.3 Pressure Drop

The pressure drop along the column is a limiting factor only when small particles are used for high speed and high efficiency separations. According to Darcy's law, the pressure drop along the column is

$$\Delta P = \frac{\phi \eta L u}{d_p^2} \qquad \text{I. 13}$$

where ΔP is the pressure drop, ϕ is the flow resistance factor, L is the column length, η is the mobile phase viscosity, u is the linear velocity, and d_p is the particle diameter. It can be seen that the pressure applied to the column is inversely proportional to the square of the particle diameter. Furthermore, from reduced parameter analysis, the optimum linear velocity is inversely proportional to the particle diameter as shown by

$$u_{opt} \approx \frac{3D_m}{d_p} \qquad \text{I. 14}$$

where u_{opt} is the optimum linear velocity and D_m is the diffusion coefficient of the solute in the mobile phase. Combining equations I.13 and I.14 yields

$$\Delta P \propto \frac{1}{d_p^3} \qquad \text{I. 15}$$

It can be seen that at the optimum linear velocity, the pressure drop along a packed column is inversely proportional to the cube of the particle diameter. Therefore, when small particles are used, much higher pressure is required to overcome the pressure drop, compared to larger particles. The pressures that can be used are limited by the commercial pumps that are available. For higher pressures, alternative pumps must be considered. This will be discussed in section I.2.2. In addition, the pressure drop along the column is proportional to the mobile phase viscosity, which decreases with an

increase in temperature. Therefore, use of elevated temperature can lessen the back pressure, allowing the use of smaller particles or higher flow rates.

I.2 High Speed and High Efficiency Separations Using Liquid Chromatography

I.2.1 Column Design

Particle size and column dimensions. As discussed previously, theory predicts that HPLC separations can be made more efficient by using columns packed with small diameter particles because of the reduced intraparticulate mass transfer resistance due to the short diffusion distances and, to a lesser extent, the small contribution of "eddy diffusion" to the plate height.[9]

In addition to the particle size, the particle configuration also plays an important role in determining the separation speed and efficiency. In practice, several particle configurations, favoring fast mass transfer, have been proposed for high speed and high efficiency separations:[10,11] (1) eliminating the support pores by using nonporous particles; (2) introducing particle transacting pores of 6000 – 8000 Å by using perfusion particles; (3) forming a continuous monolithic polymeric network of support instead of a bed of discrete particles.

Besides particle size and configuration, the column diameter influences the separation efficiency. Due to the wall-effect, the use of smaller column diameter lowers the resistance to mass transfer (C term), producing higher column efficiency.[12,13] In addition, eddy diffusion (A term) decreases as a result of smaller flow rate distribution over the column cross section as column diameter decreases.[14] Therefore, use of a smaller diameter column favors higher separation efficiency.[15]

Nonporous particles. For nonporous particles, the stationary phase is coated on the outside of a solid microsphere. A thin porous layer allows fast rates of mass transfer. Due to the lack of stagnant mobile phase, the C term is significantly reduced compared to porous particles and the nonporous particles should provide better efficiency, especially when the column is operated at a linear velocity higher than the optimum.[16,17]

In the early 1980s, Unger's group introduced very small nonporous silica particles for protein separations.[18,19] A high flow rate and steep gradient have been used for separation of five proteins in 8 s on 2 μm nonporous silica particles.[20] Furthermore, 1.5 μm nonporous particles have been employed for rapid separation of small molecules.[21,22]

The only limitation of nonporous particles is their limited loading capacity, which is approximately two orders of magnitude lower than porous packings.[2] This problem can be reduced by using very small particles, roughening the particle surface, and creation of a fimbriated layer of stationary phase.

Superficially porous particles[23,24] have an ultra-pure solid silica core with a thin porous shell. This type of particle was actually first used for high speed separations in HPLC in the 1970s.[25] However, very large particles were used at that time. Recently, Kirkland *et al.* have developed a new process to prepare ~3-6 μm particles with a porous shell of 0.1-1 μm. These particles have been used for high speed separations of polypeptides and proteins.[26,27]

Perfusion particles. Perfusion packings were developed by Afeyan and co-workers in the 1980s.[28,29] The use of perfusion particles represents another approach to improve separation speed and performance. As with nonporous particles, the advantage of perfusion chromatography is a reduction of stagnant mobile phase effects; however,

the result is achieved in a much different way. Perfusion packings have through pores, which allow flow through the particle, thus reducing the amount of stagnant mobile phase and the diffusion distance. Therefore, the solute will spend less time in mass transfer, producing narrower peaks. It was reported that use of perfusion packings accelerated intraparticle mass transfer of macromolecules by one to two orders of magnitude.[11] A high speed reversed-phase separation of proteins with a 24-s gradient has been achieved using a perfusion packing. Four out of five proteins in a mixture were resolved in 12 s.[30]

Monolithic columns. Monolithic columns have been used for high speed and high efficiency separations. Since such stationary phases contain no particles but only flow-through pores, the usual mass transfer restrictions for large molecules in particle packed columns are not observed with monolithic columns.[31,32] Therefore, van Deemter curves for some monolithic columns were much flatter at high flow rates, compared to conventional columns.[33] Furthermore, plate heights for some monolithic columns were independent of flow rate for proteins.[31] These features allow the operation of monolithic columns at very high flow rates for fast separations with no significant loss in efficiency. It was demonstrated that 4 protein standards could be resolved in 30 s using a reversed-phase monolithic poly(stryrene-*co*-divinylbenzene) column at a mobile phase flow rate of 25 mL min^{-1}.[34] Using a similar monolithic column in the reversed-phase mode, 3 polystyrene standards were separated in 4 s.[34]

I.2.2 Instrumentation Design for High Speed and High Efficiency Separations

High speed liquid chromatography requires not only a stationary phase that provides low mass transfer and low kinetic resistance, but also specially designed instrumentation capable of providing high flow rate, fast eluent gradients, and

temperature control over a wide super-ambient temperature range. When capillary liquid chromatography is used for high speed and high efficiency separations, the demand for very small extra-column dispersion is extremely stringent and, consequently, the extracolumn volume must be extremely small.

Capillary liquid chromatography. The use of miniaturized column liquid chromatography techniques in analytical chemistry improves separation efficiency, speeds up the separation, reduces solvent consumption, and enhances detection performance with the use of concentration sensitive detection devices.[35,36] However, as the column diameter is reduced, all system components that could cause extracolumn band broadening, such as connecting tubing, detector, and injector, must be reduced accordingly. Otherwise, they will cause significant loss in column efficiency, resulting in decreased separation resolution.

If the column internal diameter decreases from d_1 to d_2, according to Chervet *et al.*,[37] all system components, including flow rate, connecting tubing, detector, and injector volumes, should be downscaled by a factor of $f = \frac{d_1^2}{d_2^2}$ to miniaturize the LC system.[37,38]

As in conventional HPLC, the loss in column efficiency due to extracolumn effects should not exceed 10%. For a specific LC system, the maximum acceptable variance can be expressed as[39]

$$\sigma_{e(acc)}^2 \le 0.10\sigma_c^2 \le 0.10(\pi r^2 \varepsilon)^2 (1+k)^2 HL \qquad \text{I. 16}$$

where $\sigma_{e(acc)}^2$ is the maximally acceptable volumetric column variance due to extracolumn effects, σ_c is the peak variance caused by the chromatographic process, r

is the column radius, ε is the porosity of the column, k is the retention factor, L is the column length and H is the column plate height. Based on this equation, the maximum acceptable extracolumn variance for 75 μm and 30 μm i.d. capillary columns with different lengths and different particle sizes were calculated as shown in Table I.1. These values are extremely small, approximately 4000 to 20000 times smaller than those with conventional 4.6 mm i.d. columns.

Ultrahigh pressure liquid chromatography. The decrease in particle size is ultimately limited by the pressure provided by the LC pumping system. As discussed earlier, the pressure drop along the column is inversely proportional to the square of the particle diameter. Rearranging equation I.13 gives

$$d_p = \left(\frac{\phi u \eta L}{\Delta p}\right)^{1/2} \qquad \text{I. 17}$$

Substituting $L = N_r h_{\min} d_p$ and $u = \frac{D_{i,m} v_{\min}}{d_p}$ into the above equation gives[40]

$$d_p(opt) = \left(\frac{\phi \eta D_{i,m} v_{\min} h_{\min} N_r}{\Delta P}\right)^{1/2} \qquad \text{I. 18}$$

It can be seen from this equation that the optimal particle size increases with the required plate number, N_r. The optimal particle size, retention time, and column length were calculated as a function of N_r as shown in Table I.2. It was assumed that the minimum column reduced plate height was 2 at a reduced velocity of 3, the back pressure was 3000 psi, the viscosity was 0.001 Pa s, and ϕ was 1000.

A back pressure of 3000 psi, as given in Table I.2, is a typical condition for conventional LC. With this pressure limitation, it is obvious that it would be impossible to use 1.5 μm or smaller particles to achieve 9000 plates in 20 s with 27 mm long column

Table I. 1. Maximum acceptable extracolumn variances for 75 μm and 30 μm i.d. capillary columns.[a]

Column i.d. (μm)	Column length (cm)	$\sigma^2_{e(acc)}$ (nL^2)			
		d_p = 1 μm		d_p = 3 μm	
		k = 0	k = 2	k = 0	k = 2
75	15	0.28	2.6	0.84	7.8
	25	0.48	4.4	1.44	13.2
	40	0.76	6.8	2.28	20.4
30	15	0.007	0.066	0.022	0.20
	25	0.012	0.11	0.037	0.34
	40	0.020	0.17	0.058	0.52

[a]Total porosity, ε, was taken as 0.70, and plate height, $2d_p$, at optimum linear velocity.

in conventional HPLC. In order to use small particles for high speed and high efficiency separations, the pressure limitation must be improved and a new HPLC must be developed.

In 1997, MacNair *et al.*[41] introduced ultrahigh pressure liquid chromatography (UHPLC) in order to take advantage of the high efficiency potential of very small particles. A commercial pneumatic amplifier pump (pressure controlled) was used to provide pressures as high as 100,000 psi. Due to the lack of a reliable ultrahigh pressure injection valve, a home-designed static splitter injection block was used for sample injection. A 66 cm × 30 μm i.d. capillary column packed with 1.5 μm nonporous C18 bonded silica particles was employed for isocratic separation. Using this column, they achieved an efficiency as high as 190,000 plates. In their study, frictional heating which occurred at ultrahigh pressures was discussed. It was reported that the frictional heat was dissipated quickly when small diameter capillary columns were used.

In 1999, MacNair *et al.*[42] introduced ultrahigh pressure gradient liquid chromatography. In this design, an exponential gradient was used instead of a linear gradient. Using gradient UHPLC, a fluorescently-labeled protein digest was separated using 1.0 μm nonporous particles at a pressure of 37,000 psi. However, sample injection was cumbersome because the separation column had to be first installed into a static splitter injection block for sample injection at low pressure, and then removed and installed in the gradient UHPLC system for separation at ultrahigh pressure.

In 1999, our group[43] reported another UHPLC system which was used for high speed and high efficiency separations. Various herbicides and benzodiazepines were separated in 60 s on a 29 cm column with efficiency as high as 350,000 plates m^{-1}. An

Table I. 2. Unretained elution times for optimum particle diameters and column lengths in HPLC for pressure-limited situation.[a]

Required plate number	d_p (μm)	T_0 (s)	L (mm)
1,000	0.5	0.2	1.1
4,000	1.0	4.0	8.0
9,000	1.5	20.3	27
36,000	3.0	324	216
1,000,000	5.0	2500	1000

[a] Assuming ϕ is 1000, viscosity is 0.001 Pa s, diffusion coefficient is 1×10^{-9} m^2 s^{-1} and back pressure is 3000 psi. A minimum value h = 2 for h assumed at a reduced velocity of 3.

ultrahigh pressure supercritical carbon dioxide-slurry packing system was used to pack fused-silica capillaries with inner diameter of 29 μm and lengths up to 70 cm with 1.5 μm nonporous particles. In addition, UHPLC was first coupled to a time-of-flight mass spectrometer (TOF/MS) for detection.[44]

Our group also investigated the practical aspects of UHPLC. In this paper[45], an ultrahigh pressure injection valve, called a "pressure balanced switching valve", was evaluated, the dependence of column efficiency on column diameter was discussed, and fast detection using TOF/MS was described. It was reported that the pressure balanced switching valve could handle pressures as high as 17,000 psi, which was particularly important for development of UHPLC for routine use.

In 2001, Tolley *et al.*[46] reported flow controlled very high pressure liquid chromatography (VHPLC). Their system was based on a commercial pump which had been modified to operate at up to 17,500 psi. A computer controlled low pressure mixer was used to generate linear gradients. Protein digests were separated by gradient VHPLC at pressures as high as 13,500 psi, and detected by either a tandem mass spectrometer using electrospray ionization or a UV/visible detector. The results using VHPLC-MS/MS for protein identification were compared to those from nanoelectrospray-MS/MS. It was found that the VHPLC method gave more sequence information and higher signal-to-noise ratio than MS/MS alone.

Safety is a concern when extremely high pressures are used in UHPLC or VHPLC. In 2003, I authored a paper[47] concerning the safety aspects of UHPLC. It was pointed out in this paper that from an energy standpoint, UHPLC is much safer than the high pressures would seem to indicate due to the low compressibility of liquid solvents

(e.g., water can only be compressed approximately 10% at 40,000 psi). Water jets and capillary projectiles under ultrahigh pressures might lead to skin penetration under limited conditions. It was proposed that the use of a plexiglass shroud to cover an initial length of the installed capillary column would eliminate any safety-related concerns about liquid jets or capillary projectiles. This work is described in detail in Chapter II of this dissertation.

Elevated temperature was also investigated by me for high speed and high efficiency separations in UHPLC.[48] Capillary columns packed with small diameter particles typically result in low permeability. Decreasing the viscosity of the mobile phase by elevating the column temperature reduced the pressure drop and facilitated the use of small particles and high flow rates that otherwise could not be used at room temperature, even under ultrahigh pressures. In my design, a water-resistant, flexible heater tape covered with insulation was used to provide the desired heat to the column. Polybutadiene-coated 1.0 μm nonporous zirconia particles were used because of their chemical stability at elevated temperature. A separation of five herbicides was completed in 60 s using 26,000 psi and 90 °C. This work is described in detail in Chapter III of this dissertation.

A particularly interesting application of UHPLV is the separation of enantiomers using either a chiral mobile phase or chiral stationary phases.[49,50] In my work, β-cyclodextrin and 2-hydroxypropyl-β-cyclodextrin were added to the mobile phase as chiral selectors to separate benzodiazapine enantiomers. Several separations were completed in 60 s with efficiencies in excess of 200,000 plates m^{-1}. Pressures up to

42,000 psi were applied in these separations. Details of this work are described in Chapter IV of this dissertation.

With the development of UHPLC, synthesis of new packing materials, which are chemically and mechanically stable, is necessary. Colon's group[51] introduced a simple one-step process to synthesize uniform, spherical organosilica nano-particles (670 nm) containing octadecyl moieties. These capillary columns packed with nano-particles were tested in UHPLC at inlet pressures of approximately 50,000 psi, showing chemical stability under acidic (pH < 1) and basic (pH > 11) conditions. Fast separations were obtained with efficiencies of 500,000 plates m^{-1}. In another study[52], I evaluated specially synthesized 1.0 μm diameter polybutadiene-encapsulated nonporous zirconia particles, which were slurry packed into 50 μm i.d. fused-silica capillary columns using UHPLC. Efficiencies up to 280,000 plates m^{-1} were obtained for the separation of antiinflammatory drugs at a pressure of 20,000 psi. Compared to octadecylsilane bonded nonporous silica, the PBD nonporous zirconia showed greater selectivity for the applications reported. These particles also showed excellent thermal and mechanical stability at a temperature of 100°C and a pressure of 20,000 psi. This study is described in detail in Chapter III of this dissertation.

Elevated temperature liquid chromatography. Since the pressure is inversely proportional to the cube of particle diameter, the pressure drop along the column length rapidly increases with a decrease in particle size. Therefore, it may be particularly appropriate to reduce the viscosity of the mobile phase by carrying out chromatography at elevated column temperatures to improve separation speed. For example, five long-chain alkylphenones were completely resolved at 150 ^{o}C in 30 s with a flow rate of 15

mL min^{-1}.[53] Increasing the temperature can enhance the sorption-desorption kinetics and transport properties of the solute, thus reducing band broadening.[54] Increasing the temperature from 25 ^{o}C to 65 ^{o}C on a zirconia packing improved the efficiency by 30%, while an increase from 25 ^{o}C to 65 ^{o}C on a silica packing improved the efficiency by 48%.[55] Therefore, elevated temperatures are also beneficial for high efficiency separations.

When elevated temperature is used in LC, certain characteristics are required: (1) chemical stability of the solute and the stationary phase at the high operation temperature; (2) homogeneous heat transfer to the separation column; and (3) precisely controlled temperature.[56,57] Silica-based stationary phases typically degrade at very high temperature. However, nonporous particles showed better chemical stability for at least 1000 h at a temperature up to 120 ^{o}C.[53] Also, sterically protected silica particles have been reported to withstand temperatures up to 90 ^{o}C.[58] In addition, styrene-divinylbenzene polymers and polybutadiene-coated zirconia particles were both resistant at temperatures up to 200 ^{o}C.[59,60] Small diameter fused silica capillaries have good heat transfer properties, which make them amenable to temperature-controlled LC, even with temperature programming.[61] The repeatability of retention time with temperature programming was 0.2% for 40–110 °C with packed capillary columns.[62] Solute stability is also critical for elevated temperature LC. However, with high speed separation, the solute residence time inside the hot column is short, which makes it possible to analyze relatively unstable compounds and complex molecules with elevated temperatures.[63]

High speed gradient HPLC. Gradient elution is widely used in HPLC for complex samples having components with widely different retention factors. Using gradient elution, the separation time is given by[64]

$$t_R \approx \frac{L}{u} + \frac{t_G}{1 - \frac{k_f}{k_0}} \qquad \text{I. 19}$$

where t_G is the gradient time and k_0 and k_f are the respective isocratic retention factors of the most retained sample components at the initial and final mobile phase compositions.

The resolution in gradient elution does not depend on the column length and the flow velocity; thus, flow velocity can be increased and, at the same time, the column length reduced to achieve fast separations at a fixed column inlet pressure.[65]

I.3 Significance and Scope of Research Described in This Dissertation

UHPLC is still in its infancy. Many questions associated with this technique still need to be answered and technical problems still remain. In Chapter II of this dissertation, safety concerns with UHPLC are discussed.

It is obvious from the previous sections that employment of small nonporous particles with ultrahigh pressure and elevated temperature can provide high speed and high efficiency separations. This dissertation mainly focuses on the application of nonporous silica and zirconia particles for fast separations in UHPLC (Chapters III and IV). The use of elevated temperatures in UHPLC for fast separations is described in Chapter III and fast chiral separations using UHPLC are discussed in Chapter IV.

In Chapter V, use of a novel ultrahigh pressure injector for gradient UHPLC is described. High efficiency separations of a protein tryptic digest using gradient UHPLC

are demonstrated. In Chapter VI, gradient separations of peptides on three different types of particles are discussed. Finally, a trypsin immobilized microreactor, coupled to liquid chromatography, is described for on-line protein digestion and separation.

I.4 References

1. Halász, I.; Endele, R.; Asshauer, J.; J. Chromatogr. 112 (1975**)** 37.
2. Guiochon, G. Anal. Chem. 50 (1978) 1812.
3. Chen, H.; Horvath, C. J. Chromatogr. A 705 (1995) 3.
4. Van Deemter, J. J.; Zuiderweg, F. J.; Kinkenberg, A. Chem. Eng. Sci. 5 (1956) 271.
5. Hawkes, S. J. J. Chem. Ed. 60 (1983) 395.
6. Giddings, J. C. Unified Separation Science, Wiley: New York, 1991
7. Snyder, L. R.; Kirkland, J. J. Introduction to Modern Liquid Chromatography*;* John Wiley: New York, 1979.
8. MacNair, J. E. Ph.D Thesis, University of North Carolina, Chapel Hill, 1998.
9. Giddings, J.C. Dynamics of Chromatography, Marcel Dekker, New York, 1965.
10. Kennedy, R. T.; German, I.; Thompson, J. E.; Witowski, S. R. Chem. Rev. 99 (1999) 3081.
11. Paliwal, S. K.; de Frutos, M.; Regnier, F. E. Meth. Enzymol. 270 (1996) 133.
12. Knox, J. H.; Parcher, J. F. Anal. Chem. 41 (1969) 1599.
13. Sternberg, J. C.; Poulson, R. E. Anal. Chem. 36 (1964) 1492.
14. Bristow, P. A.; Knox, J. H. Chromatographia 10 (1977) 279**.**
15. Li, Y. M.; Liao, J. L.; Kakazato, K.; Mohammad, J.; Terenius, L.; Hjerten, S. Anal. Biochem. 223 (1994) 153.
16. Lommen, D. C.; Snyder, L. R. LC GC 11 (1993) 223.
17. Hanson, M.; Unger, K. K. LC GC 15 (1997) 170.
18. Janzen, R.; Unger, K. K.; Giesehe, H.; Kinkel, J. N.; Hearn, M. T. W. J. Chromatogr. 397 (1987) 91.

19. Unger, K. K.; Jilge, G; Kinkel, J. N.; Hearn, M. T. W. J. Chromatogr. 359 (1986) 61.

20. Jenke, D. R. J. Chromatogr. Sci. 34 (1996) 362.

21. Issaeva, T.; Kourganov, A.; Unger, K. J. Chromatogr. A 846 (1999) 13.

22. Chollet, D.; Castella, E.; Combe, P.; Arnera, V. J. Chromatogr. B 683 (1996) 237.

23. Kirkland, J. J. J. Chromatogr. Sci. 38 (2000) 535.

24. Kirkland, J. J. Truszkowaki, F. A.; Dilks Jr. C. H.; Engel, G. S. J. Chromatogr. A 890 (2000) 3.

25. Kirkland, J. J. J. Chromatogr. 185 (1979) 1.

26. Snyder, J. L.; Kirkland, J. J.; Glajch, J. L.; Practical HPLC Method Development, 2nd ed, Wiley, New york, 1997, Chapter 5.

27. Stadalius, M. A.; Berus, J. S.; Snyder, L. R. LC· GC 6 (1988) 494.

28. Afeyan, N. B.; Gordon, N. F.; Mazsaroff, I.; Varady, L.; Fulton, S. P.; Yang, Y. B.; Regnier, F. E. J. Chromatogr. 519 (1990) 1.

29. Regnier, F. E. Nature, 350 (1991) 634.

30. Fulton, S. P.; Afeyan, N.B.; Gordon, N. F.; Regnier, F. E. J. Chromatogr. 547 (1991) 452.

31. Wang, Q. C.; Svec, F.; Frechet, J. M. J. Anal. Chem. 65 (1993) 2243.

32. Liao, J. L.; Li, Y. M.; Hjerten, S. Anal. Biochem. 234 (1996) 27.

33. Minakuchi, H.; . J. Chromatogr. A 716 (1995) 107.

34. Petro, M.; Svec, F.; Frechet, J. M. J. J. Chromatogr. A. 752 (1997) 59.

35. Karlsson, K. E.; Novotny, M. Anal. Chem. 60 (1988) 1882.

36. Kennedy, R. T.; Jorgenson, J. W. Anal. Chem. 61 (1989) 1128.

37. Chervet, J.P.; Ursem, M. Anal. Chem. 68 (1996) 1507.

38. Vissers, J. P. C.; Claessens, H. A.; Cramers, C. A. J. Chromatogr. A 779 (1997) 1.

39. Vissers, J. P. C. J. Chromatogr. A. 856 (1999) 117.

40. Poppe, H. J. Chromatogr. A 778 (1997) 3.

41. MacNair, J. E.; Lewis, K. C.; Jorgenson, J. W. Anal. Chem. 69 (1997) 983.

42. MacNair, J. E.; Patel, K. D.; Jorgenson, J. W. Anal. Chem. 71 (1999) 700.

43. Lippert, J. A.; Xin, B.; Wu, N.; Lee, M. L. J. Microcol. Sep. 11 (1999) 631.

44. Wu, N.; Collins, D. C.; Lippert, J. A.; Xiang, Y.; Lee, M. L. J. Microcol. Sep. 12 (2000) 462.

45. Wu, N.; Lippert, J. A.; Lee, M. L. J. Chromatogr. A 911 (2001) 1.

46. Tolley, L.; Jorgenson, J. W.; Moseley, M. A. Anal. Chem. 73 (2001) 2985.

47. Xiang, Y; Maynes, D. R.; Lee, M. L. J. Chromatogr. A 991 (2003) 2.

48. Xiang, Y; Yan, B; Yue, B; McNeff, C. V.; Carr, P. W.; Lee, M. L. J. Chromatogr. A 983 (2003), 83.

49. Xiang, Y.; Wu, N.; Lippert, J. A.; Lee, M. L. Chromatographia 55 (2002) 399.

50. Gong, Y; Xiang, Y; Yue, B; Xue, G; Bradshaw, J. S.; Lee, H. K.; Lee, M. L. J. Chromatogr. A 1002 (2003) 63.

51. Cintron, J. M.; Colon, L. A. Analyst 127 (2002) 701.

52. Xiang, Y.; Yan, B.; McNeff, C. V.; Carr, P. W.; Lee, M. L. J. Chromatogr. A 1002 (2003) 71.

53. B. Yan, J. Zhao, J. S. Brown, J. Blackwell, P. W. Carr, Anal. Chem. 72 (2000) 1253.

54. Chen, H.; Horvath, C. Anal. Meth. Instrum. 1 (1993) 213.

55. Dolan, J. W.; Snyder, L. R.; Wolcott, R. G.; Haber, P.; Baczek, T.; Kaliszan, R. J. Chromatogr. A 857 (1999) 41.

56. Maa, Y.-F.; Horvath, C. J. Chromatogr. 445 (1988) 71.

57. Greibrokk, T.; Andersen, T. J. Chromatogr. A. 1000 (2003) 743.

58. Kirkland, J. J.; Dilks, Jr. C. H. LC GC 11(1993) 292.

59. Ingelse, B. A.; Janssen, H.-G.; Cramers, C. A.; J. High Resolut. Chromatogr. 21 (1998) 613.

60. Zhao, J.; Carr, P. W. Anal. Chem. 72 (2000) 302.

61. Molander, P.; Haugland, K.; Fladseth, G.; Lundanes, E.; Thorud, S.; Thomssen, Y.; Greibrokk, T. J. Chromatogr. A 892 (2000) 67.

62. Bowermaster, J.; McNair, H.; J Chromatogr. Sci. 22 (1984) 165.

63. Thompson, J. D.; Carr, P. W. Anal. Chem. 74 (2002) 1017.

64. L.R. Snyder, in Cs. Horvath (Editor), HighPerformance Liquid Chromatography — Advances and Perspectives, Vol. 1, Academic Press, New York, 1980, p 207.

65. L.R. Snyder, M. A. Stadalius and M. A. Quarry, Anal. Chem. 55 (1983) 1412.

CHPATER II

SAFTY CONCERNS IN ULTRAHIGH PRESSURE LIQUID CHROMATOGRAPHY

II.1 Introduction

Because the pressure drop across the column is inversely proportional to the cube of the particle size when a column is operated at optimum linear velocity, for columns packed with particles smaller than 2 μm in diameter, much higher pressures are required to operate at optimum flow rates, compared to columns containing larger particles.[1]

In 1997, MacNair *et al.* introduced UHPLC in order to take advantage of the high efficiency potential of very small particles.[2] Subsequent studies have further demonstrated high efficiency and high speed in UHPLC.[3-7] Commercial pneumatic amplifier pumps (pressure controlled) used in these studies reached pressures as high as 5,000 bar (72,000 psi). These pumps were used for packing columns as well as for chromatography.

Tolley *et al.* recently reported the use of flow control in UHPLC.[8] Their system was based on a commercial pump which had been modified to operate at up to 20 kpsi. UHPLC requires some custom-made components or special modification of commercial instruments to withstand ultrahigh pressures. For example, home-designed static-split injection valves were used for sample introduction because conventional injection valves could only endure pressures of 4,200-6,000 psi. For safety reasons, MacNair *et al.* modified all original liquid seal components in their pump, and built a 3/16 in. thick steel box to enclose all of their UHPLC system components.[2,4] However, until now, little

attention has been paid to carefully evaluating the safety concerns resulting from column rupture or failure in UHPLC during operation.

Column rupture in UHPLC can lead to two general safety concerns: liquid jets and capillary projectiles. In industry, high pressure liquid jets are used for a variety of purposes, such as manufacturing, cleaning, and dismantling.[9] In medical applications, liquid jets are used for cutting soft tissue.[10,11] However, high pressure liquid jet applications have also resulted in injuries because of their extremely high power densities.[12-14] A liquid jet could form in UHPLC if the capillary column broke or the on-column frits failed. Furthermore, other components, such as the injection valve, tubing, purge valve, pressure transducer and tubing connections, could wear out after being used for a period of time, which could also lead to formation of liquid jets. For example, to close a typical injection valve, a smooth cone-shaped surface of a needle tip is pressed into a channel orifice. The seal could fail after repeated use. It has been reported that the skin can be penetrated at a liquid jet power density of 1000-1500 W mm^{-2}, and bone is penetrated at a power density of 2200-3500 W mm^{-2}.[15] Incorrect installation of the capillary, breakage of the capillary or failure of the ferrule used in the capillary connector could lead to capillary projectiles being discharged in the liquid jet from the injection valve or tubing. The sharp capillary fragments represent the greatest potential risk of injury.

In this chapter, liquid jets and capillary projectiles caused by failures or ruptures in pressure-controlled UHPLC were investigated. Laboratory experiments were carried out to study the formation of liquid jets and capillary projectiles. Theoretical calculations were performed to estimate the power densities of liquid jets and the impact force of

capillary projectiles under ultrahigh pressures. Modifications and practices to prevent any possible injury from ultrahigh pressure liquid jets or capillary projectiles are suggested.

II.2 Experimental

II.2.1 Materials and Chemicals

HPLC-grade water was obtained from Fisher Scientific (Fair Lawn, NJ). Prior to use, the water was filtered through a 0.22 μm Durapore® membrane filter (Millipore, Bedford, MA) and degassed thoroughly. SFC-grade carbon dioxide and compressed nitrogen were purchased from Airgas (Salt Lake City, UT). Fused silica tubing was obtained from Polymicro Technologies (Phoenix, AZ).

II.2.2 UHPLC System

The experimental UHPLC apparatus is shown in Figure II.1. A double-head air-driven liquid pump (Model DSHF-302, Haskel, Burbank, CA, USA) with a piston area ratio (air drive area to liquid piston area) of 346 was used to generate the liquid pressure needed. The maximum air supply pressure was 150 psi, resulting in a pump pressure limit of 52 kpsi. The internal volume of the pump was 4.5 mL. A cylinder containing compressed nitrogen was used to drive the pump. The outlet of this pump was connected to a 3-way valve (called the main valve, Model 60-13HF2, High Pressure Equipment, Erie, PA, USA), one port of which was connected to a 2-way valve (called the pump vent valve, Model 60-11HF2, HiP, Erie, PA) and the other port to a tee (Model 60-23HF2, HiP, Erie, PA). The high pressure tee interconnected a high pressure transducer and an

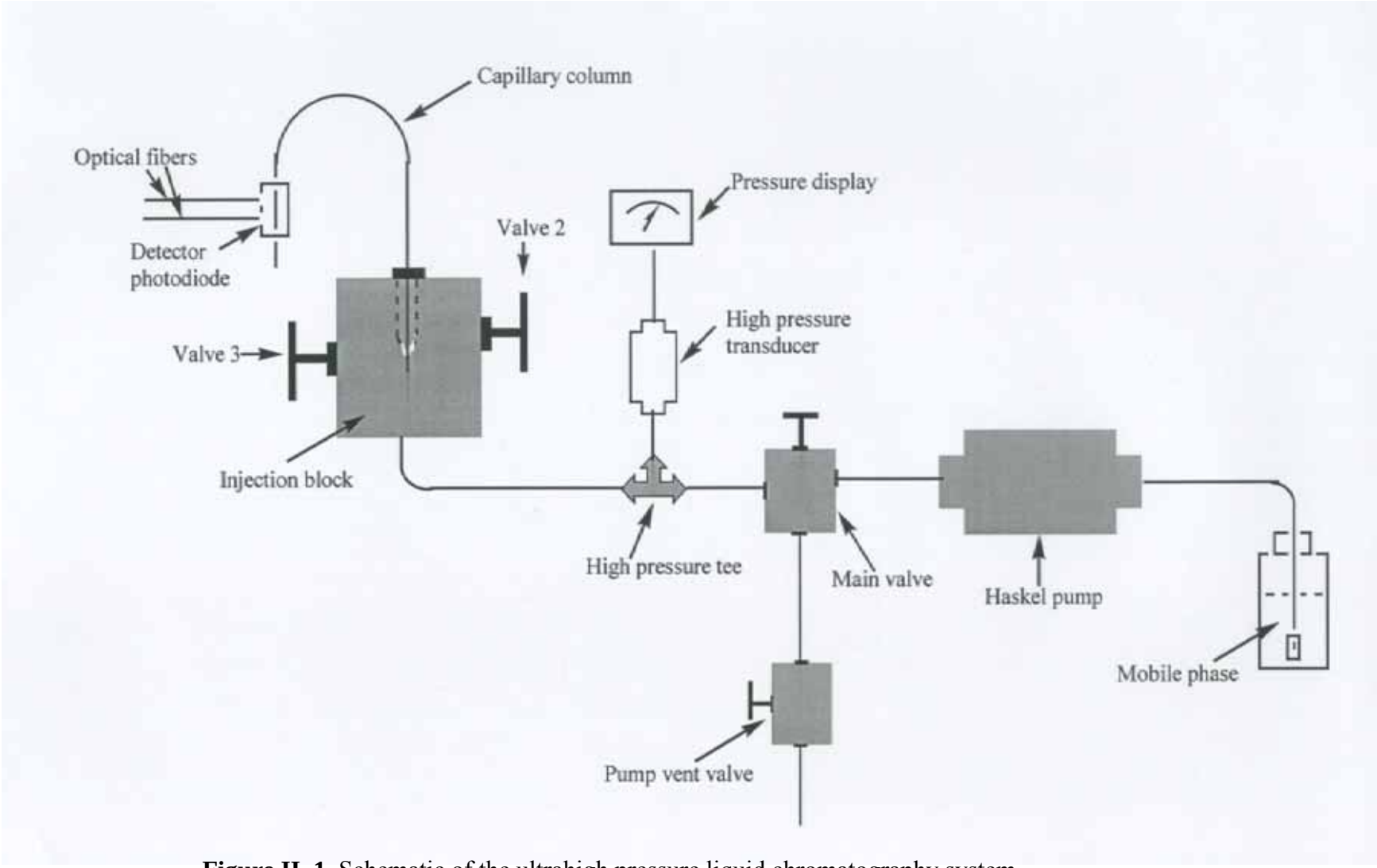

Figure II. 1. Schematic of the ultrahigh pressure liquid chromatography system.

injection block. Stainless steel tubing (1/8" o.d x 0.020" i.d, HiP, Erie, PA) was used for these connections. The high pressure transducer allowed real-time monitoring of the column inlet pressure, from 0-60,000 psi. The injection block, called the static-splitter injector, incorporated three valves and four ports. Valve 1 was used to isolate the pump from the injection block (not shown in Figure II.1). Valves 2 and 3 were used to open the sample and waste ports. When valves 2 and 3 were opened and valve 1 was closed, sample could be loaded by filling the internal channel of the injection block with a syringe. After sample loading, valves 2 and 3 were closed. For sample injection, the pump pressure was adjusted to 800 psi, and then valve 1 was opened and closed as quickly as possible, allowing the mobile phase to carry the sample into the separation column. After injection, it was necessary to flush the sample channel by opening valves 1 and 2, and then valves 1 and 3. Figure II.2 shows a photograph of the UHPLC system as described above.

II.2.3 Measurement of the Liquid Jet Velocity

Knowledge of the liquid jet velocity is necessary for calculation of the power density. Generally, the liquid jet velocity is hard to measure directly. In pressure controlled UHPLC, if a liquid jet occurs, it can only last for a short time period until the pump reservoir becomes empty. The time between the start of liquid jet formation and complete pump volume expulsion was measured. The total volume of liquid from the jet was also collected and measured. The average liquid jet velocity could then be calculated from the total volume expelled divided by the product of the expulsion time and jet cross sectional area. The liquid used for measurement of the liquid jet velocity was water.

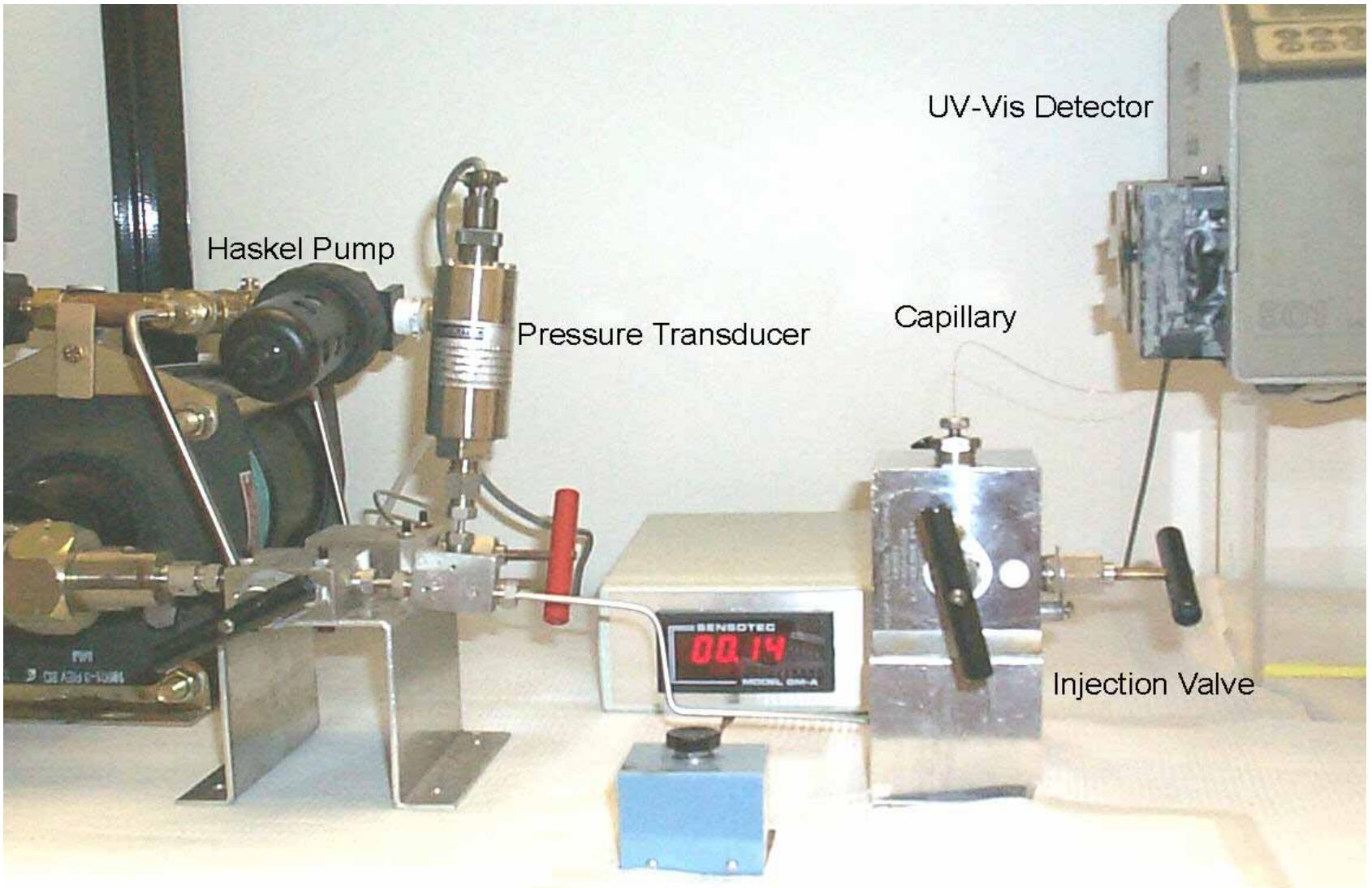

Figure II. 2. Photograph of the ultrahigh pressure liquid chromatography system.

II.3 Results and Discussion

II.3.1 Internal Energy

The amount of stored energy in a system is a safety concern because too much stored energy may lead to an explosion or catastrophic failure. However, the actual amount of stored energy in the system is quite low, due to the low compressibility of solvents (i.e., water can be compressed approximately 10% at 40,000 psi). If air is compressed to 40,000 psi, the stored energy is on the order of 10^8 J Kg^{-1}, while for water at the same pressure, the stored energy is on the order of 10^5 J Kg^{-1}, or three orders of magnitude smaller. Thus, from an energy standpoint, UHPLC is much safer than the high pressures would seem to indicate.

Nevertheless, ruptures or failures during operation in UHPLC are possible, and they can result in the formation of liquid jets and/or particle projectiles. Particle projectiles can represent the whole capillary with inlet end dislodged, capillary fragments and/or particles of packing materials. Details concerning formation and potential health risks of liquid jets and projectiles are discussed in the following sections.

II.3.2 Liquid Jets

When the mobile phase is ejected out of a small diameter capillary or through an orifice under ultrahigh pressure, a liquid jet is formed. There are three potential causes of liquid jets in UHPLC: first, breakage or dislodgement of the capillary column; second, blow-out of the on-column frits; and third, wearing out of system parts, such as the injection valve, tubing, purge valve, pressure transducer or tubing connections. In practice, liquid jets are rarely experienced from the third cause since these typically

involve large volumetric flow rates and the pump pressure decreases quickly (i.e., the pump can only maintain ultrahigh pressure when there is a low flow rate). In addition, liquid jets are only remotely possible for well-packed columns from the second cause. Therefore, the main safety concern arises from liquid jets originating from breakage or dislodgement of the capillary column.

High speed liquid jets can impose a cutting potential. Previous studies have shown that the skin is penetrated at a jet power density of 1000-1500 W mm^{-2}.[15] The power density can be calculated simply as the ratio of the hydraulic power and the area affected by the jet

$$Power \quad density = \left(\rho Q \frac{V^2}{2A} \right) \qquad \text{II. 1}$$

where Q is the volumetric flow rate (mL s^{-1}), ρ is the fluid density (g mL^{-1}), A is the area affected by the jet (mm^2), and V is the average velocity of the liquid jet (m s^{-1}).

Calculation of the power density requires knowledge of the velocity or the volumetric flow rate of the liquid jet, which is hard to measure directly. In pressure controlled UHPLC, when a liquid jet occurs, it will last until the pump reservoir is empty. This pump reservoir drain time can be measured. The average volumetric flow rates of various liquid jets were determined by dividing the total reservoir volume by the measured pump reservoir drain time. However, when ultrahigh pressures and short capillaries (capillaries remaining after breakage) are used, these drain times are hard to measure precisely due to the high speed flow rates.

A simplified form of the mechanical energy equation for viscous flow through pipes can be used to describe the velocity of the liquid jet formed due to rupture in UHPLC:

$$V = \sqrt{\frac{2\Delta P}{\rho}(1 + f\frac{L}{D})} \qquad \text{II. 2}$$

where V is the exit average velocity from the broken capillary (m s^{-1}), ΔP is the pressure difference supplied by the pump (Pa), ρ is the fluid density (g m^3), L is the length of capillary remaining (1-2 cm), D is the capillary inside diameter (cm), and f is the friction factor. Since f is dependent on V, the solution to Equation II.2 must be iterative. The empirical volumetric flow rates obtained as described earlier were compared with those calculated from equation II.2 (Table II.1). It was found that the experimental results were in agreement with the theoretical calculations. Therefore, equation II.2 was used for further prediction of liquid jet velocities at ultrahigh pressures.

When connecting the capillary to steel tubing or to the injector via Vespel/graphite ferrules, the shortest feasible capillary length inside the injector is approximately 1 cm. Therefore, a worst-case scenario for liquid jet formation under our UHPLC conditions (i.e., remaining column length of 1.0 cm after breakage and a maximum operating pressure of 40,000 psi) was considered as shown in Figure II.3. Also, shown in Figure II.3 are the times required for the pump reservoir to empty.

As the capillary exit, the power density of the jet can be quite high as shown in Figure II.4. As the diameter of the jet exit orifice becomes smaller, the power density decreases because of the reduction in volumetric flow rate. Unfortunately, the orifice diameter would have to be less than 5 μm to pose absolutely no significant health threat.

Table II. 1. Comparison of experimental drain times and flow rates with theoretical calculations.[a]

Pressure	Experimental measurement		Theoretical calculation	
(kpsi)	Drain time (s) [b]	Flow rate (mL s^{-1})[c]	Drain time (s) [b]	Flow rate (mL s^{-1})[c]
6.00	25.2	0.163	25.2	0.153
9.00	19.7	0.198	20.3	0.192
15.0	14.4	0.271	15.2	0.256
21.0	11.7	0.332	12.6	0.310
25.0	10.6	0.369	11.4	0.342
35.0	—	—	9.5	0.413
40.0	—	—	8.8	0.445

[a] Assuming 2 cm capillary remaining after breakage.

[b] n=4.

[c] 4.1 mL pump reservoir volume.

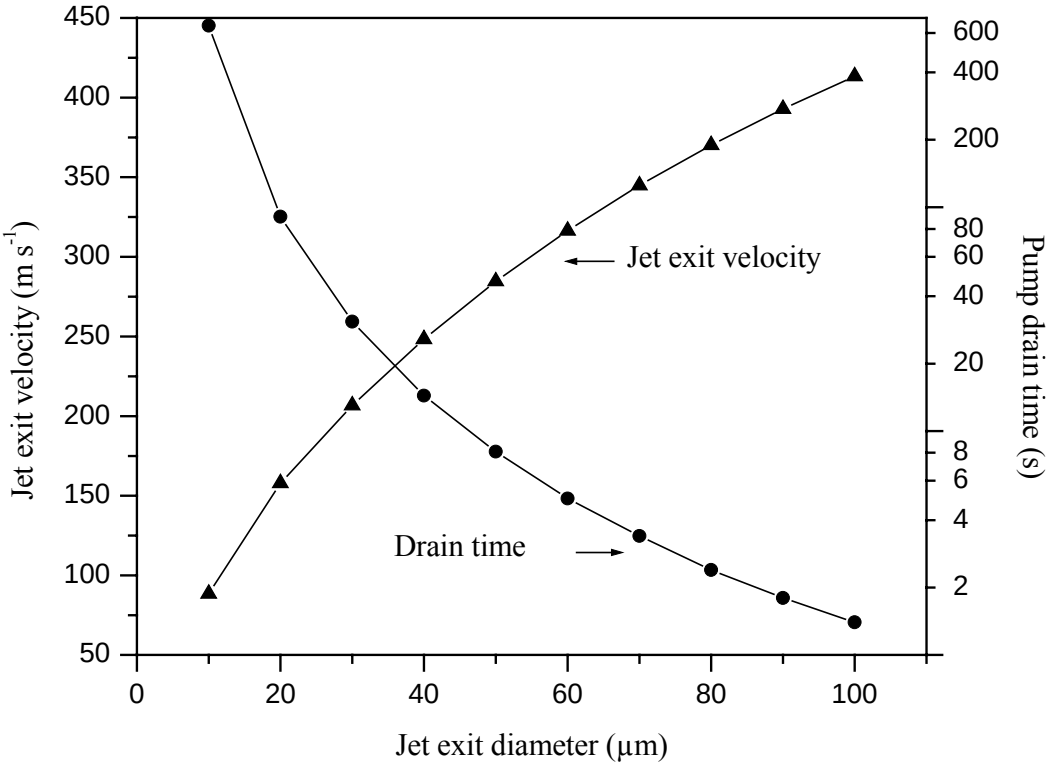

Figure II. 3. Liquid jet exit velocity and time for pump cavity to empty vs. capillary diameter for a capillary length of 0.01 m and a pump pressure of 40,000 psi.

However, the jet velocity decreases with distance from the exit due to viscous interactions with the surrounding air; thus, the power density decreases. Also the jet tends to break up into droplets due to the surface tension of the liquid. Because of these effects, the damage potential is greatly reduced at even short distances from the jet exit. For example, a jet operating at a pressure of 45,000 psi with a liquid jet diameter of 0.15 mm would cut plastic at a 10 mm stand-off, but would have no cutting power at a distance of 30 mm. Yanaida has shown that for liquid jets in air, at 200 diameters (200 *d*) from the jet exit, the diameter of the jet increases to 4 times the exit diameter.[16] Thus, the velocity of the jet decreases to about $1/16^{th}$ of the exit velocity. For capillaries of $d = 10$ and 100 μm, this distance is 2 mm and 2 cm, respectively. Also shown in Figure II.4 is the liquid jet power density at a distance of 200 *d* vs. the exit diameter. A safety factor of 2 was utilized in determining the power density; thus, the values are conservative.

Note in Figure II.4 that at the jet exit, the power density is larger than 1000-1500 W mm^{-2} for most diameters at 40,000 psi. However, at 200 *d* the power density is below this value for all cases. The breakup distance, i.e., the predicted distance where the jet breaks up into droplets, was calculated based on a correlation provided by Grant and Middleman.[17] The breakup distance under our conditions was at most 2.5 cm and, once breakup occurred, the danger of damage to soft tissue was eliminated. Thus, at distances greater than 2-2.5 cm (worst case), the danger due to the liquid jet was minimal.

The worst case for liquid jet formation was considered above. In fact, the risk decreases if rupture occurs further from the pressure inlet end of the capillary because the pressure drops gradually along the capillary length due to the resistance of the packed bed. Also, the densely packed particles in the capillary cause a delay in the formation of

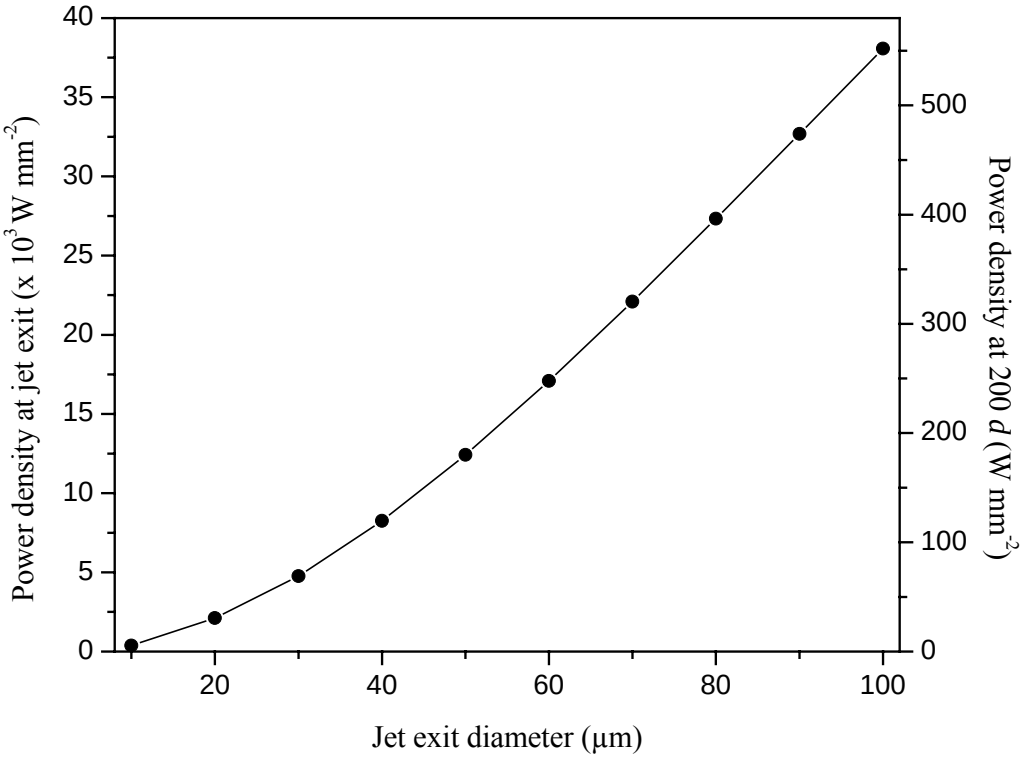

Figure II. 4. Liquid power density at the jet exit and at 200 *d* vs. *d* for a capillary length of 0.01 m and a pump pressure of 40,000 psi.

the liquid jet because it takes time to push the packing materials out of the capillary. This delay allows the operator to take some precautionary measures, such as turning off the pump.

II.3.3 Capillary Projectiles

Capillary projectiles can be formed in UHPLC when the capillary end is discharged at high speed from the injector. This may be due to either breakage of the capillary, failure of the Vespel/graphite ferrules, or incorrect installation of the capillary in the injector. Under this scenario, the existence of capillary projectiles in addition to the liquid jet is of concern. Incorrect installation of the capillary [not tightening the capillary connector in the injector (see Figure 5 in reference 4 for details)] represents the worst case since the entire capillary may be ejected at high speed. This situation was created experimentally to produce projectiles and to study the effectiveness of various safety modifications (discussed in the next section). Since it was impractical to measure projectile speeds, theoretical calculations were used for further safety considerations.

If the capillary is completely removed, the size of the orifice through which liquid can be ejected is 360 μm (outer diameter of the capillary used), and viscous effects can be neglected so that the velocity can be computed from equation II.2 where $f = 0$. However, the pump cannot maintain a pressure of 40,000 psi with such a large flow rate. In fact, under these conditions, the exiting jet velocity would be 166 m s^{-1}, with a corresponding pump pressure of 2,000 psi. For this jet velocity, the power density at the exit would be approximately 2300 W mm^{-2}; however, at 50 *d* (1.8 cm) from the jet exit, the jet velocity is conservatively estimated to be approximately 83 m s^{-1} and the power density, 575 W mm^{-2}. Thus, beyond 1.8 cm, there is no danger from the liquid jet.

Propelled projectiles in the jet offer the greatest potential for injury. The worst case corresponds to a start up of the pump system with the capillary unrestrained. In this case, the capillary would accelerate out the end of the steel tubing or injector like a projectile. Assuming a long, straight projectile of diameter 360 μm, a force balance can be performed on the projectile to determine the velocity at which it would leave the tubing

$$\sum F = m\frac{dv}{dt} = m\frac{d^2x}{dt^2} \qquad \text{II. 3}$$

where v is the velocity (m s^{-1}) of the projectile and x is the position (m) of capillary projectile inside the tubing or injector. Also

$$\sum F = PA = P\pi R^2 \qquad \text{II. 4}$$

and

$$m = \rho_{capillary} \forall = \rho_{capillary} \pi R^2 L \qquad \text{II. 5}$$

where P is the pressure (Pa), A is the cross-sectional area (cm^2), R is the capillary outer radius (cm), $\rho_{capillary}$ is the capillary density (g mL^{-1}), $\forall$ is the volume (mL) of the fused silica capillary , and L is the length (cm) of the capillary ejected.

Substituting equations II.4 and II.5 into equation II.3 gives

$$P\pi R^2 = \rho_{capillary} \pi R^2 L \frac{d^2x}{dt^2} \qquad \text{II. 6}$$

Rearranging terms, the above equation can be written as

$$\frac{d^2x}{dt^2} = \frac{P}{\rho_{capillary} L} \qquad \text{II. 7}$$

Solving equation II.7, we obtain

$$x = \frac{Pt^2}{\rho_{capillary} L^2} \qquad \text{II. 8}$$

When x is approximately equal to x_b, the initial length of capillary inside the tubing or injector, a force will no longer be applied. The time when this occurs is

$$t = \left(\frac{\rho_{capillary} L^2 x_b}{P}\right)^{1/2} \qquad \text{II. 9}$$

From this time, the ejection velocity can be computed from

$$\frac{dx}{dt} = v = \frac{P}{\rho_{capillary} L} t \qquad \text{II. 10}$$

Assuming a length of capillary in the tubing or the injector of 1 cm, the ejection velocity was modeled as a function of total capillary (projectile) length. The results are shown in Figure II.5.

Although the pump cannot maintain a pressure of 40,000 psi long term because the actual pump pressure is limited by the volumetric flow rate capability of the pump, due to liquid compression, the maximum pump pressure (40,000 psi) can be exerted on the capillary end initially. The maximum projectile velocity can be as great as 350 m s^{-1}, and this velocity represents an upper limit. However, the actual velocity will be much smaller because: (1) there is usually some restraining force on the capillary (it is not simply free to be ejected); (2) the capillary will not typically move as a straight, rigid whole when it is ejected, resulting in rapid deceleration; (3) the capillary will likely break since the initial length will be typically 15-30 cm, and the breakage energy will reduce the kinetic energy of the ejected capillary; and (4) there is a pressure drop along the capillary, which reduces the initial force on the projectile, depending on the point of breakage.

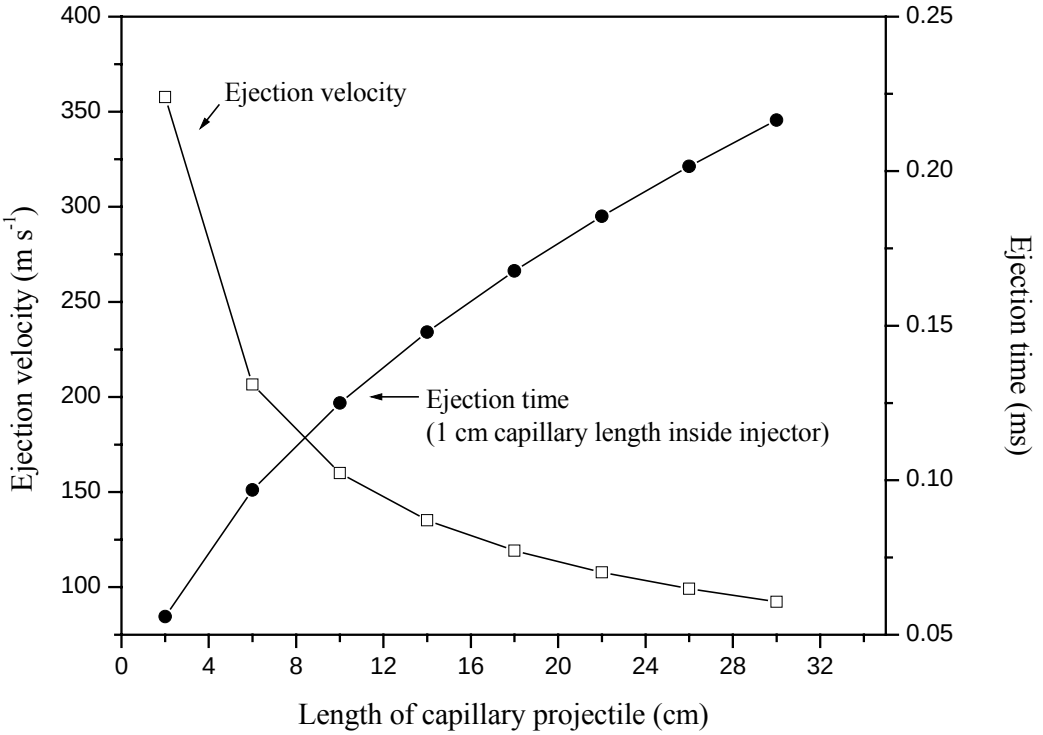

Figure II. 5. Projectile ejection velocity and ejection time for a capillary length of 0.01 m inside the injector vs. capillary projectile length at a pump pressure of 40,000 psi.

II.3.4 Specific Recommendations

Modeling the ejection dynamics accurately is somewhat difficult because of their complex dynamic behavior. It can be said, however, that the maximum possible velocity of ejected projectiles from the steel tubing will be much less than 350 m s^{-1}. Even though the masses of the ejected capillaries would be small, ranging from 4-71 mg for 2-30 cm lengths, at these velocities, penetration of soft tissue would certainly occur, and damage to the eyes could be severe. This danger, however, can be eliminated by installing a plastic shroud over a short section of capillary column that extends out of the injector. There are two considerations regarding the required thickness of the plastic cover: penetration of the plastic, or impact and spalling on the exterior surface causing secondary projectiles. The maximum impact pressure of the ejected capillary is conservatively estimated as the product of the fused silica density and the square of the maximum ejection velocity. For the worst possible case of an ejection velocity of 350 m s^{-1}, the maximum possible impact pressure will be less than 40,000 psi. By comparing the impact force, $P\pi R^2$, with the force required to penetrate the cover, $\pi Rt\tau$, whether or not penetration is possible can be determined. In these equations, R is the radius (mm) of the projectile, t is the thickness (mm) of the plastic cover, and τ is the tensile strength (psi) of the plastic. Since $\pi Rt\tau$ is much greater than $P\pi R^2$ for plexiglass (approximately 5 times), for a thickness of 3.2 mm (1/8 inches), there is no danger of penetration. The fused silica is also brittle compared to the ductile plexiglass, with a tensile strength (6900 psi) less than that of the plexiglass (9800 psi). Thus, the projectile should disintegrate at impact, resulting in a tremendous loss in energy and significantly decreasing the potential

loading on the shroud. Thus, spalling cannot occur, and a plexiglass cover of 3.2 mm thickness is adequate for containment of any failure.

Containment has been demonstrated with a very simple setup as shown in Figure II.6. A plastic bottle with a small hole in the side was installed to contain the first several cm of the capillary. The capillary exited the plastic bottle at an almost right angle to the inlet capillary axis. The capillary was secured at the hole with epoxy. The inlet of the capillary was installed in the injector incorrectly (not tightening the capillary connector in the injector) so that the worst case scenario would result. As predicted, when the capillary was ejected, the loose end flew directly to the bottom of the inverted bottle and broke into pieces. Plastic bottles of different sizes with wall thickness of 1.5 mm, which is in the safety range as discussed earlier, were evaluated. The experiments were repeated 5 times with an applied pressure of 40,000 psi for every bottle. It was found that as long as the projectiles are contained, safety is assured. Another advantage of installing a shroud is that water jets are also contained.

II.4 Conclusions

Rupture of the column and failure of the system components in UHPLC could lead to hazardous high speed liquid jets and capillary projectiles. Our analysis of liquid jets and capillary projectiles was based on the worst case. Even for the worst case, the power density of a liquid jet at a distance of 200 *d*, or approximately 2 cm, was lower than 1000-1500 W mm^{-2}. Therefore, capillary (particle) projectiles impose the greatest potential for injury. However, any possible injury can be eliminated by enclosing the first section of the capillary column in a V045I Plexiglass shroud.

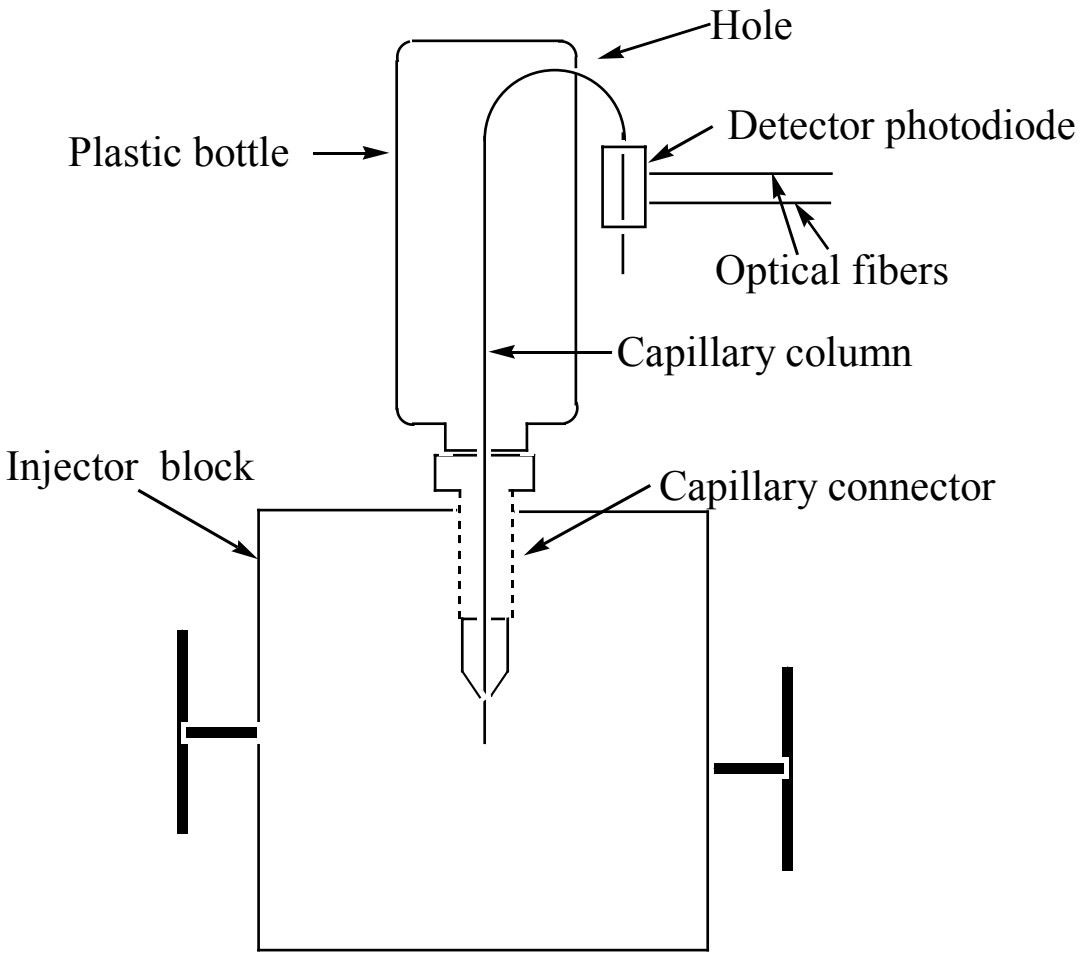

Figure II. 6. Schematic of the UHPLC inlet system with safety modification.

II.5 References

1. Jenke, D. R. J. Chromatogr. Sci. 34 (1996) 362.

2. MacNair, J. E.; Lewis, K. C.; Jorgenson, J. W. Anal. Chem. 69 (1997) 983.

3. Lippert, J. A.; Xin, B.; Wu, N.; Lee, M. L. J. Microcol. Sep. 11 (1999) 631.

4. MacNair, J. E.; Patel, K. D.; Jorgenson, J. W. Anal. Chem. 71 (1999) 700.

5. Wu, N.; Collins, D. C.; Lippert, J. A.; Xiang, Y.; Lee, M. L. J. Microcol. Sep. 12 (2000) 462.

6. Wu, N.; Lippert, J. A.; Lee, M. L. J. Chromatogr. A 911 (2001) 1.

7. Xiang, Y.; Wu, N.; Lippert, J. A.; Lee, M. L. Chromatographia 55 (2002) 399.

8. Tolley, L.; Jorgenson, J. W.; Moseley, M. A. Anal. Chem. 73 (2001) 2985.

9. Axmann, H,-D.; Flügel, M.; Laurinat, A.; Louis, H.; Proc. 12th Internat. Conf. Jetting Technology−Applications and Opportunities, N. G. Allen, Ed., (1994) 317.

10. Honl, M.; Rentzsch, R.; Üebeyli, H.; Hille, E.; Morlock M. and Louis, H.; Proc. 15th Internat. Conf. Jetting Technology, R. Ciccu, Ed., (2000) 183.

11. Piek, J.; Wille, C.; Warzok, R.; Gaab, M. R. J. Neurosurg. 89 (1998) 861.

12. Calhoun, J. H.; Gogan, W. J.; Viegas, ST. F.; Mader, J. T. Foot and Ankle 10 (1989) 40.

13. Summers, D. A.; Viebrock, J. Proc. 9th Internat. Symp. Jet Cutting Technology, J. Sendai, Ed., (1988**)** 423.

14. Weltmer, J. B.; Pack, L. L. J. Bone Joint Surg. 70 (1988) 1221.

15. Axmann, H,-D.; Krause, M.; Laurinat, A.; Louis, H.; Meiβner, T. Proc. 13th Internat. Conf. Jetting Technology−Applications and Opportunities, C. Gee, Ed., (1996**)** 309.

16. Yanaida, K. Proc. 2nd Internat. Symp. Jet Cutting Technology, Cambridge, UK,

April (1974) A2-19.

17. Grant, R. P.; Middleman, S. AIChE J., 12 (1966) 669.

CHAPTER III

FAST SEPARATIONS USING ELEVATED TEMPERATURE ULTRAHIGH PRESSURE LIQUID CHROMATOGRAPHY

III.1 Introduction

III.1.1 Elevated Temperature UHPLC

As shown with equation I.4 in Chapter I, reducing the particle diameter (d_p) of chromatographic packing materials is one of most efficient methods to achieve high speed and high efficiency separations.[1] Theoretically, the use of small nonporous particles further assists the achievement of high performance separations by eliminating diffusion of solute into and out of the stagnant mobile phase contained in the pores of porous particles.[2,3] The particle diameter of nonporous particles can be reduced below 2 μm while still retaining their mechanical strength, which is important when very high or ultrahigh pressure is used.[4] Columns containing small nonporous particles have exhibited excellent ultrafast separations for both macromolecular compounds and small molecules. Therefore, use of small nonporous particles has become very popular recently. Ohmacht *et al.* used 1.5 μm nonporous particles to separate selected peptides, vitamins, proteins and tryptic fragments of proteins.[5,6] A 15-s separation of 3 peptides was demonstrated. However, the three peaks were not completely resolved due to the low total efficiency provided by the short 33 mm long column. Obviously, longer columns packed with small nonporous particles are necessary to achieve high resolution in short analysis times.

The pressure drop across the column is inversely proportional to the cube of the particle size at optimum linear velocity, as discussed in Chapter I, when a column is

operated at optimum linear velocity.[7,8] Therefore, for columns packed with particles smaller than 2 μm in diameter, much higher pressures are required to operate at optimum linear velocities compared to columns containing large particles.[8] Lower flow rates result in degraded column efficiency because of increased band broadening by solute longitudinal diffusion.[9] However, the applicability of high flow rates for fast separations using small particle packed columns is limited by the pressure that the conventional LC pump system (~6,000 psi upper pressure limit) can supply and the back pressure that the other components of the chromatographic system (injector, column and valves) can withstand.

In 1997, MacNair *et al.* reported the use of ultrahigh pressures to overcome the significant pressure drop that results from using small particles in LC.[10] A static splitter injection block, which can withstand pressures as high as 72,000 psi, was used for sample injection. Mobile phase pressures as high as 72,000 psi were supplied to a 46 cm column packed with 1.0 μm particles to generate more than 200,000 theoretical plates in 6 min. Over 100 peaks from a protein digest were resolved in 30 min using a 27 cm column with UHPLC.[11] In 1999, Wu *et al.*[12] separated selected combinatorial chemistry samples, pharmaceutical compounds, and herbicide standards in less than 100 s. Recently, I demonstrated[13] fast chiral separations of chlorthalidone and oxazepam enantiomers in 60 s. It has been proven that UHPLC is a powerful chromatographic technique for high speed and high efficiency separations.

Use of elevated temperature in LC has been advocated primarily as a means of decreasing the back pressure of the column, and shortening the separation time and increasing the column efficiency.[14,15] Increasing the temperature of the mobile phase

decreases its viscosity; thus, the back pressure is greatly reduced, allowing the use of higher flow rates, longer columns, or smaller particles that otherwise could not be used.[16,17] Therefore, the significant pressure drop resulting from using small particles in LC can be overcome by either ultrahigh pressure, elevated temperature or both. For most solutes, analysis time can be reduced at elevated temperature because the enthalpy of solute transfer from the mobile phase to the stationary phase is favorable.[18,19] For example, at 150 ^{o}C and a flow rate of 15 mL min^{-1} with a 5 cm by 4.6 mm (i. d.) column packed with 3 μm polystyrene-coated porous zirconia particles, five long-chain alkylphenones were completely resolved in under 30 s.[19] This is a 50-fold reduction in time compared to the same separation at ambient temperature. Elevated temperature also facilitates high efficiency separations.[20,21] Generally, for fast separations, much higher mobile phase velocities than the optimum are used. The resulting efficiency of the column at these high velocities is determined by the mass transfer characteristics of the system. Elevated temperatures increase the diffusivities of the analytes, improving mass transfer and, hence, efficiency.[22,23]

Due to their relatively low mass and heat capacity, packed capillary columns are more suitable for elevated temperature LC than conventional columns because radial temperature effects are negligible.[23-25] Capillary columns provide both efficient dissipation of frictional heat and minimization of radial temperature gradients that otherwise would be problematic when using ultrahigh pressures to generate high mobile phase linear velocities.[10] Precisely controlled temperature is critical for elevated temperature UHPLC.[26] It is well known that preheating the mobile phase in addition to thermostating the column can help to avoid unacceptable peak broadening caused by a

temperature difference between the incoming eluent and the column.[23,27,28] In addition, development of a stationary phase that is chemically stable at elevated temperatures is particularly important for elevated temperature UHPLC.

III.1.2 Zirconia-based Stationary Phases for UHPLC

The most widely used nonporous particles have been silica-based particles. Most silica-based stationary phases are thermally unstable in aqueous solution and can only be used at temperatures marginally higher than ambient. Sterically protected silica-based stationary phases have shown better thermal stability, but are still limited for use at very high temperatures (> 100 ^{o}C).[29,30] In addition, most silica-based stationary phases must be used between pH 2 and pH 9. Recently, there has been a rising interest in zirconia-based stationary phases because they are mechanically and chemically stable over relatively wide pressure and pH ranges. Over the past decade, Carr and co-workers have produced a series of thermally stable stationary phases, which allow very high temperatures (up to 200 ^{o}C) to be used in LC. Chemically and thermally stable zirconia particles coated with polybutadiene (PBD),[31-35] polystyrene (PS),[36,37] and carbon (C)[38] have allowed separations at temperatures exceeding 200 ^{o}C. Studies on efficiency, selectivity and thermodynamic properties of PBD-ZrO_2, PS-ZrO_2, and C-ZrO_2 stationary phases have shown the advantages of high temperature LC. In 2001, Carr's group developed a new process for synthesis of spherical and unaggregated nonporous zirconia particles.[39] It was claimed that these microspheres were suitable for ultrafast chromatography at elevated temperature.

III.1.3 Fast Separations in Elevated Temperature UHPLC Using An Aqueous Buffer as Mobile Phase

In comparison to porous particles for reversed phase chromatography, nonporous particles show some differences. Primarily, nonporous particles have reduced surface area, leading to much less solute retention when the same mobile phase is used. Alternatively, compared to porous particles, less organic content or even no organic content in the mobile phase is needed to achieve similar solute retention. It was reported that neat water was used as mobile phase for the separation of organic hydrocarbons on trifluoropropylsiloxane modified nonporous particles.[40] In addition, the polarity of water decreases markedly as its temperature is raised. Therefore, an aqueous-only mobile phase can be adjusted to the same polarities as mixtures of methanol and water which are typically employed as eluents in reversed phase LC for moderately polar and nonpolar analytes by merely controlling the temperature.[41-45] Temperature programming with neat water may be used to mimic solvent programming within a specific polarity range.[44] Therefore, increasing the solvent temperature and reducing the phase volume ratio of the stationary phase when using nonporous particles make possible the use of water as mobile phase to achieve reasonable retention factors for certain analytes.

The organic solvent content in the mobile phase can be a significant source of chemical waste. Aqueous-only mobile phases, on the other hand, are environmentally "friendly". They are nonflammable, and their use eliminates organic vapor emissions from eluent waste containers. Since water is the most ultraviolet transparent solvent for HPLC, the best detection limits should be possible when using UV absorbance detection. In addition, having no organic solvent in the mobile phase makes the LC method

compatible with other detection methods such as flame ionization detection.[40,46] In fact, when using deuterium oxide as a mobile phase, HPLC was compatible with high field NMR spectroscopy detection.[47]

In my research, I found that polybutadiene-encapsulated nonporous zirconia was very suitable for "green" analyses. Separations of selected pharmaceutical drugs using only water or an environmentally friendly water buffer as mobile phase were achieved using this stationary phase. Elevated temperature was applied to ultrahigh pressure liquid chromatography for fast and efficient separations.

In this chapter, 1.0 μm diameter polybutadiene-encapsulated nonporous zirconia particles were evaluated in UHPLC and compared with octadecylsilane modified nonporous silica particles. Elevated temperature UHPLC was developed and the effects of temperature and pressure on linear velocity, efficiency and resolution are discussed. Also, 1.0 μm polybutadiene-encapsulated nonporous zirconia particles and 1.0 μm isohexylsilane modified nonporous silica particles were applied in elevated temperature UHPLC for high speed and high efficiency separations. Separations on 1.0 μm polybutadiene-encapsulated nonporous zirconia particles using aqueous-only mobile phases are described in the last section of this chapter.

III.2 Experimental

III.2.1 Elevated Temperature UHPLC

The UHPLC system[12] was previously described in detail (see Chapter II). Water-resistant, flexible heat tape (Watlow Heatcon, Seattle WA, USA) covered with insulation was used to provide the desired heat to the chromatographic system. Due to differences

in thermal conductivities and masses, the tubing between the pump and the injector, the ultrahigh pressure injector, and the column were heated separately. Heat tape was found to provide homogenous heating to the whole injection block. In addition, the original small diameter connecting tubing between the pump and injector was changed to a larger size (9/16" o.d.× 3/16" i.d.), which preheated a larger amount of mobile phase. Otherwise, flushing excess sample away during split injection could lead to significant loss of preheated mobile phase, which would cause a temperature change in the column, leading to band broadening and/or peak splitting. Each heat tape segment was connected to a temperature controller (Omega, Stamford, CT, USA), which thermostated the whole system to ± 0.2 °C at temperatures up to 150 °C. A linear restrictor (1 m × 30 μm i.d.) was attached to the end of the column to prevent bubble formation, especially at temperatures higher than the boiling points of water and acetonitrile.

III.2.2 Column Preparation

The high pressure packing system used to prepare columns for this study has been described previously.[48] Briefly, a Model DSF-150-C1 air-driven pneumatic amplifier pump (Haskel, Burbank, CA, USA) was used to drive packing solvent through the column. One end of a fused silica capillary was connected to a Valco 1/16" union (Valco, Houston, TX, USA) with a piece of PEEK tubing (Upchurch, Oak Harbor, WA, USA) and a stainless steel screen or frit (0.5 μm pore size) to retain the particles in the capillary, thus eliminating the need to make an initial frit. The other end of the capillary to be packed was connected to a modified Swagelok reducing union, which acted as the packing material reservoir and was connected to the Haskel pump via 1/8" o.d. tubing.

Slurries of silica particles were made by mixing nonporous particles in a 33% acetone/67% hexane solution. Then the slurry was transferred to the packing reservoir. Liquid carbon dioxide from a gas cylinder was used to drive the silica particle slurry into the capillary column. Both the column and the reservoir were placed in an ultrasonic bath (Branson Ultrasonic, Danbury, CT, USA) that was set at room temperature and turned on from the beginning until the column was completely filled. The initial pressure was generally 900 psi (60 atm). The pressure was increased gradually to maintain a constant packing rate until the column was completely filled. The final packing pressure generally ranged from 15 to 20 kpsi. The column was then left to depressurize overnight.

The frit-making process used here was similar to that of Boughtflower *et al.*[49] A Haskel pump (Lincoln, NE, USA) was used for column rinsing and conditioning. First, the packed capillary was wetted with acetonitrile/water (80:20 v/v) (1 h at 15,000 psi with column in ultrasonic bath) and then flushed with water using the same conditions. An outlet frit was formed a few centimeters from the end of the packed bed using a resistive heating device (InnovaTech, Hertfordshire, UK) while water was pumped through the column. The capillary was depressurized slowly over 10 min and then reversed. Excess packing material was removed from the capillary, and the bed was consolidated by pumping acetonitrile/water (80:20 v/v) overnight, and then water for 1 h. The inlet frit was then formed at a certain distance from the outlet frit. A window for on-column detection was created as close as possible to the outlet frit by burning off the polyimide coating using the same heating device.

Slurries of zirconia particles were made by mixing nonporous zirconia particles in a 50% chloroform/50% cyclohexanol solution. Then, the slurries were sonicated for

more than 1 h before being transferred to the packing reservoir. A syringe pump was used to fill the solvent reservoir of the pneumatic amplifier pump with isopropanol, which was subsequently driven with nitrogen gas pressure. The packing process for zirconia particles was the same as for silica particles. Since it was not possible to sinter the zirconia particles to make frits, 1.5 μm bare silica particles were introduced into the capillary for several centimeters both before and after packing with zirconia particles. Internal frits were made by sintering the silica particles at a distance of 3 mm from the beginning of the zirconia particle bed using a method similar to that described for the silica particle packed columns.

III.2.3 Materials and Chemicals

Nonporous zirconia particles (1.0 μm diameter) used in this study were supplied by Zirchrom Separations (Anoka, MN, USA). Scanning electron microscopy (JEOL 8401, JEOL, Peabody, MA, USA) was used to determine the polybutadiene-encapsulated zirconia particle size distribution. Particle size distributions of the final product were determined by images of hundreds of particles. The figures shown are representative of the entire sample collected. To verify that there were no internal pores, the microspheres were dispersed in epoxy resin (#8778, Cole-Parmer, Chicago, IL, USA), polished to expose the interior of some microspheres, sputter-coated with a 50 Å layer of platinum and then viewed by electron microscopy.

Octadecylsilane (C_{18}) and isohexylsilane-modified (C_6) nonporous silica particles (1.5 μm diameter, Kovasil MS-H) were purchased from Chemie Uetikon (Uetikon, Switzerland). These particles were chemically bonded with a short, branched alkylsilane, resulting in a rigid and sterically hindered stationary phase which was stable at low pH

and high temperature.[8,9] C_{18} bonded porous silica particles (1.5 μm diameter) were obtained from Alltech (Deerfield, IL, USA).

HPLC-grade acetonitrile, chloroform, and water were obtained from Fisher (Fair, Lawn, NJ, USA), and HPLC-grade hexane was purchased from EM Sciences (Gibbstown, NJ, USA). HPLC-grade isopropanol were purchased from Mallinckrodt (Phillipsburg, NJ, USA). Fused silica capillary tubing was purchased from Polymicro Technologies (Phoenix, AZ, USA). All buffers and solvents were filtered through Durapore® membrane filters (0.22 μm pores) (Millipore, Bedford, MA, USA) before use. Similarly, samples were filtered through polytetrafluoroethylene (PTFE) syringe filters (0.2 μm pores, Chromacol, Trumbull, CT, USA). Zeflor™ filter membranes with pore size of 3.0 μm were supplied by Gelman Science (Ann Arbor, MI, USA) and used to filter the particle slurry before packing.

III.3 Results and Discussion

III.3.1 Instrumental Considerations and Performance

In order to obtain high efficiency separations using elevated temperatures in LC, it is necessary to preheat the mobile phase to the column temperature to avoid unacceptable peak broadening. The chromatograms in Figure III.1 show the difference in performance of UHPLC with different temperature control designs. When only the column was heated to 60 °C (Figure III.1B), as compared to when the whole system was operated at room temperature (Figure III.1A), the separation time decreased. When the injector and connecting tubing were also heated to 60 °C (Figure III.1C), the separation time decreased even further and the separation efficiency greatly improved. This design

was further evaluated by measuring the repeatability of retention and efficiency of parabens at elevated temperature. The RSD values for retention time and plate number for parabens at 80 °C range from 0.2-0.4% and 1.2-4.3%, respectively. These results confirm the claim of others that the incoming mobile phase must be heated to avoid problems of peak distortion and retention-time changes.[27-29] In addition to heating the column and injector, we changed the original small diameter connecting tubing between the pump and injector to a larger one (9/16" o.d. × 3/16" i.d.), which preheated a larger amount of mobile phase. With a narrow-bore column and this heating strategy, radial temperature effects were minimized.

III.3.2 Effect of Temperature on Separation

Effect of temperature on mobile phase linear velocity. Figure III.2 shows the relationship between column inlet pressure and mobile phase linear velocity at different temperatures for 1.0 μm PBD-coated particles. The average linear velocity at 80 °C is approximately 2.6 times higher than that at room temperature when the same inlet pressure is used. As expected, elevated column temperature decreases the pressure drop by decreasing the mobile phase viscosity as predicted in equation I.13. Therefore, faster separation should be possible using elevated temperature. It should be noted that linear velocity and not pressure itself is the actual parameter that affects chromatographic performance. For convenience, however, since the outlet of the column is always at atmospheric pressure and the pressure is easier to measure than the linear velocity, pressure is used in this study to indicate a relative increase or decrease in velocity.

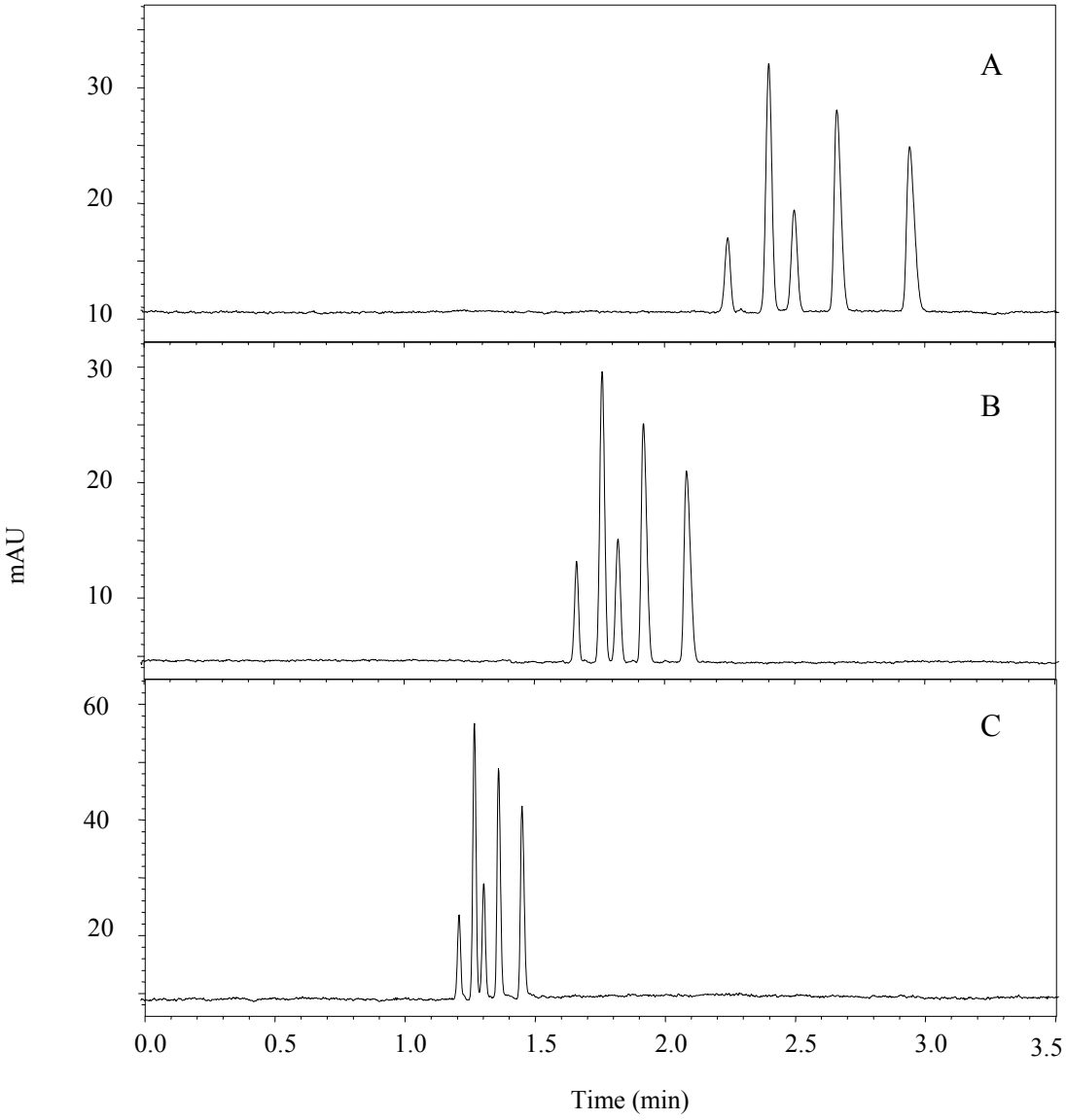

Figure III. 1. Effect of heating strategy on performance in UHPLC. Conditions: 15 kpsi inlet pressure; 15 cm × 50 μm i.d. fused silica capillary column packed with 1.0 μm Kovasil MS-H nonporous particles; water (20 mM NH_4Ac, pH = 3.5)/acetonitrile (65:35, *v*/*v*); 215 nm UV detection; uracil as marker; parabens as test solutes; (A) column at 22 °C; (B) column at 60 °C; (C) column and injector at 60 °C.

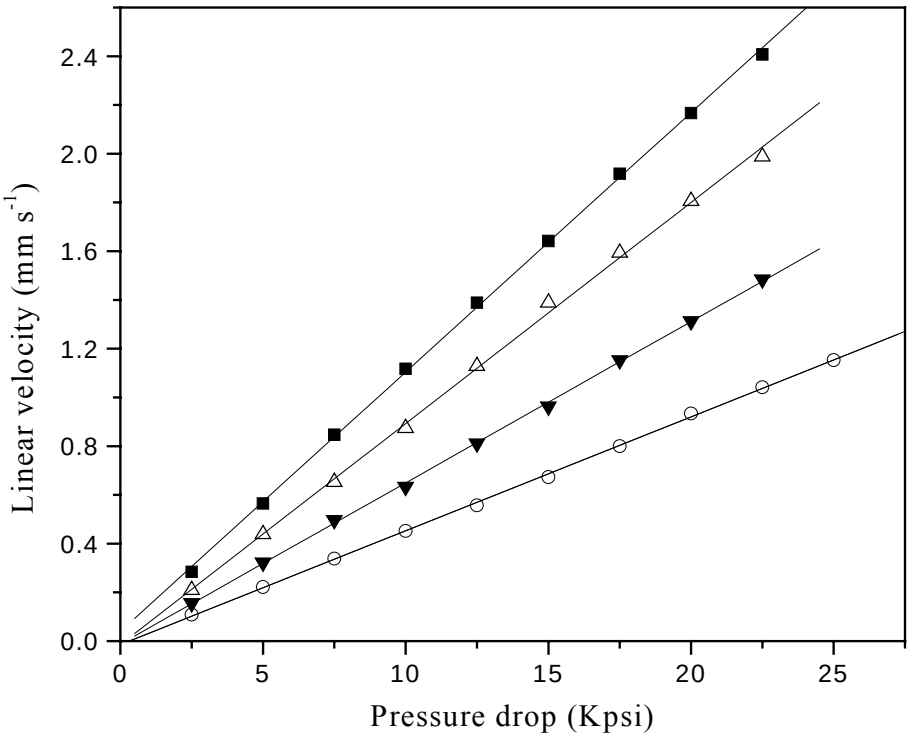

Figure III. 2. Effect of temperature on pressure drop and linear velocity. Conditions: 13 cm × 50 μm i.d. fused silica capillary column packed with 1.0 μm PBD-encapsulated nonporous zirconia particles; water (40 mM NaH_2PO_4, pH = 7.0)/acetonitrile (65:35, *v*/*v*); 215-nm UV detection; uracil as marker; parabens as test solutes. (○) 22 °C; (▼) 40 °C; (△) 60 °C; (■) 80 °C.

Effect of temperature on column efficiency. The van Deemter equation can be used to evaluate column efficiency at different temperatures

$$H = A + \frac{B}{u} + Cu \qquad \text{III. 1}$$

where

$$A = 2\lambda d_p \qquad \text{III. 2}$$

$$B = 2\gamma D_m \qquad \text{III. 3}$$

$$C = \frac{2kd_f^2 u}{3D_s(1+k)^2} + \frac{\chi(1+6k+11k^2)d_p^2 u}{24(1+k)^2 D_m} + \frac{(1-\phi^{'}+k)^2 d_p^2 u}{30(1-\phi^{'})(1+k)^2 \gamma D_m} \qquad \text{III. 4}$$

and where λ is the packing constant, d_p is the mean particle diameter of the packing, γ is the tortuosity constant due to the packing, k is the retention factor, d_f is the mean stationary phase film thickness, χ is a geometric factor, $\phi^{'}$ is the fraction of the total mobile phase in the pores, D_m is the diffusion coefficient of the solute in the mobile phase and D_s is the diffusion coefficient of the solute in the stationary phase.

Theoretically, the effect of temperature on the *A* term is uncertain. The *B* term, representing longitudinal diffusion, increases with increasing temperature, but only becomes significant at low linear velocities. The *C* term, which represents adsorption/desorption kinetics and mass transport between phases, decreases with increasing temperature. Therefore, efficiencies at linear velocities greater than the optimum are better at higher than at room temperature.

The dependence of plate height (*H*) on interstitial linear velocity (μ_e) at different temperatures was plotted as shown in Figure III.3. The actual data, represented by markers, were fitted using the van Deemter equation. Efficiencies as high as 350,000

plates m^{-1} were obtained at the optimum linear velocities at different temperatures. As expected, efficiencies at linear velocities > 1.0 mm s^{-1} were better at elevated temperatures than at room temperature. Temperature effects on the *A*, *B*, and *C* terms were investigated and the results are listed in Table III.1. It can be seen that the *B* term increases with increasing temperature, which is mainly due to an increase in D_m at elevated temperature. Compared to room temperature, the *C* term at 40, 60 and 80 °C decreases as expected and is much smaller at 80 °C than at room temperature. As described in equation III.4, both changes in *k* and D_m at elevated temperatures could have an effect on the *C* term. Generally, an increase in the diffusion coefficient of the solute in the mobile phase is the main reason for the decrease in the *C* term, which helps to produce faster and higher efficiency separations.

Lower efficiencies were obtained in this study than we typically obtain in capillary LC, especially when using 1 μm silica particles in UHPLC. The reasons for this are: (a) coated zirconia particles are known to provide lower efficiencies than bonded silica particles, (b) efficient packing of zirconia particles is challenging due to their tendency to agglomerate, and (c) higher than optimum linear velocities were used.

Effect of temperature on retention factor. The effect of temperature on retention factor, *k*, can be described using the van't Hoff equation

$$\ln k = -\frac{\Delta H}{RT} + \frac{\Delta S^o}{R} + \ln \phi \qquad \text{III. 5}$$

where ΔH and ΔS^o are the enthalpy and entropy of transfer from the stationary phase to the mobile phase, respectively, and ϕ is the phase ratio of the column. The dependence of

Table III. 1. Effect of temperature on the *A*, *B*, and *C* terms in the van Deemter equation.

T (°C)	A (μm)	B (10^3 μm s^{-1})	C (10^3 s^{-1})
22	2.32	0.22	0.70
40	2.30	0.36	0.61
60	2.28	0.44	0.55
80	2.27	0.63	0.36

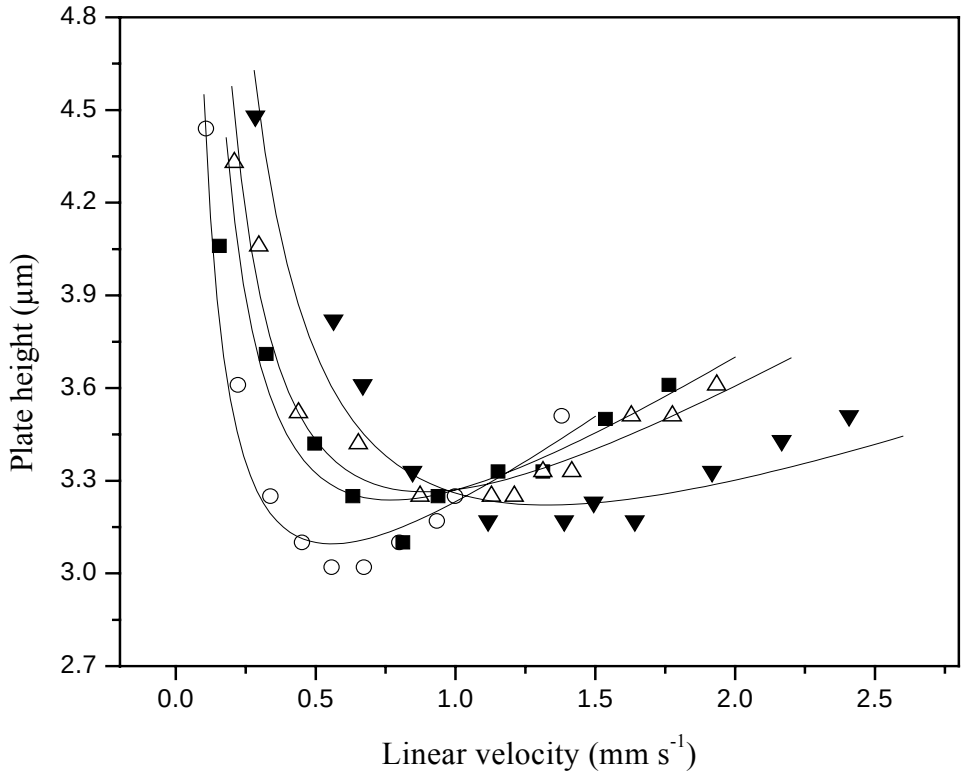

Figure III. 3. Van Deemter curves for different temperatures. Conditions are the same as in Figure III.1. Lines represent fitted van Deemter curves. (○) 22 °C; (▼) 40 °C; (△) 60 °C; (■) 80 °C.

retention factor on temperature for four parabens over the temperature range of 22 to 80 °C was observed. The analytes eluted with good peak shapes at each temperature tested. Linear relationships for *ln k* vs. *1/T* were obtained with correlation coefficients greater than 0.98 for each compound. The enthalpy values are consistent with typical enthalpy interactions in reversed phase systems.[23]

Changes in selectivity with temperature can be caused by either enthalpy or entropy changes. The latter is usually brought about by shape related changes in the stationary phase. In this study, no major changes in selectivity were observed as the temperature was varied, presumably because the sample studied was a homologous series.

Figure III.4 shows separations of four parabens at different temperatures. All separations were conducted at constant pressure. With an increase in temperature, the linear velocities (flow rates) were increased due to a decrease in mobile phase viscosity (dead time decreased from 3.68 min to 1.62 min); at the same time, solute retention also decreased due to an increase in speed of adsorption/desorption (retention factor decreased from 0.54 to 0.25). Therefore, there was an approximate 3-fold reduction in the analysis time (from 6 min at 25 °C to about 2 min at 80 °C). Even though there was a significant decrease in analysis time, the overall quality of the separation is still quite acceptable.

III.3.3 Effect of Pressure on Separations

The dependency of retention factor on pressure was investigated as shown in Figure III.5. Slight increases in retention factors with an increase in inlet pressure were observed. Similar observations were reported for silica packed columns.[10,15-16]

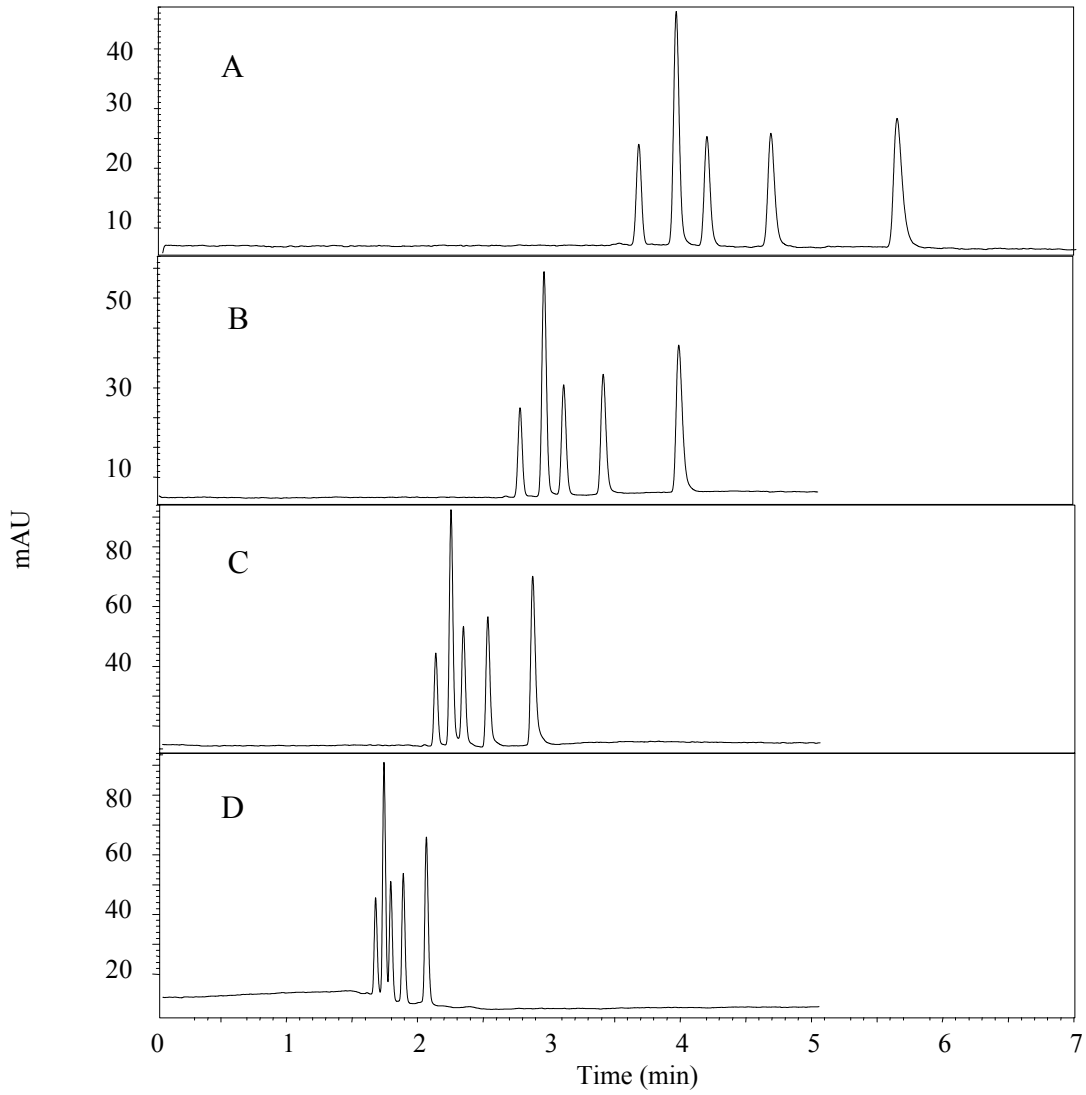

Figure III. 4. Effect of temperature on the separation of parabens. Conditions: (A) 25 °C; 15,000 psi inlet pressure; 15 cm × 50 μm i.d. fused silica capillary column packed with 1.0 μm PBD-encapsulated nonporous zirconia particles; water (40 mM NaH_2PO_4, pH = 7.0)/acetonitrile (60:40, *v*/*v*); other conditions are the same as Figure III.1; (B) 40 °C; (C) 55 °C; (D) 80 °C; other conditions are the same as in (A).

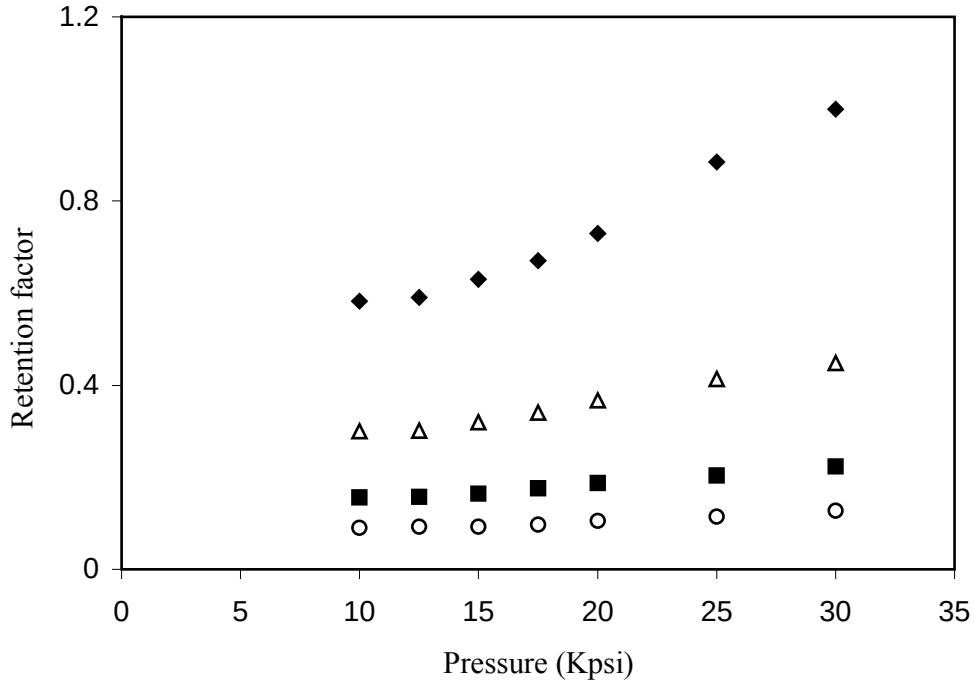

Figure III. 5. Effect of pressure on retention factor. Conditions: 15 cm × 50 μm i.d. fused silica capillary column packed with 1.0 μm PBD-encapsulated nonporous zirconia particles; water (40 mM NaH_2PO_4, pH = 7.0)/acetonitrile (65:35, *v*/*v*); 215 nm UV detection; uracil as marker. Peak identifications: (○) methyl paraben, (■) ethyl paraben, (△) propyl paraben, (♦) butyl paraben.

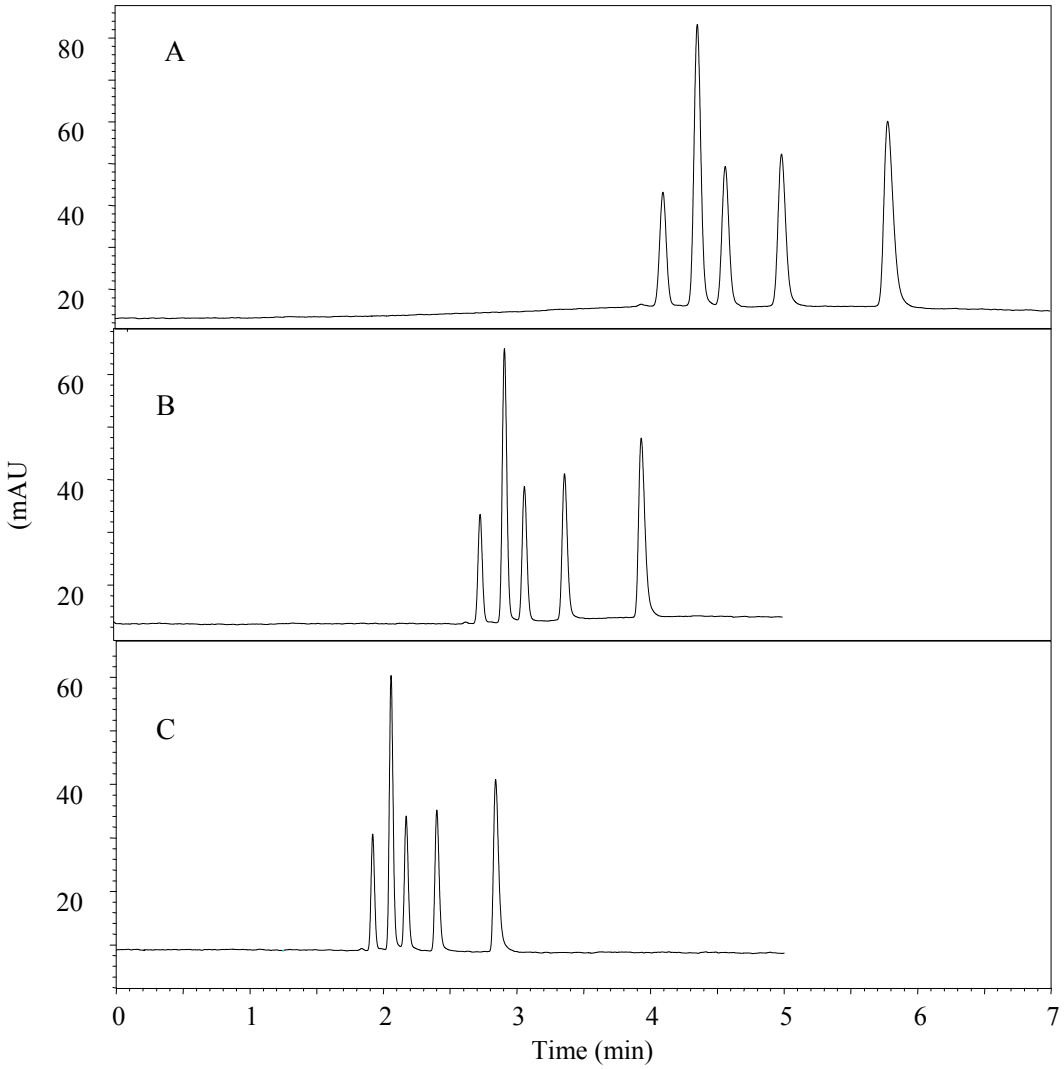

Figure III. 6. Effect of pressure on the separation of parabens. Conditions: (A) 40 °C; 10,000 psi inlet pressure; other conditions are the same as in Figure III.4; (B) 15,000 psi; and (C) 20,000 psi; other conditions are the same as in (A).

Figure III.6 shows separations of four parabens at different pressures. When the pressure increased from 10 kpsi to 20 kpsi, the analysis time was reduced from 5.8 to 2.8 min, or approximately 2-fold. However, resolution values for peaks 2 and 3 were 2.18 and 2.08 at 10 and 20 kpsi, respectively, indicating no significant loss in resolution. This may be due to two reasons. First, the van Deemter curve for the small particle packed column tends to be relatively flat, which means there is little loss in efficiency with an increase in pressure.[10,13,16] Second, retention factors of solutes increase with an increase in pressure.[10,16]

III.3.4 Combined Effects of Pressure and Temperature on Separation

A test mixture of four parabens was used to investigate the combined effects of pressure and temperature on separation. The mobile phase linear velocity in a packed column can be obtained by rearranging equation I.12

$$u = \Delta P d_p^2 / \phi L \eta \qquad \text{III. 6}$$

It can be seen that the linear velocity is directly proportional to the pressure applied.

For temperatures ranging from the freezing point to near the normal boiling point, the relationship between viscosity and temperature can be expressed by[31]

$$\ln \eta = a + b / T \qquad \text{III. 7}$$

where a and b are empirically determined constants, and T is the temperature. Substituting equation III.7 into equation III.6 gives

$$u = \Delta P d_p^2 / \phi L e^{a+b/T} \qquad \text{III. 8}$$

Thus, an increase in column operating temperature results in a decrease in the mobile phase viscosity, finally leading to an increase in linear velocity. In this study, it was found that the linear velocity was approximately proportional to the temperature (in °C) in the range of 22 °C to 77 °C.

Generally, for high speed separations, high linear velocities are used, which can be achieved by increasing the pressure, elevating the column temperature, or both simultaneously. Separation time (i.e., retention time for the most retained compound) is obviously affected by temperature and pressure. For example, at 55 °C and 13 kpsi, the separation time (Figure III.7C) was approximately 1.42 min, 2.2-fold faster than when using 22 °C and 10 kpsi (Figure III.7A). At 22 °C and 25 kpsi (Figure III.7B), the separation time was 1.72 min, an approximately 1.8-fold reduction (compared to Figure III.7A). For the separations in Figures III.7B and III.7C, the same linear velocities were used. The shorter separation time in Figure III.C is due to less retention of the solutes at elevated temperature as described by equation III.5. Also, higher efficiencies were obtained at elevated temperature. The average plate numbers for 4 parabens in Figures III.7B and III.7C were 42,000 and 45,000, respectively.

In LC, the resolution is affected by selectivity, α, retention factor, k, and plate number, N, as given by

$$R_s = 0.25N^{0.5}(\alpha - 1)[k/(k+1)] \qquad \text{III. 9}$$

Both temperature and pressure influence α, k and N (see Table III.2). When the pressure was increased from 10 to 25 kpsi, slight increases in $k/(k+1)$ and $(\alpha-1)$ were observed, however, there was an approximate 20% loss in average separation efficiency. Comparatively, when the temperature was elevated from 22 to 55 °C, there was no

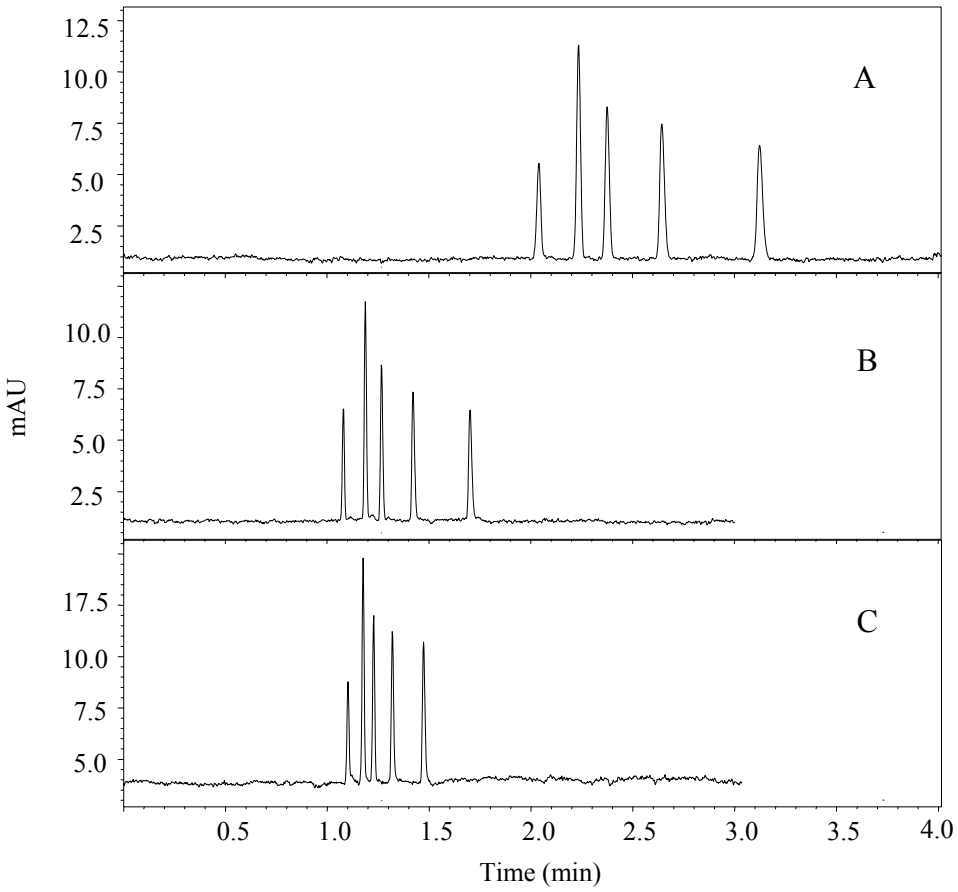

Figure III. 7. Effect of temperature and pressure in UHPLC of parabens. Conditions: 15 cm × 50 μm i.d. fused silica capillary column packed with 1.0 μm Kovasil MS-H nonporous particles; water (20 mM NH_4Ac, pH = 3.5)/acetonitrile (65:35, *v*/*v*); 215 nm UV detection; uracil as marker; parabens as test solutes; (A) 10 kpsi inlet pressure, 22 °C; (B) 25 kpsi inlet pressure, 22 °C; (C) 13 kpsi inlet pressure, 55 °C.

Table III. 2. Effects of pressure and temperature on resolution of parabens in UHPLC.[a,b]

Compound	10 Kpsi, 22 °C			25 Kpsi, 22 °C			10 Kpsi, 55 °C		
	k/(k+1)	α-1	N (plates)	k/(k+1)	α-1	N (plates)	k/(k+1)	α-1	N (plates)
Methyl paraben	0.086		57,000	0.088		46,000	0.068		50,000
Ethyl paraben	0.14	0.73	55,000	0.15	0.80	46,000	0.11	0.70	50,000
Propyl paraben	0.22	0.78	55,000	0.24	0.83	44,000	0.17	0.71	54,000
Butyl paraben	0.34	0.78	51,000	0.37	0.82	47,000	0.26	0.69	57,000

[a]Conditions: 15 cm × 50 μm i.d. fused silica capillary column packed with 1.0 μm nonporous Kovasil MS-H particles; water (20 mM NH_4Ac, pH = 3.5)/acetonitrile (65:35, v/v); 215 nm UV detection; uracil as marker.

[b]n = 3

significant reduction in separation efficiency. Even for the most retained compound, butylparaben, an increment in efficiency was observed, mainly due to an improvement in peak shape at elevated temperature. However, reductions in $k/(k+1)$ and $(\alpha-1)$ were experienced with an increase in temperature. Reductions in $k/(k+1)$ for the first and last eluting peaks were 32% and 34%, respectively. At the same time, losses in $(\alpha-1)$ were 4% and 13% for these two peaks. Temperature significantly affects retention and selectivity, while pressure mainly affects efficiency.

III.3.5 Fast Separations on Nonporous Silica Particles Using Elevated Temperature UHPLC

A test mixture of 7 barbitals was used to illustrate the effects of combining ultrahigh pressure and elevated temperature for fast and high efficiency separations. At room temperature and 10 kpsi, the separation was completed in approximately 6.5 min (Figure III.8A). When the temperature was increased to 80 °C, the separation time was shortened to 1.8 min (Figure III.8B). Finally, by increasing the pressure from 10 kpsi to 35 kpsi, only 33 s were required for separation (Figure III.8C). Even though there was an approximate 12-fold decrease in analysis time, the overall quality of the separation was still good. All of the peaks were baseline resolved, except for peaks 5 and 6, which had a resolution of 1.32. The average plate number for all seven peaks was approximately 200,000 plates m^{-1} for the 30-s separation in Figure III.8C. In addition, the detector response at 80 °C (Figures III.8C) was significantly improved (approximately 2-fold) relative to that at 22 °C (Figures III.8A and III.8B). This was due to the narrow peaks that were obtained.

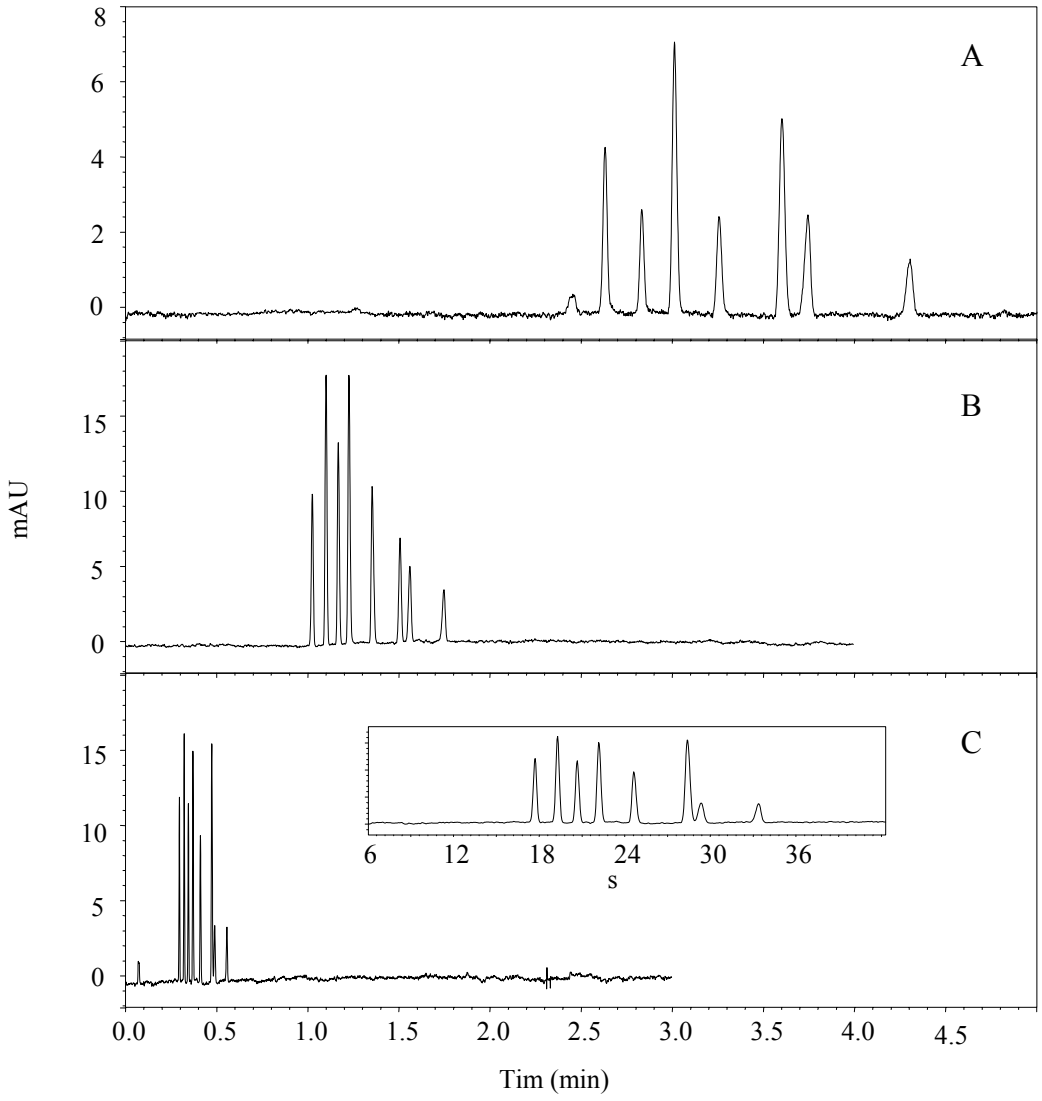

Figure III. 8. Effect of temperature and pressure in UHPLC of barbitals. Conditions: 15 cm × 50 μm i.d. fused silica capillary column packed with 1.0 μm Kovasil MS-H nonporous particles; water (20 mM NH_4Ac, pH = 3.5)/acetonitrile (80:20, *v*/*v*); 215 nm UV detection; uracil as marker; (A) 10 kpsi inlet pressure, 22 °C; (B) 10 kpsi inlet pressure, 80 °C; (C) 35 kpsi inlet pressure, 80 °C.

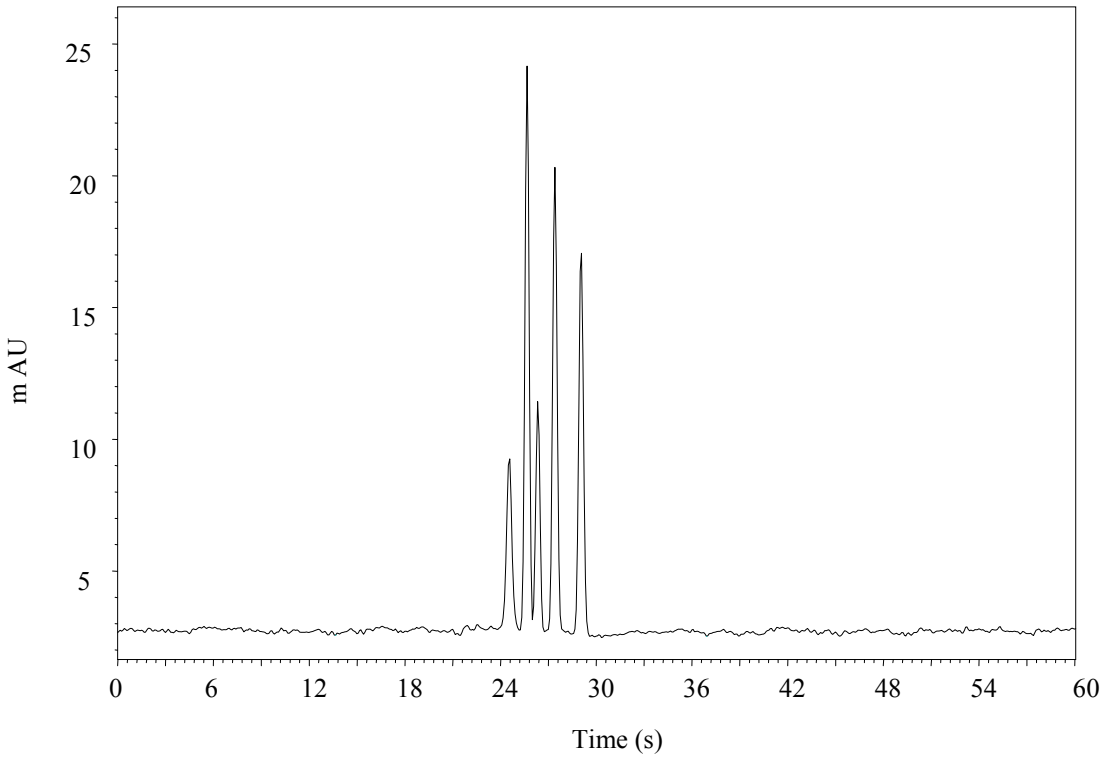

Figure III. 9. Fast UHPLC of parabens. Conditions: 30 kpsi inlet pressure, 80 °C; water (20 mM NH_4Ac, pH = 3.5)/acetonitrile (60:40, *v*/*v*); other conditions are the same as in Figure III.7.

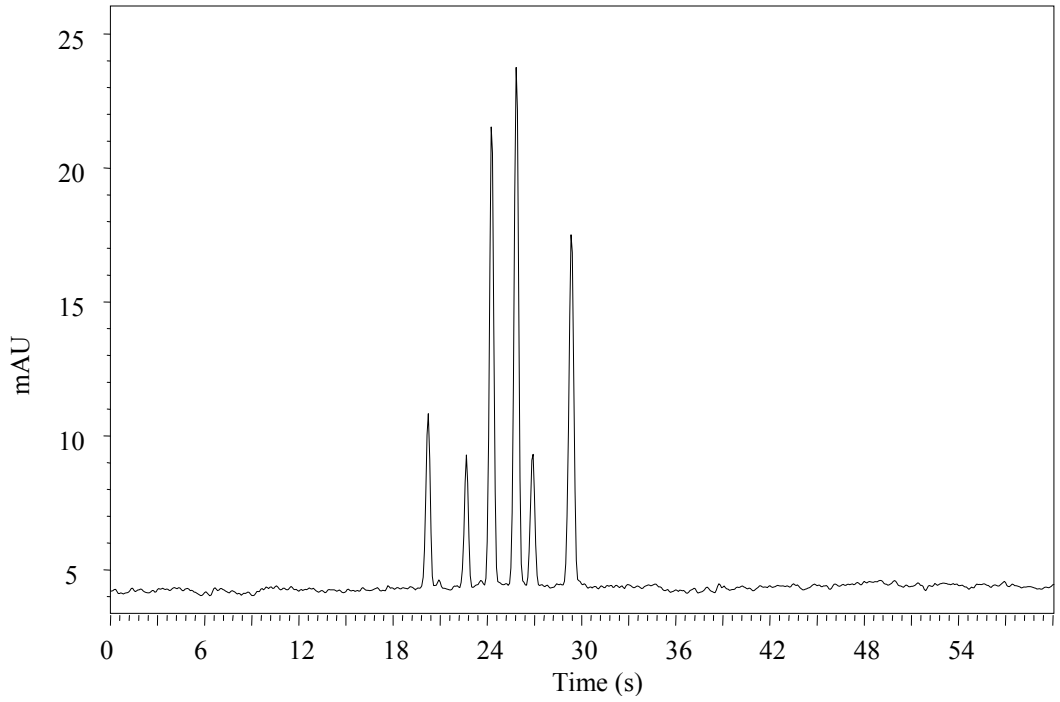

Figure III. 10. Fast UHPLC of herbicides. Conditions: 30 kpsi inlet pressure, 80 °C; water (20 mM NH_4Ac, pH = 3.5)/acetonitrile (65:35, *v*/*v*); other conditions are the same as in Figure III.7.

Figure III.9 demonstrates a very fast separation of parabens. Compared to Figure III.1A, the separation time decreased from 3 min to 30 s, an approximate 6-fold reduction. This separation was obtained at 80 °C and 30 kpsi. Peaks 1 and 2 overlap slightly, however, the other peaks are resolved. In Figure III.10, a separation of 5 herbicides was completed in 30 s by combining both ultrahigh pressure and elevated temperature. In this separation, all peaks were resolved. The efficiency for the last eluting solute was approximately 33,000 plates.

III.3.6 Fast Separations on Polybutadiene-encapsulated Nonporous Zirconia Particles Using Elevated Temperature UHPLC

Characterization of 1 μm polybutadiene-encapsulated nonporous zirconia particles. The best chromatographic efficiencies are obtained with well packed columns, which significantly depend on particle uniformity.[50] Figure III.11A shows a scanning electron micrograph of a representative batch of nonporous zirconia particles prepared in this study. Nitrogen adsorption, confocal fluorescence microscopy and fluoride desorption uptake measurements demonstrated that the synthesized particles were nonporous.[42] The particle size distribution for this batch of particles is given in Figure III.11B. It can be seen that these particles were nonaggregated and spherical. The mean diameter was 1.14 μm and the standard deviation was 0.22 μm.

The dependence of plate height (H) on mobile phase linear velocity (u) was plotted as shown in Figure III.12. The data were fit to the van Deemter equation as shown by the solid line. The minimum plate height (approximately 3.5 μm) was obtained at a linear velocity of 0.5 mm s^{-1}. Previous work using well-packed columns containing 1.5 μm nonporous silica showed little change in column performance with increase in

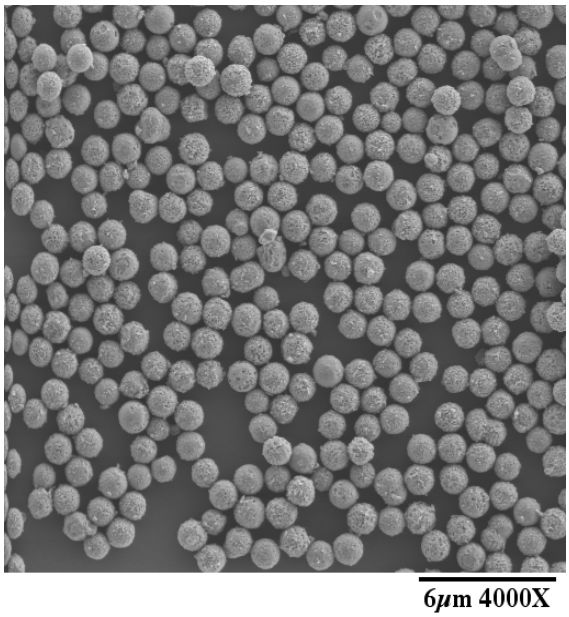

(A)

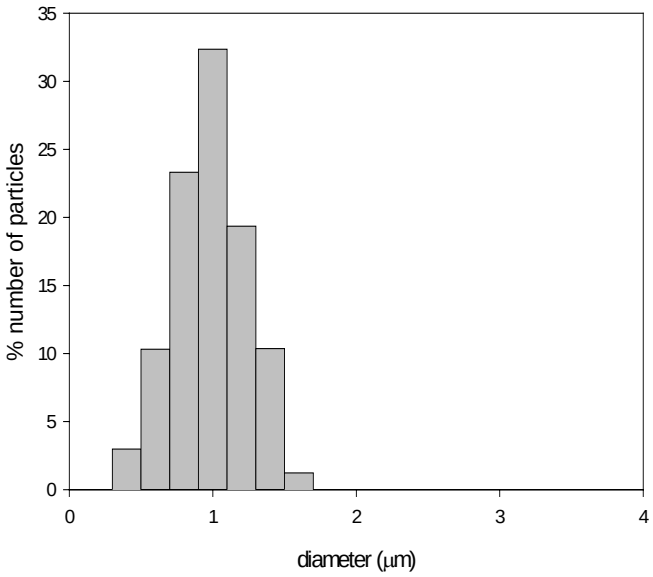

(B)

Figure III. 11. (A) Scanning electron micrograph of zirconia microspheres. (B) Size distribution of the sample shown in (A) determined by analysis of 356 particles.

flow rate.[10,11,13,14] As is seen in Figure III.12, the van Deemter curve obtained using the zirconia column was also relatively flat at linear velocities much higher than u_{opt}. However, the efficiencies obtained using the zirconia packed columns are not as good as those obtained with silica packed columns, probably due to less favorable mass transfer characteristics of polymer-encapsulated particles compared to typical C_{18} bonded phases.

Comparison of polybutadiene-encapsulated zirconia with C_{18} bonded silica. In reversed phase LC over a reasonable range in mobile phase composition, the logarithm of retention factor (k) is linearly proportional to the number of methylene groups in a homologous series of analyte molecules.[34] Four paraben standards were used to investigate the reversed phase nature of the polybutadiene-encapsulated zirconia particles, and a good linear relationship between $ln\ k$ and n_{CH2} was found. It was also found that as organic modifier content in the mobile phase decreased, the retention of parabens on the encapsulated zirconia decreased as is generally observed for conventional ODS bonded phases. These results verify (as expected) that polybutadiene-encapsulated zirconia behaves similarly to an ODS bonded reversed phase.

Figure III.13 shows chromatograms of barbitals using C_{18} bonded nonporous silica particles (Figure III.13A) and polybutadiene-encapsulated nonporous zirconia particles (Figure III.13B). It can be seen that most barbital standards are resolved on both stationary phases, and solute elution orders are the same, indicating a similar retention mechanism in both separations. The average efficiency for the zirconia particles is more than 200,000 plates m^{-1}, which is comparable to that obtained using C_{18} bonded particles (i.e., 210,000 plates m^{-1}). However, k values for the zirconia column were lower than those for the C_{18} bonded silica, except for the first peak. This could be due to differences

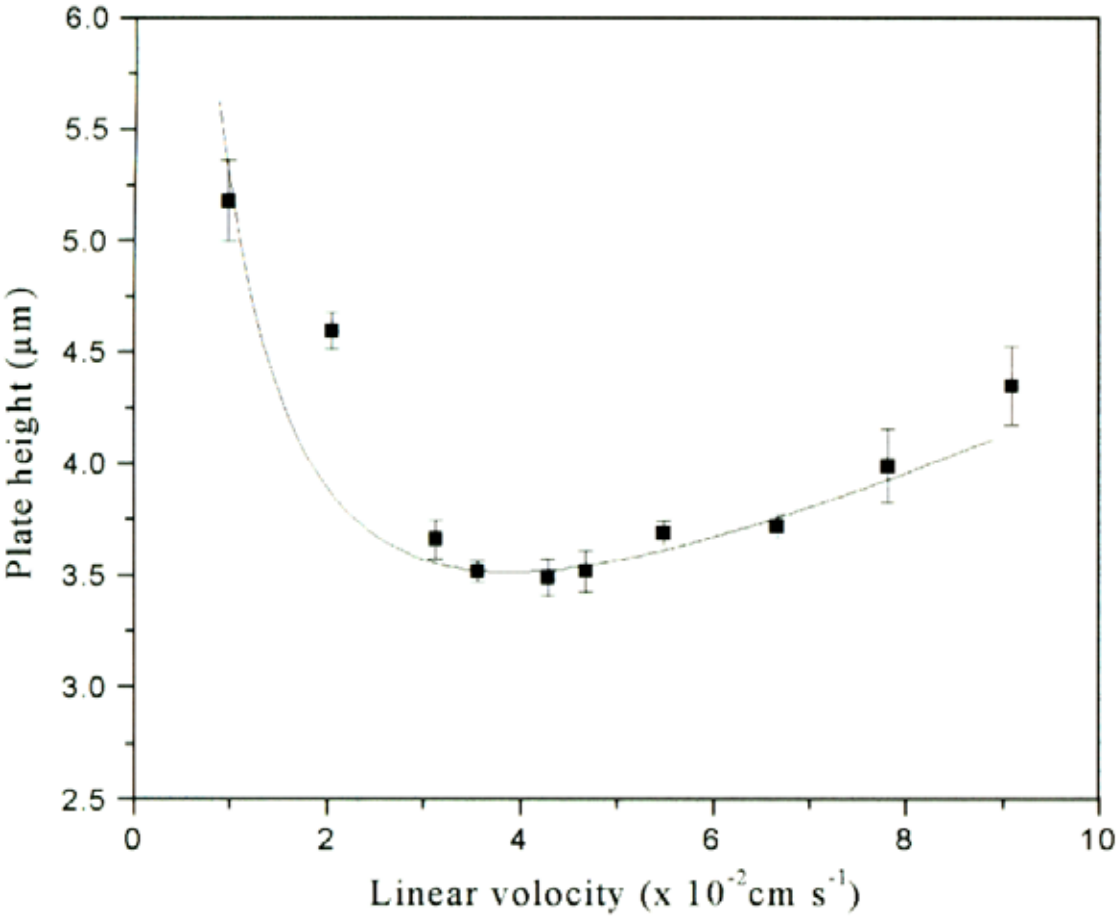

Figure III. 12. UHPLC van Deemter plot for ascorbic acid. Conditions: 15 cm × 50 μm i.d. fused silica capillary columns packed with 1.0 μm PBD-encapsulated nonporous zirconia particles; water (40 mM NaH_2PO_4, pH = 7.0)/acetonitrile (80:20, *v*/*v*); 254 nm UV detection, three columns were evaluated.

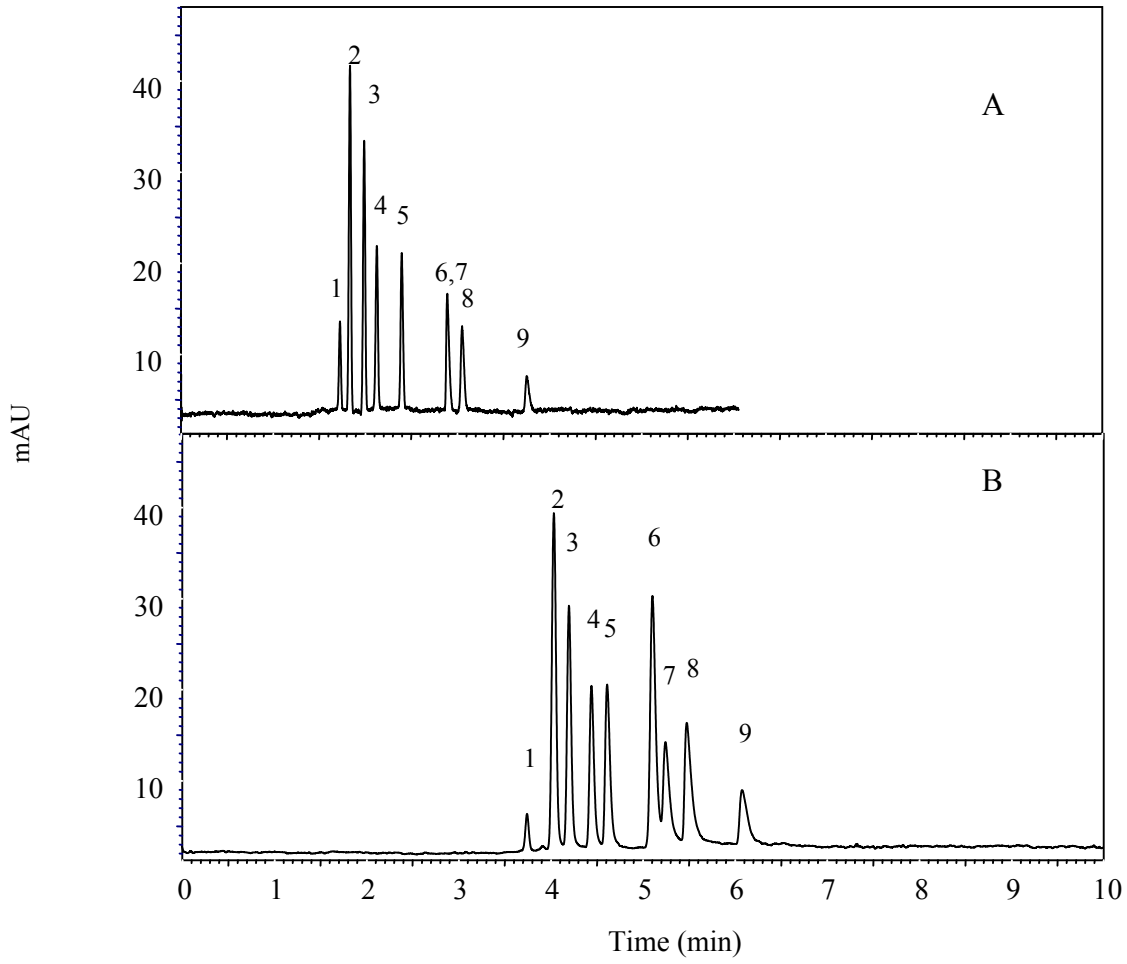

Figure III. 13. UHPLC chromatograms of barbitals. Conditions: (A) 22 °C; 15,000 psi inlet pressure; 16 cm × 50 μm i.d. fused silica capillary column packed with 1.0 μm Kovasil C_{18} bonded nonporous particles; water (40 mM NaH_2PO_4, pH = 7.0)/acetonitrile (80:20, *v*/*v*); 220-nm UV detection; uracil as marker. (B) 16 cm × 50 μm i.d. fused silica capillary column packed with 1.0 μm PBD-encapsulated nonporous zirconia particles; water (40 mM NaH_2PO_4, pH = 7.0)/acetonitrile (75:25, *v*/*v*); other conditions are the same as in (A). Peak identifications: (1) uracil, (2) allobarbital, (3) barbital, (4) phenobarbital, (5) butalbital, (6) hexabarbital, (7) amobarbital, (8) pentobarbital, (9) secobarbital.

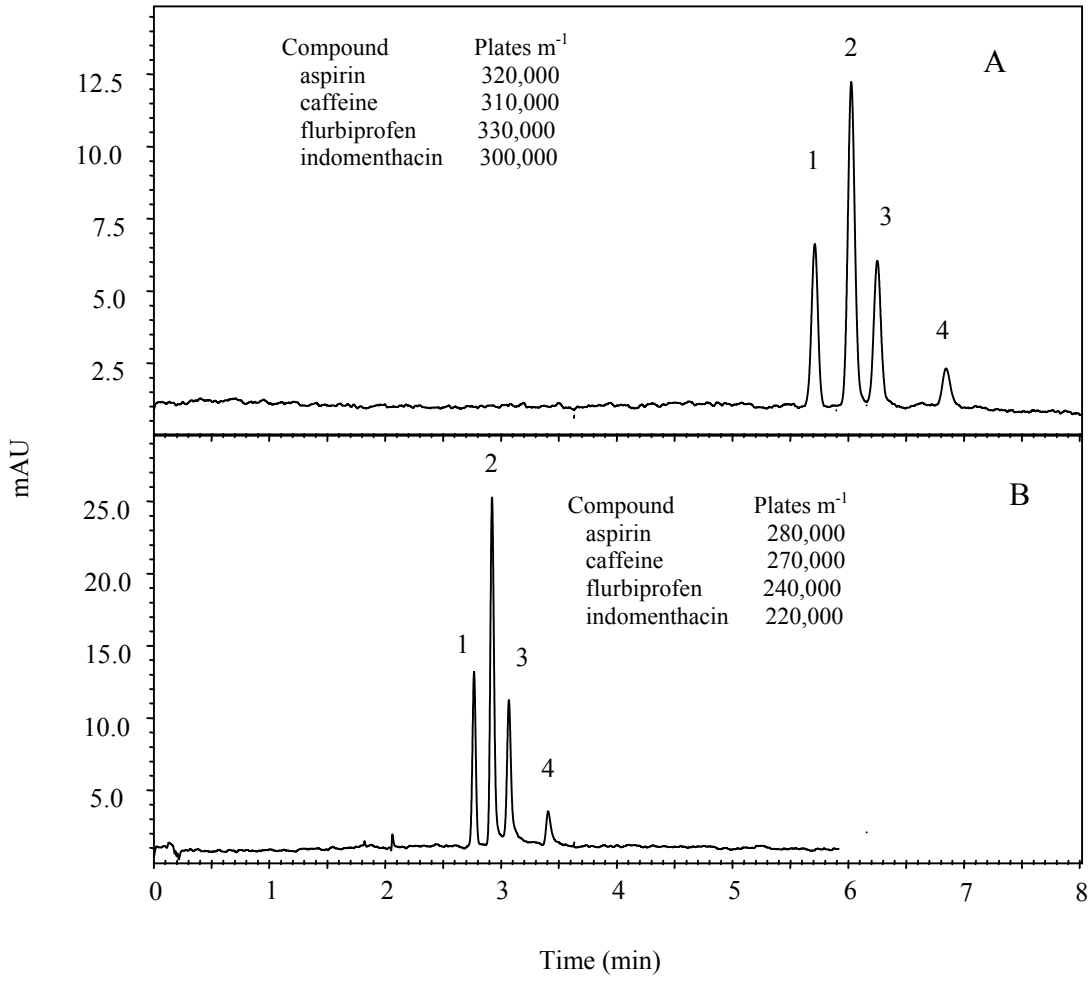

Figure III. 14. UHPLC chromatogram showing the effect of pressure on separation of anti-inflammatory drugs. Conditions: (A) 10,000 psi inlet pressure; 15 cm × 50 μm i.d. capillary column packed with 1 μm PBD-encapsulated nonporous zirconia particles; water (40 mM NaH_2PO_4, pH = 7.0)/acetonitrile (80:20, *v*/*v*); 215 nm UV detection; uracil as marker. (B) 20,000 psi inlet pressure; other conditions are the same as in (A). Peak identifications: (1) aspirin, (2) caffeine, (3) flurbiprofen, (4) indomenthacin.

in either partition coefficients or phase ratios, or both.[34] Peaks 6 and 7 are not resolved on the C_{18} bonded silica column, even with less organic modifier. This pair of peaks is resolved using the zirconia column with resolution of 1.2.

Figure III.14 shows separations of 4 anti-inflammatory drugs using inlet pressures of 10 and 20 kpsi. The separation time was reduced in half when the pressure was raised from 10 to 20 kpsi. The average efficiency at 20 kpsi was 250,000 plates m^{-1}, which represents a 21% loss compared to the average efficiency obtained at 10 kpsi. However, all of the drug compounds were still baseline resolved at 20 kpsi. The resolution values for peaks 2 and 3 were 2.01 and 2.34 at pressures of 10 and 20 kpsi, respectively. The increase in resolution is mainly due to an increase in retention factor with increase in pressure as shown in Figure III.5.

Fast separations on nonporous zirconia particles using elevated temperature UHPLC. Temperature plays a significant role in all chromatographic techniques. The use of elevated temperature in LC has been advocated primarily as a means of decreasing the back pressure of the column, shortening the separation time and increasing the column efficiency.[23] It has been demonstrated that encapsulated zirconia particles are stable at a temperature of 100 °C for over 7000 column volumes.[34] The exceptional thermal stability of zirconia allows the use of elevated temperature UHPLC for fast separations. Figure III.15B shows the separation 8 polycyclic aromatic hydrocarbons at a temperature of 100 °C using a pressure of 20 kpsi. Compared to Figure III.15A, the separation time was reduced from 25 min to 2.7 min, an approximate 10-fold reduction. The overall quality of the resolution at elevated temperature and ultrahigh pressure is still quite acceptable, and peak shapes are improved significantly at elevated temperature.

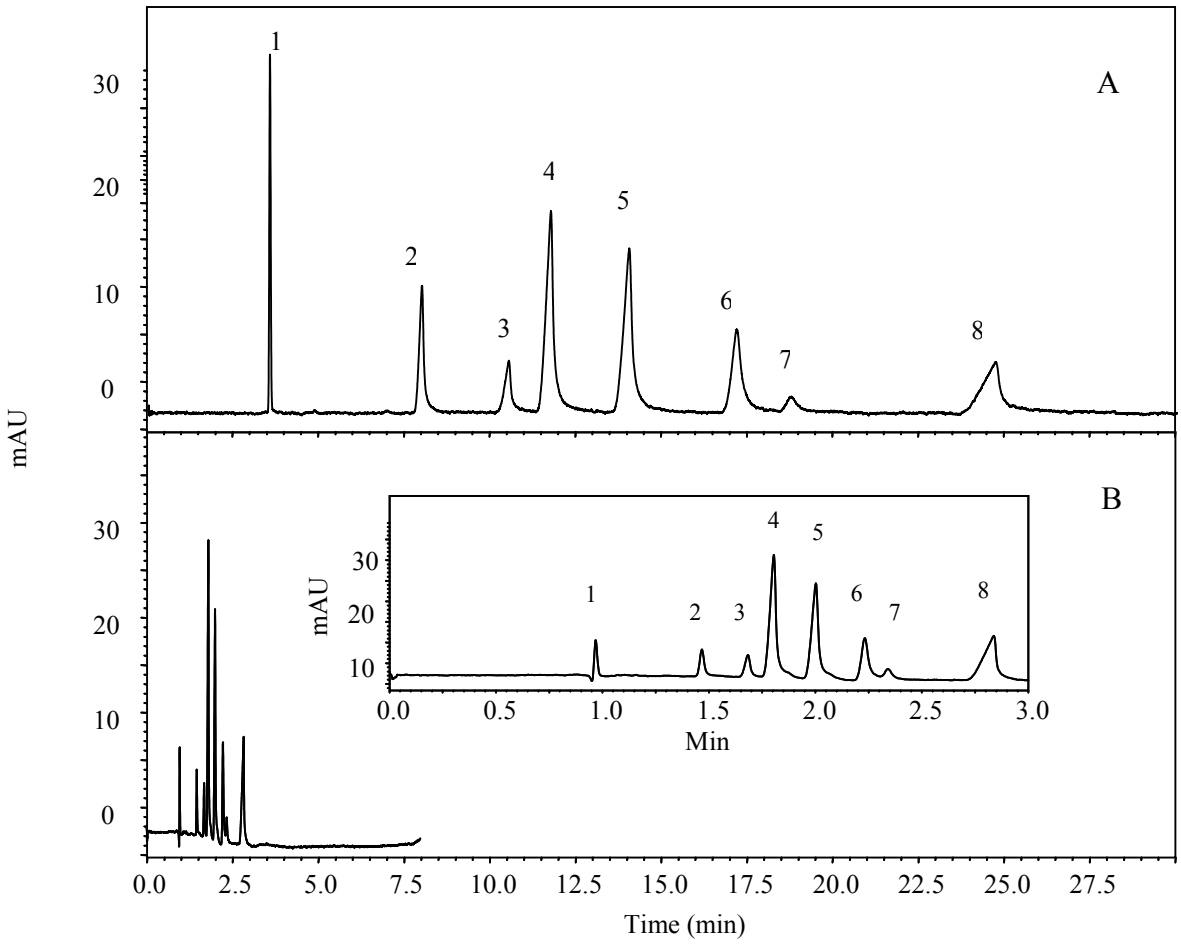

Figure III. 15. UHPLC chromatograms of polycyclic aromatic hydrocarbons. Conditions: (A) 22 °C; 15,000 psi inlet pressure; 14.5 cm × 50 μm i.d. fused silica capillary column packed with 1.0 μm PBD-encapsulated nonporous zirconia particles; water (40 mM NaH_2PO_4, pH = 7.0)/acetonitrile (55:45, *v*/*v*); 254 nm UV detection. (B) 100 °C; 20,000 psi inlet pressure; 14.5 cm × 50 μm i.d. fused silica capillary column packed with 1.0 μm polybutadiene-encapsulated nonporous zirconia particles; water (40 mM NaH_2PO_4, pH = 7.0)/acetonitrile (58:42, *v*/*v*); other conditions are the same as in (A). Peak identifications: (1) uracil, (2) naphthalene, (3) acenaphthylene, (4) biphenyl, (5) fluorine, (6) phenanthrene, (7) anthracene, (8) fluoranthene.

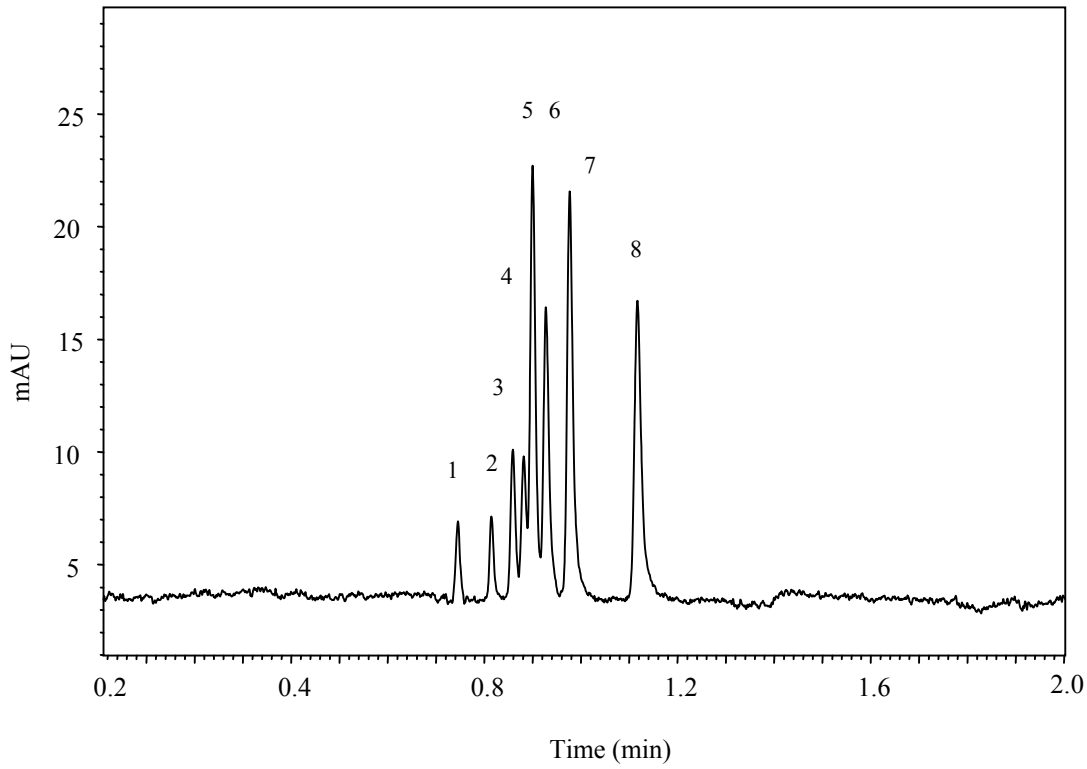

Figure III. 16. UHPLC chromatogram of benzodiazepines. Conditions: 100 °C; 22,000 psi inlet pressure; 14.5 cm × 50 μm i.d. fused silica capillary column packed with 1.0 μm PBD-encapsulated nonporous zirconia particles; water (40 mM NaH_2PO_4, pH = 7.0)/acetonitrile (68:22, *v*/*v*); 215 nm UV detection. Peak identifications: (1) uracil, (2) clorazepate, (3) flunitrozepam, (4) clonazepam, (5) chlordiazepoxide, (6) oxazepam, (7) clorazepate, (8) diazepam.

Separation of 6 benzodiazepine samples within 1.2 min is demonstrated in Figure III.16. Again this speed was possible because of the use of elevated pressure and temperature. The plate number for the last peak is approximately 26,000 plates.

High speed separation of herbicides using elevated temperature UHPLC is demonstrated in Figure III.17. At room temperature, the separation was completed in 8 min as shown in Figure III.17A. Using a pressure of 26 kpsi and a temperature of 90 °C, the separation was achieved in 60 s with all peaks baseline separated, except peaks 3 and 4 (Figure III.17B). In addition, an efficiency of 200,000 plates m^{-1} was obtained for this separation. Comparatively, it would be necessary to increase the pressure to approximately 80 kpsi to achieve a 60 s separation of herbicides at room temperature.

Operating at higher than optimum linear velocities produces very fast separations, but results in some efficiency loss. The separation in Figure III.17B was conducted at a linear velocity of approximately 3.0 mm s^{-1}, while the optimum linear velocity at 80 °C was approximately 1.2 mm s^{-1}. At a linear velocity 2.5 times higher than the optimum, 26,000 plates for a 13 cm long column is still quite good. The inherently high efficiencies of columns containing small particles allow us to sacrifice some efficiency for speed.

III.3.7 UHPLC Using Aqueous Buffer as Mobile Phase

Effects of phase volume ratio and stationary phase polarity on retention factor. The solubility parameter model originally developed to describe the thermodynamics of mixing of regular solutions has been used to theoretically estimate retention factor in reversed phase LC. The retention factor can be related to solubility parameter data as[44]

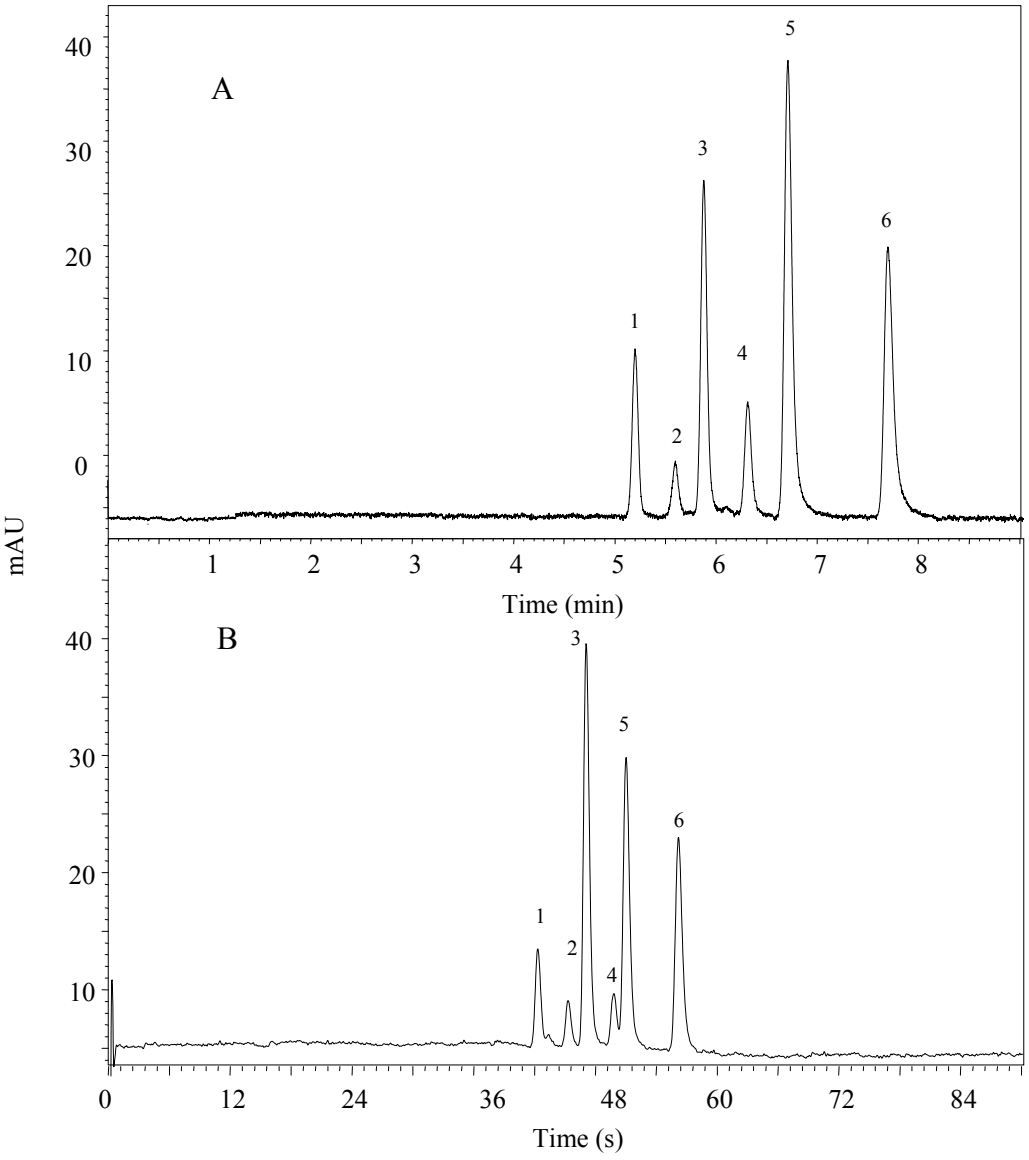

Figure III. 17. Fast separation of herbicides. Conditions: (A) 22 °C; 10,000 psi inlet pressure; 13 cm × 50 μm i.d. fused silica capillary column packed with 1.0 μm PBD-encapsulated nonporous zirconia particles; water (40 mM NaH_2PO_4, pH = 7.0)/acetonitrile (55:45, *v*/*v*); 215-nm UV detection; uracil as marker. (B) 90 °C; 25,000 psi inlet pressure; other conditions are the same as in (A).

$$\log k = \log k_0 + \frac{2V_i}{2.3RT}(\delta_m - \delta_i)(\delta_w - \delta_m)(\%water) + \frac{V_i}{2.3RT}(\delta_w - \delta_m)^2(\%water)^2 \quad \text{III. 10}$$

where

$$\log k_0 = \frac{Vi}{2.3RT}[(\delta_m - \delta_i)^2 - (\delta_s - \delta_i)^2] + \log\varphi \quad \text{III. 11}$$

and δ_i, δ_s, δ_m, and δ_w are the solubility parameters (polarities) for the analyte, stationary phase, initial mobile phase, and water, respectively, V_i is the molar volume of the analyte, R is the gas constant, T is the absolute temperature, φ is the phase volume ratio, (i.e. the ratio of stationary phase volume to mobile phase volume), and k_0 is the retention factor obtained in pure solvent, (i.e., with 0% water).

Based on equation III.10, increasing the polarity of the stationary phase will result in an increase in the (δ_s-δ_i) term, finally leading to a lower retention factor for a given analyte, mobile phase, and phase volume ratio. In addition, decreasing the phase volume ratio (φ) will lead to a decrease in k_0, finally resulting in reduction in retention factor for a given analyte, mobile phase, and stationary phase. Therefore, a reasonable retention factor can be achieved by either increasing the polarity of the stationary phase or reducing the phase volume ratio or both with an aqueous mobile phase. Short-chain alkyl, hydrophilic, polar-endcapped, polar-enhanced or polar-embedded stationary phases have been designed to help retain polar analytes with aqueous mobile phase.[51] A lower phase volume ratio can be achieved by decreasing the amount of stationary phase on the particles. The use of nonporous particles gives less surface area and less densely bonded stationary phase.

The effects of porosity (phase volume ratio) and polarity of the stationary phase on retention factor were investigated as shown in Figure III.18. In this study, three

capillary columns of the same length and i.d. were packed with 1.5 μm C_{18} bonded porous silica, 1.5 μm C_{18} bonded nonporous silica and 1.5 μm C_6 bonded nonporous silica, respectively. It can be seen that for the C_6 bonded nonporous silica, a lower amount of organic solvent in the mobile phase is required for the same retention factor, compared to the C_{18} bonded silicas. This is due to the relatively high polarity of the C_6 stationary phase. The C_{18} bonded porous silica requires much more organic solvent than the other two nonporous silicas. In order to achieve a retention factor of 0.23 for catechol, 95%, 90% and 30% water are required for 1.5 μm C_6 bonded nonporous silica, 1.5 μm C_{18} bonded nonporous silica and 1.5 μm C_{18} bonded porous silica, respectively.

The great difference between nonporous and porous particles is due to the large surface area of the porous particles, which translates into a large amount of stationary phase, resulting in a high phase volume ratio (volume of stationary phase to mobile phase). In addition, 1.0 μm nonporous polybutadiene-encapsulated zirconia particles show smaller retention factor than any of the three silica particles studied. For clarity, these results were not shown in Figure III.18. Comparatively, it is possible to use 1.0 μm nonporous polybutadiene-encapsulated zirconia particles and 1.5 μm C_6 bonded nonporous silica for separations using only water as mobile phase.

Effect of temperature and pressure on absolute retention. Previous studies have demonstrated that the polarity of water decreases markedly as its temperature is raised. Therefore, water has been described as a moderately polar solvent under high temperature conditions, comparable to traditional organic-water phases.[45-47] In addition, elevated temperature can reduce the viscosity of the mobile phase, shorten the separation time, and increase the column efficiency. This allows the use of relatively long columns

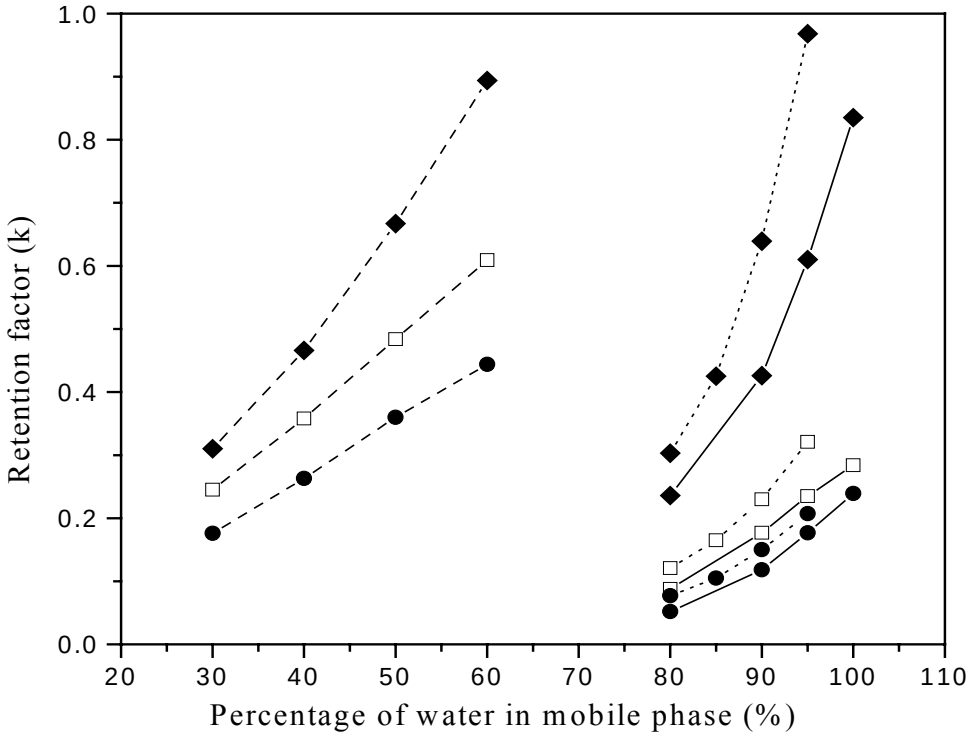

Figure III. 18. Effects of polarity and volume phase ratio on retention factor. Conditions: 16 cm × 50 μm i.d. fused silica capillary column; 10 kpsi inlet pressure; 215 nm UV detection; (long dash) 1.5 μm C_{18} bonded porous silica particles; (short dash) 1.5 μm C_{18} bonded nonporous silica particles; (line) 1.5 μm C_6 bonded nonporous silica particles; (◆) resorcinol; (□) catechol; (●) 4-methylcatechol; uracil as marker.

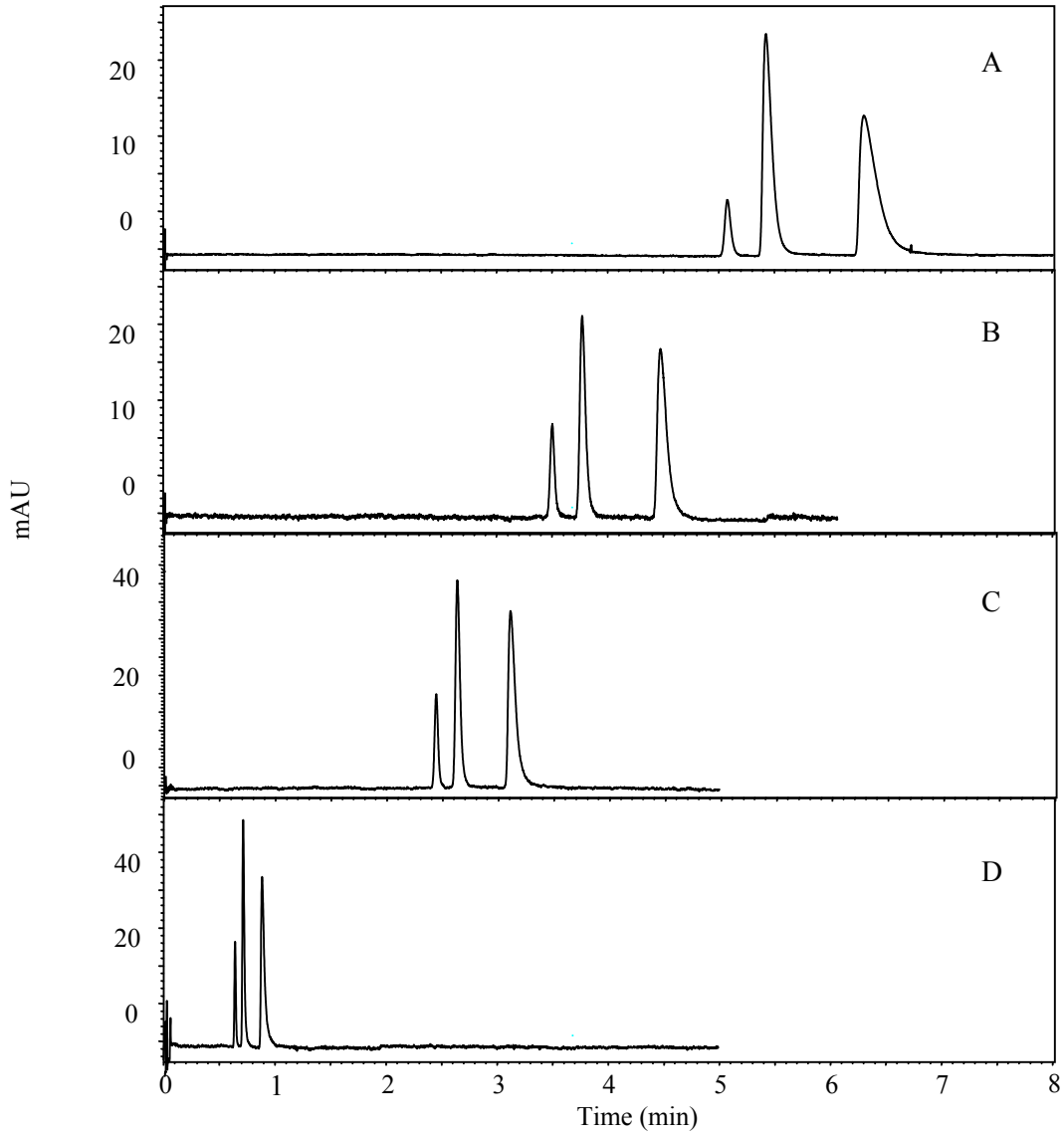

Figure III. 19. Effects of temperature and pressure on the separation of cardiac stimulants using water buffer as mobile phase. Conditions: 16 cm × 50 μm i.d. fused silica capillary column packed with 1.0 μm PBD-encapsulated nonporous zirconia particles; water (40 mM NaH_2PO_4, pH = 7.0); 215 nm UV detection; (A) 22 °C, 10 kpsi inlet pressure; (B) 40 °C; 10 kpsi inlet pressure. (C) 60 °C, 10 kpsi inlet pressure; (D) 80 °C, 20 kpsi inlet pressure.

packed with very small particles.[18]

The effects of elevated temperature on separation were investigated as shown in Figure III.19. Three cardiac stimulant drugs were separated using water as a mobile phase. The separation time was shortened from 7 min to 1 min by increasing the temperature from 22 °C to 80 °C and the pressure from 10 kpsi to 20 kpsi. In addition, the detector response at 80 °C (Figures III.19C and III.19D) was improved approximately 2-fold relative to that at 22 °C (Figures III.19A and III.19B). This was due to the narrow peaks that were obtained at elevated temperature.

Separations using polybutadiene-encapsulated nonporous zirconia. Figures III.20 and III.21 show separations of five analgesic drugs and five barbitals, respectively, using 1.0 μm nonporous polybutadiene-encapsulated zirconia particles with water as a mobile phase. Most peaks were baseline resolved, and the last eluting compound in both figures gave tailing peaks. Elevating the temperature helps to achieve fast separations by accelerating the flow rate and speeding the solute-stationary phase sorption-desorption kinetics. A temperature of 60 °C was used in both separations to obtain reasonable resolution since both separation retention factor and selectivity decrease with an increase in temperature. Based on Figure III.18, it should be theoretically possible to resolve these compounds using a column packed with 1.5 μm C_6 bonded nonporous silica using water as mobile phase. However, it was found that the barbitals could not be eluted from this column, and most of the analgesic drugs tailed seriously during the first several runs with water as mobile phase, even at elevated temperature. After the column was operated using water as mobile phase for several runs, these compounds could be eluted; however,

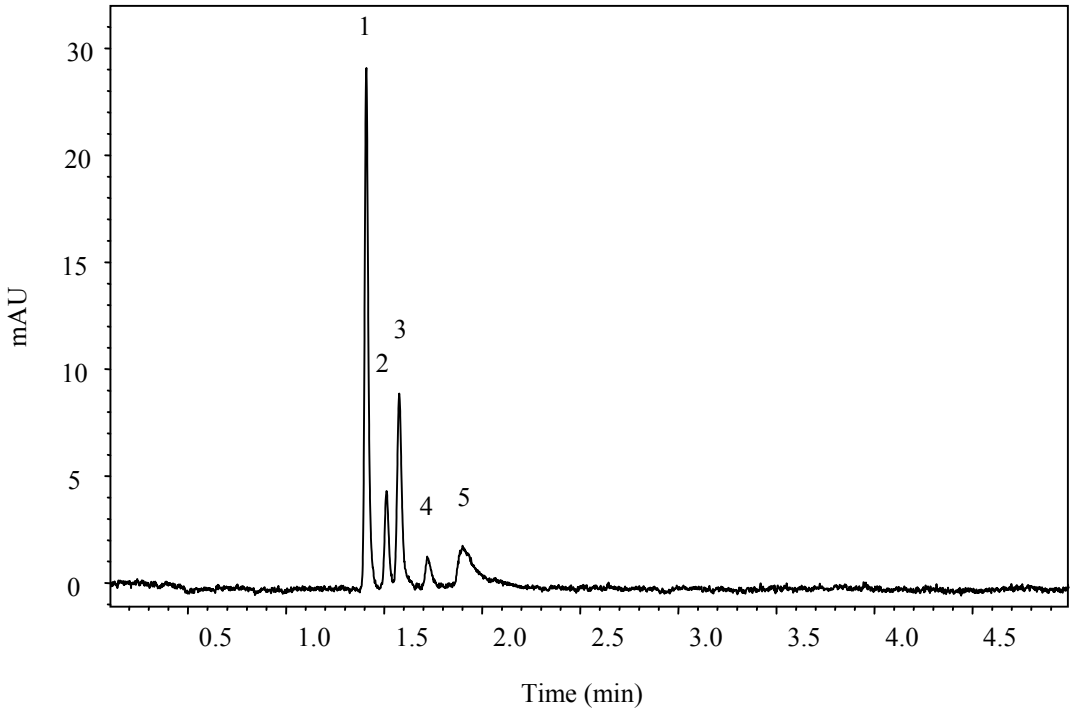

Figure III. 20. UHPLC chromatogram of analgesic drugs using water as mobile phase. Conditions: 16 cm × 50 μm i.d. fused silica capillary column packed with 1.0 μm PBD-encapsulated nonporous zirconia particles; water (40 mM NaH_2PO_4, pH = 7.0); 215 nm UV detection; 60 °C, 20 kpsi inlet pressure. Peak identifications: (1) aspirin, (2) acetaminophen, (3) fenoprofen, (4) flubiprofen, (5) diflunisal.

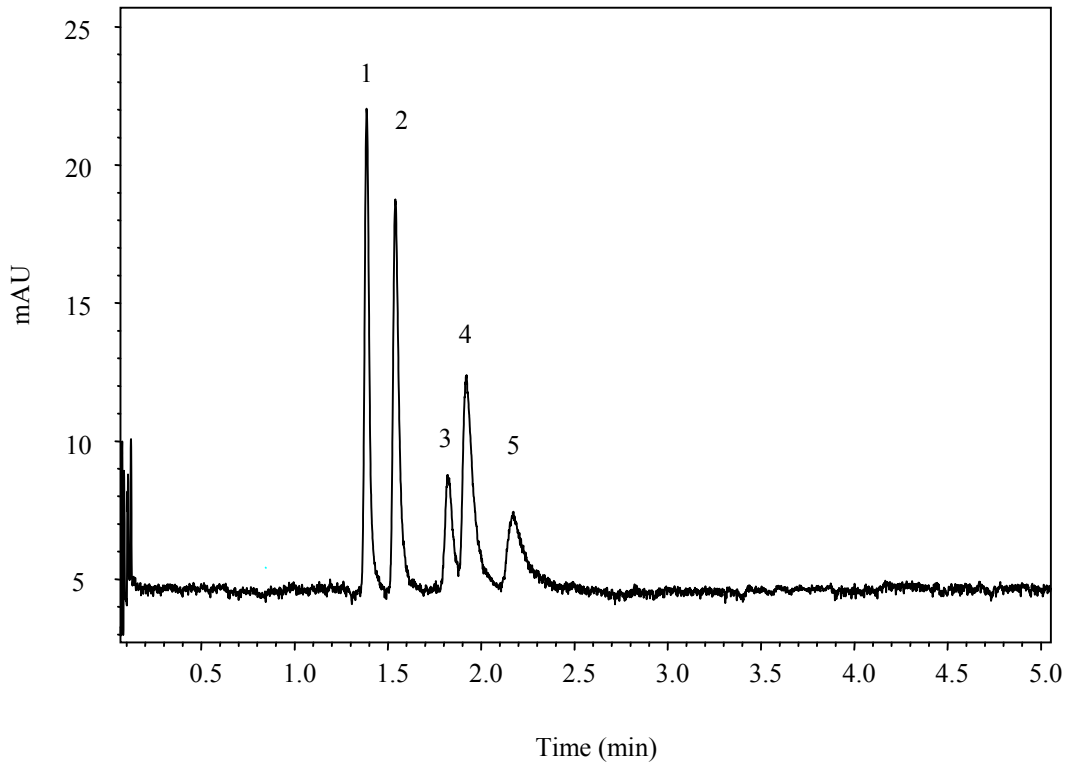

Figure III. 21. UHPLC chromatogram of barbitals using water as mobile phase. Conditions: water (5 mM NaF); other conditions are same as in Figure III.3. Peak identifications: (1) allobarbital, (2) butalbital, (3) pentobarbital, (4) secobarbital, (5) hexobarbital.

retention times decreased until they eluted with the dead time. It was believed that phase collapse occurred when using 1.5 μm C_6 bonded nonporous silica because of retention loss and retention irreproducibility. This phenomenon was not found when using 1.0 μm nonporous polybutadiene-encapsulated zirconia particles.

III.4 Conclusions

Use of elevated temperature reduces the mobile phase viscosity and speeds up solute sorption/desorption, leading to fast separation without significant loss of resolution. A combination of elevated temperature with ultrahigh pressure further facilitates high speed and high efficiency separations. This combination was used for fast separations of pharmaceuticals and herbicide standards on both silica-based and zirconia-based nonporous particles. Separations as fast as 30 s were achieved with efficiencies as high as 26,000 plates.

Use of polybutadiene-encapsulated nonporous zirconia particles with diameter of approximately 1.0 μm was described. The new particles were slurry packed into a 50 μm i.d. fused silica capillary column and evaluated using elevated temperature UHPLC. Column efficiencies as high as 350,000 plates m^{-1} were obtained with polybutadiene-encapsulated particles. The dependency of solute retention on pressure was determined. These particles showed reversed phase behavior. A column was used to separate anti-inflammatory drugs and barbitals. Efficiencies as high as 280,000 plates m^{-1} were obtained for the separation of anti-inflammatory drugs at a pressure of 20,000 psi. The particles demonstrated good thermal stability for fast separations of herbicides and benzodiazepins at temperatures up to 100 °C using pressures as high as 30 kpsi.

Effects of stationary phase polarity and phase volume ratio for four different particle types on solute retention were investigated. Polybutadiene-encapsulated nonporous zirconia particles provide a smaller phase volume ratio, requiring less organic solvent in the mobile phase to achieve the same retention. Elevating the temperature decreases the polarity of water, making it possible to use heated water as mobile phase to achieve some selectivity. In this chapter, three separations were demonstrated using nonporous zirconia particles and water as mobile phase in elevated temperature UHPLC.

III.5 References

1. Halasz, I.; Endele, R.; Asshauer, J. J. Chromatogr. 12 (1975) 37.
2. Barder, T.J.; Wohlman, P. J.; Thrall, C.; DuBois, P. D. LC GC 15 (1997) 918.
3. Issaeva, T.; Kourganov, A.; Unger, K. K. J. Chromatogr. A 846 (1999) 13.
4. Shen, Y.; Yang, Y.; Lee, M. L. Anal. Chem. 69 (1997) 628.
5. Ohmacht, R; Boros, B.; Kiss, I.; Jelinek, L. Chromatographia 50 (1999) 75.
6. Ohmacht, R; Kiss, I. Chromatographia 42 (1996) 595.
7. Giddings, J. C. Dynamics of Chromatography, Dekker: New York, 1965, Chapter 5.
8. Snyder, L.; Kirkland, J. J. Introduction to Modern Liquid Chromatography; Wiley: New York, 1979.
9. Van Deemter, J. J.; Zuiderweg, F. J.; Kinkenberg, A. Chem. Eng. Sci. 5 (1956) 271.
10. MacNair, J. E.; Lewis, K. C.; Jorgenson, J. W. Anal. Chem. 69 (1997) 983.
11. MacNair, J. E.; Patel, K. D.; Jorgenson, J. W. Anal. Chem. 71 (1999) 700.
12. Wu, N.; Lippert, J. A.; Lee, M. L. J. Chromatogr. A. 911 (2001) 1.
13. Xiang, Y.; Wu, N.; Lippert, J. A.; Lee, M. L. Chromatographia 55 (2002) 399.
14. Colin, H.; Diez-masa, J. C.; J. Chromatogr. 435 (1988) 1.
15. Dolan, J. W. LC·GC 20 (2002) 524.
16. Ooma, B. LC·GC 4 (1996) 306.
17. Houdiere, F.; Fowler, P. W. J.; Djordjevic, N. M. Anal. Chem. 69 (1997) 2589.
18. Mant, C.; Hodges, R. HPLC of Peptides and Proteins: Analysis and Conformation; CRC Press: Boca Raton, FL, 1990.
19. Yan, B.; Zhao, J.; Brown, J. S.; Blackwell, J.; Carr, P. W. Anal. Chem. 72 (2000) 1253.

20. Greibrokk, T.; Andersen, T. J. Sep. Sci. 24 (2001) 899.

21. Antia, F. D.; Horváth, Cs. J. Chromatogr. 435 (1988) 1.

22. Li, J. W.; Hu, Y.; Carr, P. W., Anal. Chem. 69 (1997) 3884.

23. Sheng, G.; Shen, Y.; Lee, M. L. J. Microcol. Sep. 10 (1997) 63.

24. Ooms, B. LC·GC International 9 (1996) 574.

25. Chen, H.; Horváth, Cs. J. Chromatogr. A. 788 (1997) 51.

26. Chen, H.; Horváth, Cs. J. Chromatogr. A. 705 (1995) 3.

27. Perchalski, R. J.; Wilder, B. J. Anal. Chem. 51 (1979) 774.

28. Lin, H.-J.; Horváth, Cs. Chem. Eng. Sci. 36 (1981) 47.

29. Hancock, W. S.; Chloupek, R. C.; Kirkland, J. J.; Snyder, L. R. J. Chromatogr. A. 686 (1994) 31.

30. Chloupek, R. C.; Hancock, W. S.; Marchylo, B. A.; Kirkland, J. J.; Boyes, B. E.; Snyder, L. R. J. Chromatogr. A. 686 (1994) 45.

31. Li, J. W.; Hu, Y.; Carr, P. W. Anal. Chem. 69 (1997) 3884.

32. Li, J. W.; Carr, P. W. Anal. Chem. 69 (1997) 2193.

33. Li, J. W.; Carr, P. W. Anal. Chem. 69 (1997) 837.

34. Li, J. W.; Carr, P. W. Anal. Chem. 69 (1997) 2202.

35. Li, J. W.; Carr, P. W. Anal. Chem. 68 (1996) 2857.

36. Zhao, J.; Carr, P. W. Anal. Chem. 70 (1998) 3619.

37. Zhao, J. Ph. D. Thesis, University of Minnesota, Minneapolis, Minnesota, 1999.

38. Weber, T. P.; Jackson, P. T.; Carr, P. W. Anal. Chem. 67 (1995) 3042.

39. Yan, B.; McNeff, C. V.; Chen, F.; Carr, P. W.; McCormick, A. V. J. Am. Ceram. Soc., 84 (2001) 1721.

40. Foster, M. D.; Synovec, R. E. Anal. Chem. 68 (1996) 2838.

41. Smith, R. M.; Chienthavorn, O.; Wilson, I. D.; Wright, B.; Taylor, S. D. Anal. Chem. 71 (1999) 4493.

42. Fields, S. M.; Ye, C. Q.; Zhang, D. D.; Branch, B. R.; Zhang, X. J.; and Okafo, N. J. Chromatogr. A 913 (2001) 197.

43. Chienthavorn, O.; Smith, R. M. Chromatographia 50 (1999) 485.

44. Smith, R. M.; Burgess, R. J. J. Chromatogr. A 785 (1997) 49.

45. Jandera, P.; Kubat, J. J. Chromatogr. A. 500 (1990) 281.

46. Miller, D. J.; Hawthorne, S. B. Anal. Chem. 69 (1997) 623.

47. Ingelse, B. A.; Janssen, H.; Cramers, C. A. J. High Resolut. Chromatogr. 21 (1998) 613.

48. Lippert, J. A.; Xin, B.; Wu, N.; Lee, M. L. J. Microcol. Sep. 11 (1999) 631.

49. Boughtflower, R. J.; Underwood, T.; Paterson, C. J. Chromatographia 40 (1995) 329.

50. Knox, J. H. J. Chromatogr. A. 831 (1999) 3.

51. Majors, R. E.; Przybyciel, M. LC GC 20 (2002) 584.

CHAPTER IV

UHPLC OF CHIRAL PHARMACEUTICALS USING A CHIRAL MODIFIER IN THE MOBILE PHASE

IV.1 Introduction

The increasing demand for enantiomerically pure compounds in the pharmaceutical industry has also stimulated the development of simple and fast analytical separation methods. It was reported that single enantiomer drugs showed continuous growth worldwide (21% sales increment from 1996 to 1997), and 269 of the top 500 drugs were marketed as single enantiomers.[1] To ensure the safety of currently used and newly developed drugs, it is essential to use rapid analytical methods for real-time control of enantiomeric purity of starting materials and products. The requirements of regulatory authorities have made compulsory the availability of enantioselective techniques to assess the stereoisomeric composition of chiral substances. Moreover, libraries of chiral compounds with application in combinatorial chemistry also require high throughput screening methods to handle the large number of chiral samples.

In recent years, the major focus of chiral analysis has centered on high performance LC. In LC, the most straightforward way to reduce the analysis time is to use short columns. However, shortening the column also decreases separation power and may not provide enough interaction with the stationary phase to achieve the needed resolution for chiral separation. Furthermore, in drug discovery, the FDA not only requires the determination of enantiomeric purity of drug substances, but also good control of impurities. Therefore, high efficiency separations are usually desirable, and high speed separations should be achieved without sacrificing resolution. An efficient

way to reduce the separation time and maintain resolution is to use small particles. In LC, the best possible efficiency in the least amount of time is obtained when using very small (<3 μm) diameter packing materials.[2] The enhanced efficiency is due to reduced intraparticulate mass transfer resistance and, to a lesser extent, decreased eddy diffusion. However, small particles stress the pressure limitations of conventional pumping systems, since the column pressure drop is inversely proportional to the cube of the particle diameter at optimum linear velocity.[3] Recently, UHPLC was introduced to overcome the pressure limitations of conventional pumping systems.[4-8] This new technique allows the use of long capillary columns packed with 1.0 and 1.5 μm nonporous particles. Efficiencies as high as 570,000 plates m^{-1} can be obtained using UHPLC.[6] Also, it has been reported that high efficiency is maintained at high linear velocities when short columns are used.[4,7] Separations of selected combinatorial chemistry samples, pharmaceutical compounds and herbicides were completed in less than 100 s using UHPLC with time-of-flight mass spectrometry.[6,7] UHPLC is a powerful new technique with high speed, high efficiency and high resolution.

Cyclodextrins and their derivatives have been used extensively for enantiomeric separations by high performance liquid chromatography (HPLC),[9] supercritical fluid chromatography (SFC),[10] gas chromatography (GC),[11] capillary zone electrophoresis (CZE),[12] and capillary electrokinetic chromatography (CEC).[13] Chemical modification of cyclodextrins with various functional groups has been investigated extensively in an attempt to improve the complexing and catalytic abilities of cyclodextrins. Various functional groups have been introduced onto the cyclodextrin rim, bringing about

changes in the depth of the cyclodextrin cavity, in the hydrogen bonding ability and various other physical properties.[14,15]

Generally, enantiomeric separations have been achieved using two different approaches: (1) use of cyclodextrin or highly soluble modified cyclodextrins as mobile phase additives in reversed phase HPLC, CE, and CEC;[16-20] and (2) use of chemically bonded cyclodextrin-silica as stationary phases, such as in HPLC, SFC, GC and CEC.[21-24]

There are several advantages of using chiral selectors in the mobile phase (mobile phase additives). Less expensive packed columns, such as reversed phase columns, can be used. Poor column efficiencies using a chiral stationary phase can be overcome by taking advantage of the high efficiencies of columns packed with small, nonporous particles. The type and concentration of cyclodextrins can be varied, and the selectivities are often different from those of corresponding chiral stationary phases. In addition, the use of chiral additives is more practical in capillary LC, because only a small amount of expensive chiral selector is needed when a capillary is used.[25] Thus, this approach can offer broader applicability for the chiral separation of complex biological samples.[26]

In this chapter, the potential of using UHPLC for fast chiral separations is described. β-Cyclodextrin (β-CD) and 2-hydroxypropyl-β-cyclodextrin (HP-β-CD) were added to the mobile phase as modifiers to produce transient diastereomeric complexes. Very small particles bonded with reversed phase were used as stationary phase. The effects of column length and inlet pressure and the influence of concentration of chiral mobile phase additive on selectivity were investigated. The influence of the injection amount on selectivity was observed.

IV.2 Experimental

IV.2.1 Materials and Chemicals

Nonporous 1.0 μm isohexylsilane-modified (C_6) packing materials (Kovasil MS-H) were obtained from Chemie Uetikon (Uetikon, Switzerland). Fused silica capillaries were purchased from Polymicro Technologies (Phoenix, AZ, USA). Chiral compounds, β-CD and HP-β-CD were purchased from Sigma-Aldrich (St. Louis, MO, USA). HPLC-grade acetonitrile, chloroform, and water were obtained from Fisher (Fair Lawn, NJ, USA). HPLC-grade isopropanol was purchased from Malllinckrodt (Phillipsburg, NJ, USA), and HPLC-grade hexane was purchased from EM Sciences (Gibbstown, NJ, USA). Photometric-grade trifluoroacetic acid was purchased from Aldrich (Milwaukee, WI, USA). All buffers and solvents for chromatographic use were filtered through 0.22 μm pore Durapore® membrane filters (Millipore, Bedford, MA, USA). Similarly, samples were filtered through 0.2 μm pore polytetrafluoroethylene syringe filters (Chromacol, Trumbull, CT, USA).

IV.2.2 Column Packing

The high pressure packing system used to prepare columns for this study was described in Chapter III.

IV.2.3 UHPLC System

Details of the experimental apparatus and procedures used to perform UHPLC have been previously described (see Chapter II).

IV.3 Results and Discussion

IV.3.1 Effect of Pressure and Column Length on Separations

Figure IV.1 shows separations of chlorthalidone enantiomers using inlet pressures of 10 and 40 kpsi. It can be seen that the separation at 40 kpsi was much faster. It is noted that when the pressure was raised from 10 kpsi to 40 kpsi, the resolution increased also. The same trend was found for separations of oxazepam and temazepam. The retention factor increased with an increase in the pressure, while selectivity and efficiency stayed constant. The dependence of retention factor on pressure is shown in Figure IV.2. Similar observations were reported by MacNair *et al.* and Wu *et al*.[4,7]

Theoretically, pressure-induced perturbations in equilibrium constants are predicted using the Gibbs equation[27]

$$\Delta V = \left(\frac{\partial \Delta G}{\partial P}\right)_T = -RT\left(\frac{\partial \ln K}{\partial P}\right)_T + \Delta n RT\kappa_S \qquad \text{IV. 1}$$

where ΔV is the partial molar volume, ΔG is the Gibbs free energy, and K is the equilibrium constant. The $\Delta n RT\kappa_S$ term in equation IV.1 accounts for the increase in molar concentration with pressure, based on the change in number of products formed from reactants (Δn) and the solvent compressibility (κ_S). In reversed phase separations with HP-β-CD as mobile phase additive, there are several possible equilibria affecting the separation process. First, solute and HP-β-CD in the mobile phase may individually partition into the stationary phase. The solute may form a complex with HP-β-CD in the mobile phase and then be absorbed into the stationary phase. There are mainly two types of equilibria involved in the separations reported in this paper: partition and complexation. It has been reported that pressure has a significant impact on

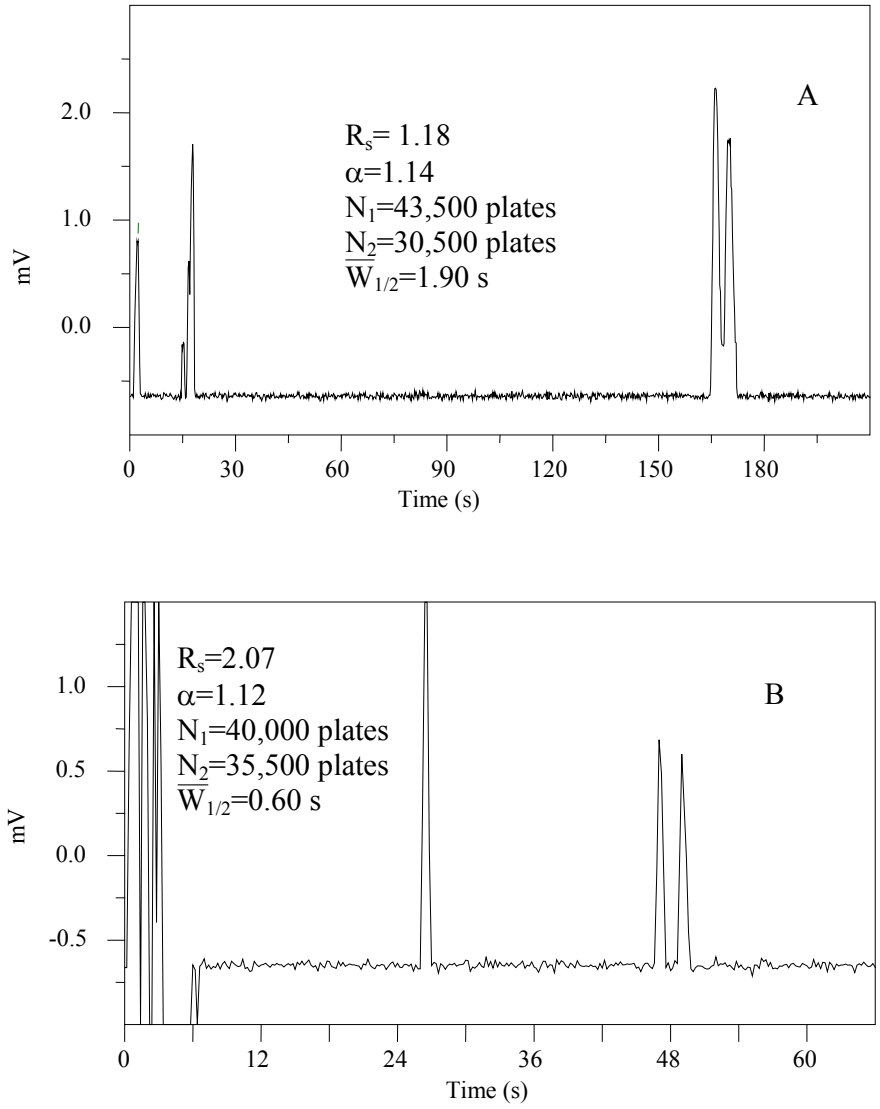

Figure IV. 1. Effect of inlet pressure on the resolution of chlorthalidone enantiomers. Conditions: (A) 10,000 psi inlet pressure; 13.5 cm × 29 μm i.d. fused silica capillary column packed with 1.0 μm Kovasil MS-H nonporous particles; 215 nm UV detection, water (0.1% TFA, pH=4, 15 mM HP-β-CD)/acetonitrile (85:15 v/v); ascorbic acid as marker; (B) 40,000 psi inlet pressure, other conditions are the same as in (A).

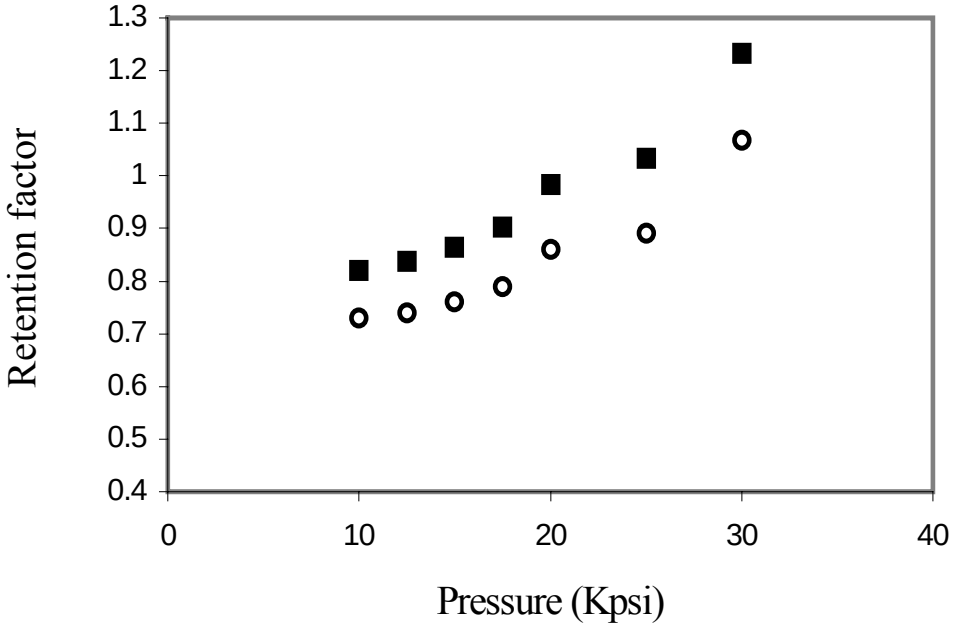

Figure IV. 2. Effect of pressure on retention factor and selectivity for chlorthalidone enantiomers. Conditions: 15 cm × 29 μm i.d. fused silica capillary column packed with 1.0 μm Kovasil MS-H nonporous particles; 215 nm UV detection, water (0.1% TFA, pH=4, β-CD)/acetonitrile (80:20 v/v); ascorbic acid as marker; ■ and ○: retention factors for chlorthalidone enantiomers.

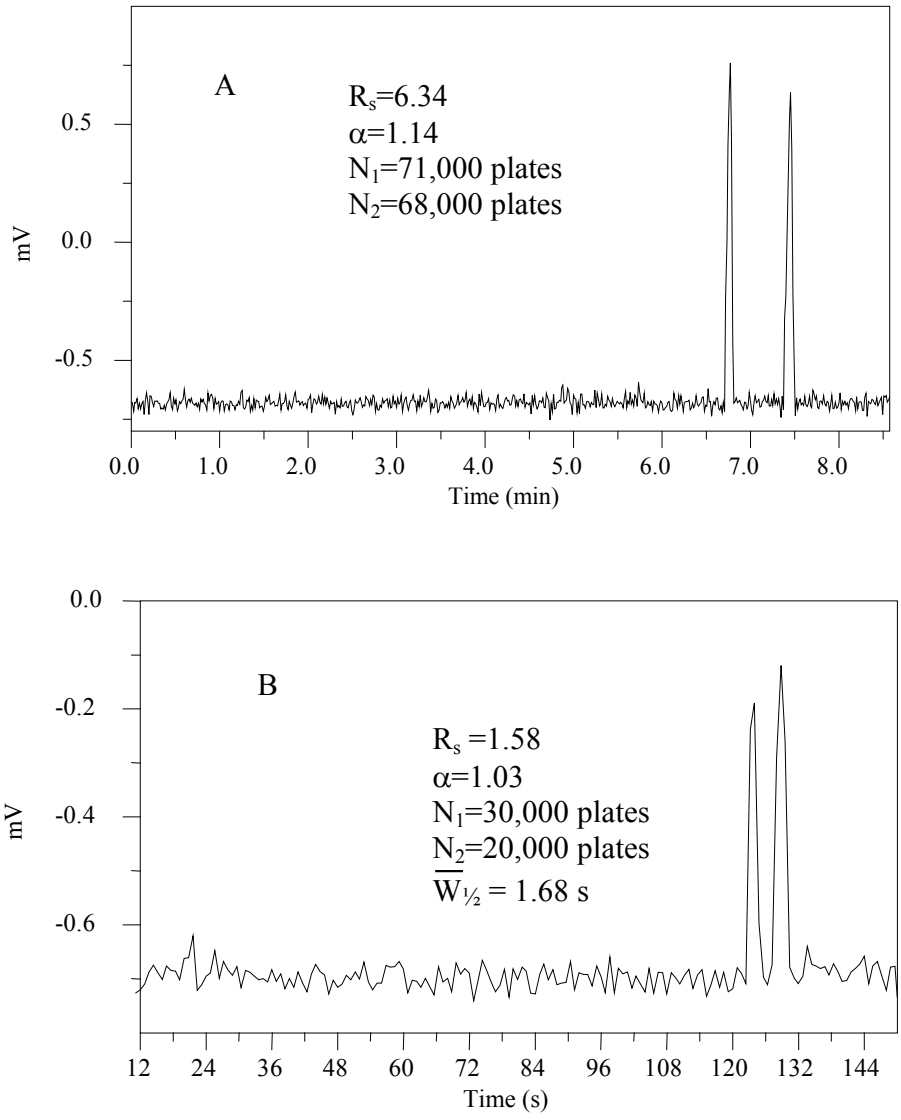

Figure IV. 3. Effect of column length on the separation of temazepam enantiomers. Conditions: (A) 20,000 psi inlet pressure; 23.5 cm × 29 μm i.d. fused silica capillary column packed with 1.0 μm Kovasil MS-H nonporous particles; 215 nm UV detection; water (0.1% TFA, pH=4, 15 mM HP-β-CD)/acetonitrile (80:20, v/v). (B) 40,000 psi inlet pressure; 13.5 cm × 29 μm i.d. fused silica capillary column packed with 1.0 μm Kovasil MS-H nonporous particles; other conditions are the same as in (A).

complexation constants.[27-29] However, pressure induced changes in the partition of solute, HP-β-CD, and solute-HP-β-CD complex between the mobile phase and stationary phase are small, because the pressure has little effect on the stationary phase partial molar volume.[19] However, MacNair *et al.*[4] and Wu *et al.*[7] both observed that retention factors increased with an increase in pressure when operating at very high pressure. In these separations, no complexation equilibria were involved. Therefore, it seems that high pressure has some effect on partition equilibria. Unfortunately, a theoretical description of this observation has not been derived to date.

Comparing Figure IV.3A with Figure IV.3B**,** the separation time was reduced by approximately one fourth by shortening the column. The resolution also decreased from 6.34 to 1.58. Loss in separation power was due to loss in plate number caused by shortening the column. By shortening the column and adjusting the mobile phase linear velocity, baseline separations of chlorthalidone in as little as 48 s and of temazepam in 2 min were obtained as shown in Figure IV.1B and Figure IV.3B**,** respectively. In these separations, an efficiency as high as 380,000 plates m^{-1} was obtained. Figure IV.4 shows baseline separations of chlorthalidone (adding β-CD) and oxazepam (adding HP-β-CD) in 60 s.

IV.3.2 Effect of β-CD and HP-β-CD Concentration on Separation

It was found that oxazepam, temazepam and chlorthalidone ematiomers could be separated by adding HP-β-CD in the mobile phase. However, only chlorthalidone could be separated using β-CD as chiral selector. HP-β-CD, a chemically modified form of β-CD, "stretched" the cyclodextrin cavity mouth and changed its hydrophobicity and,

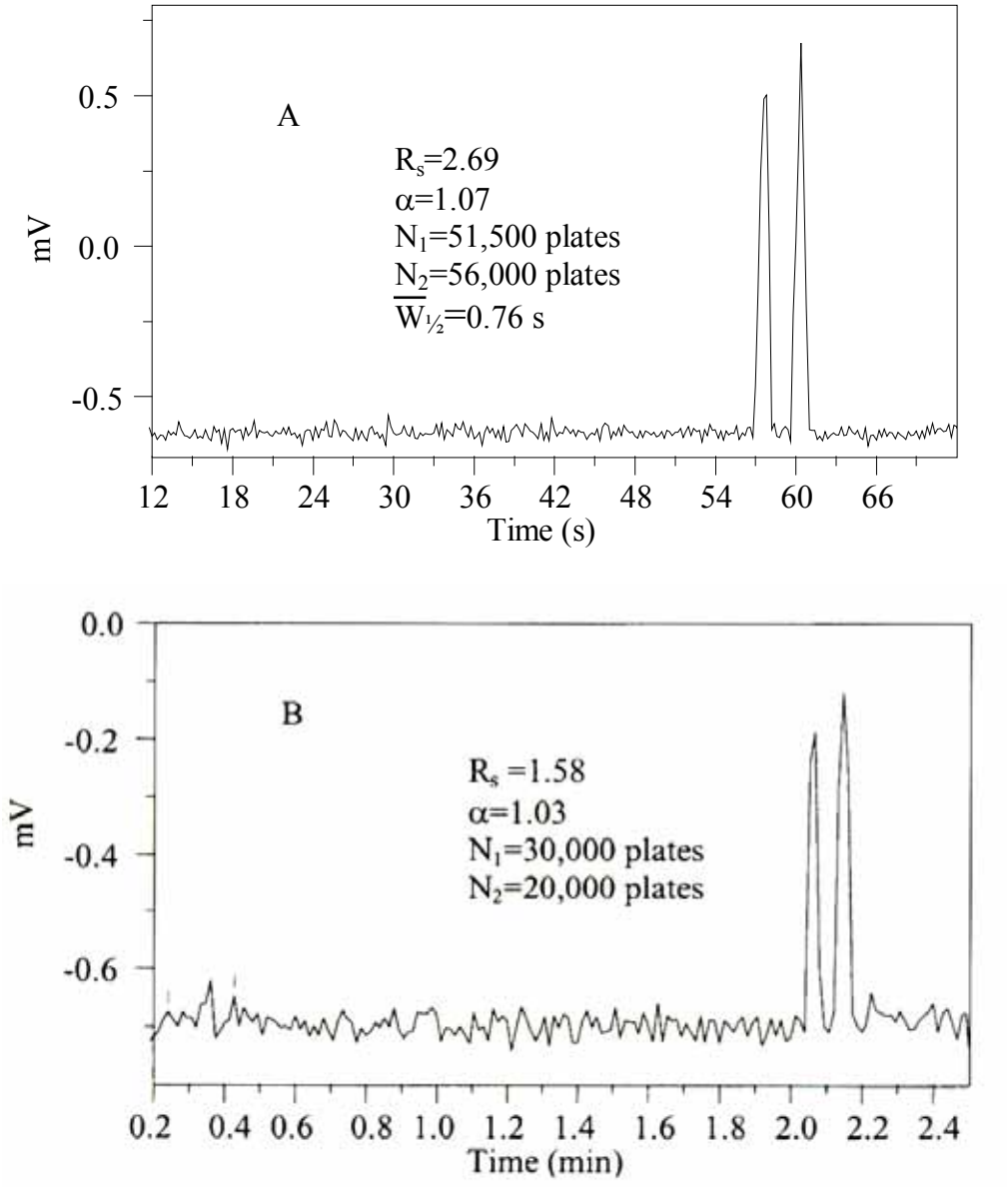

Figure IV. 4. Chromatogram of oxazepam and chlorthalidone enantiomers. Conditions: (A) 42,000 psi inlet pressure; water (0.1% TFA, pH=4, 15 mM HP-β-CD)/acetonitrile (74:26, v/v); other conditions are the same as in Figure IV.1(B); (B) water (0.1% TFA, pH=4, 15 mM β-CD)/acetonitrile (85:15, v/v); other conditions are the same as in Figure IV.1B.

hence, stereoselectivity of the inclusion process. Comparing the structure of HP-β-CD to native β-CD, the hydroxyl moiety of the derivatized hydroxypropyl group in HP-β-CD is free to rotate, which allows for closer approach between the hydroxyl groups and any hydrogen bonding moiety present in the analyte.[16]

Enantioselectivity generally improved with increasing β-CD and HP-β-CD concentration as shown in Table IV.1 for chlorthalidone. This trend was also found for temazepam and oxazepam. However, the resolution of the enantiomers was the highest when the concentration of β-CD or HP-β-CD reached 20 mM. Above this concentration, no further net interactions occurred between the chiral selectors and analytes, and the additives began to compete with the complexes for interaction with the stationary phase. Therefore, the enantiomeric selectivity was diminished. This explanation is supported by the observation that the retention factor decreased significantly when the additive concentration was higher than 20 mM (see Table IV.1). It was also observed that addition of β-CD to the mobile phase led to a greater increase in selectivity than addition of HP-β-CD. To obtain a chiral separation with a CD, at least one of the solute-CD interactions must be stereochemically dependent.[30] Therefore, different selectivities can be expected by addition of β-CD or HP-β-CD.

IV.3.3 Effect of Sample Injection Amount on the Separation

It was found in this study, as expected, that sample injection in UHPLC had a great effect on separation efficiency as shown in Figure IV.5. In this work, a static-split injection technique was used. For the static-split injector, the injected sample amount increases with an increase in injection pressure and time, which is determined by the time

Table IV. 1. Effect of β-CD and HP-β-CD concentration on resolution of chlorthalidone enantiomers.[a]

β-CD concentration (mM)	R_s	Retention factor		α	HP-β-CD concentration (mM)	R_s	Retention factor		α
		k_1	k_2				k_1	k_2	
5	1.43	0.80	0.84	1.05	5	0.84	0.73	0.76	1.04
10	2.46	0.77	0.85	1.10	10	1.20	0.69	0.72	1.04
15	3.69	0.77	0.88	1.14	15	1.26	0.67	0.70	1.05
20	4.24	0.74	0.88	1.19	20	1.43	0.66	0.70	1.06
25	4.08	0.66	0.80	1.33	25	1.38	0.57	0.60	1.05

[a] Conditions: 15,000 psi inlet pressure; 14 cm × 29 μm i.d. fused silica capillary column packed with 1.0 μm Kovasil MS-H nonporous particles; 215 nm UV detection, water (0.1% TFA, pH=4, β-CD or HP-β-CD)/acetonitrile (85:15 v/v); ascorbic acid as marker.

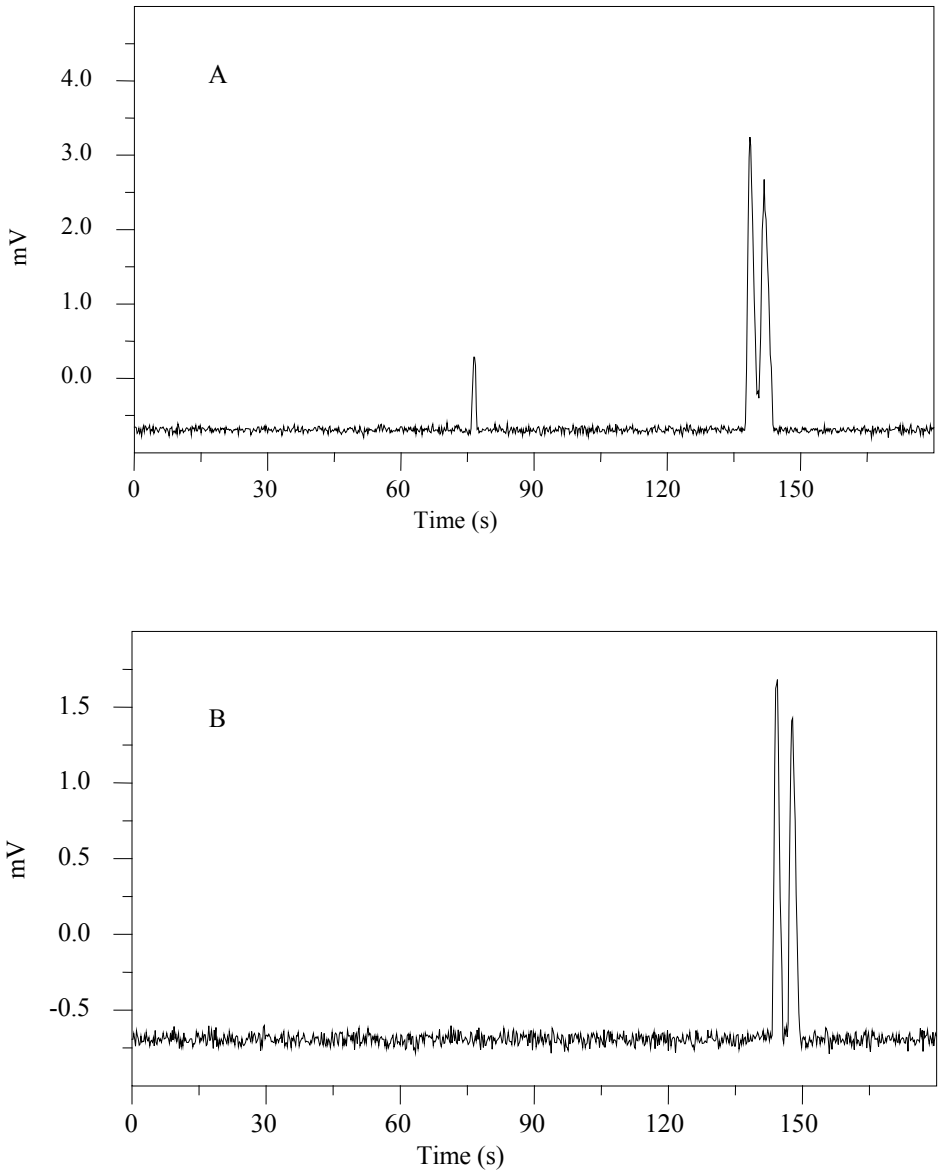

Figure IV. 5. Effect of sample injection amount on the separation of chlorthalidone enantiomers. Conditions: 15, 000 psi inlet pressure; 14 cm × 29 μm i.d. fused silica capillary packed with 1.0 μm nonporous Kovasil MS-H particles; water (0.1% TFA, pH=4, 5 mM β-CD)/acetonitrile (85:15 v/v); ascorbic acid as marker; 215 nm UV detection; injection time: (A) 3 s; (B) 2 s.

interval for valve switching. The injected sample amount can be estimated by these two factors, although it is difficult to control in practice. It was found when the same sample concentration and the same injection pressure were used, a small injection amount obtained using approximately 2 s produced much higher efficiency (120,000 plates in Figure IV.5B) than that using approximately 3 s (38,000 plates in Figure IV.5A).

IV.4 Conclusions

Fast chiral separations were achieved using capillary columns packed with 1.0 μm nonporous C_6 modified silica particles. Addition of HP-β-CD and β-CD in the mobile phase is an easy and feasible approach for chiral separations when capillary columns are used. It was found that addition of β-CD to the mobile phase provided better selectivity than HP-β-CD for chlorthalidone. It was observed that small sample injection volume favors higher enantiomeric resolution. Using UHPLC, several enantiomeric pairs were baseline resolved in 60 s and the fastest separation was completed in 30 s. .

IV.5 References

1. Maier, N. M.; Franco, P.; Lindner, W. J. Chromatogr. A 906 (2001) 3.
2. Snyder, L. R.; Kirkland, J. J. Introduction to Modern Liquid Chromatography, Wiley, New, York, 1979, Chapter 5.
3. Chen, H.; Horvath, Cs. J. Chromatogr. A 705 (1995) 3.
4. MacNair, J. E.; Lewis, K. C.; Jorgenson, J. W. Anal. Chem. 69 (1997) 983.
5. MacNair, J. E.; Patel, K. D.; Jorgenson, J. W. Anal. Chem. 71 (1999) 700.
6. Lippert, J. A.; Xin, B.; Wu, N.; Lee, M. L. J. Microcol. Sep. 11 (1999) 631.
7. Wu, N.; Collins, D. C.; Lippert, J. A.; Xiang, Y.; Lee, M. L. J. Microcol. Sep. 12 (2000) 462.
8. Wu, N.; Lippert, J. A.; Lee, M. L. J. Chromatogr. A 911 (2001) 1.
9. Armstrong, D. W.; Ward, T. J.; Armstrong, R. D.; Beesley, T. E. Science, 232 (1986) 1132
10. Shen, Y.; Wu, N. J. ; Tang, Q. L.; Chen, Z.; Bradshaw, J. S.; Lee, M. L. J. Microcol. Sep. 12 (2000) 475.
11. Ramos, M. D; Teixeira, L. H. P.; Neto, F. R. D.; Barreiro, E. J.; Rodriguez, C. R.; Fraga, C. A. M. J. Chromatogr. A 985 (2003) 321.
12. Vincent, J. B.; Sokolowski, A. D.; Nguyen, T. V.; Vigh, G. Anal. Chem. 69 (1997) 4226.
13. Schurig, V.; Wistuba, D. Electrophoresis 20 (1999) 2313.
14. Vigh, G.; Sokolowski, A. D. Electrophoresis 18 (1997) 2305.
15. Armstrong, D. W.; Han, S. M. CRC Crit. Rev. Anal. Chem. 19 (1988) 175.
16. Han, S. M. Biomedical Chromatography 11 (1997) 259.

17. Hefnawy, M. M.; Stewart, J. T. Anal. Lett. 32 (1999) 159.

18. Moeder, C.; O'Brien, T.; Thompson, R.; Bicker, G. J. Chromatogr. A 736 (1996) 1.

19. Roussel, C.; Favrou, A. J. Inclusion Phenomena and Molecular Recognition in Chemistry 16 (1993) 283.

20. Ward, T.J. Anal. Chem. 66 (1994) 632A.

21. Stalcup, A. M.; Gahm, K. H. Anal. Chem. 68 (1996) 1369.

22. Lipkowitz, K. B.; Pearl, G.; Coner, B.; Peterson, M. A. J. Am. Chem. Soc. 119 (1997) 600.

23. Lipkowitz, K. B.; Pearl, G.; Coner, B.; Peterson, M. A. J. Am. Chem. Soc. 119 (1997)

24. Gong, Y.; Lee, H.K. Helv. Chim. Acta. 85 (2002) 3283.

25. Novotny, M. V.; Ishii, D. Microcol. Sep., Elsevier Science, New York, 1985.

26. Deng, Y.; Maruyama, W.; Yamamura, H.; Kawai, M.; Dostert, P.; Naoi, M. Anal. Chem. 68 (1996) 2826.

27. Evans, C. E.; Davis, J. A. Anal. Chim. Acta. 397 (1999) 163.

28. Hoenigman, S. M.; Evans, C. E. Anal. Chem. 69 (1997) 2136.

29. Ringo, M. C.; Evans, C. E. Anal. Chem. 69 (1997) 642.

30. Li, S.; Purdy, W. C. Chem. Rev. 92 (1992) 1457.

CHAPTER V

GRADIENT ULTRAHIGH PRESSURE LIQUID CHROMATOGRAPHY USING A NOVEL VALCO INJECTOR ASSEMBLY

V.1 Introduction

As described in previous chapters, UHPLC has been developed to overcome the great pressure drop in long columns packed with small particles and to take advantage of small particles for high speed and high efficiency separations.[1,2] Subsequent studies have further demonstrated that UHPLC is a powerful separation technique.[3-7]

As a new and promising technique, UHPLC still needs to be improved. Most UHPLC systems are pressure controlled. Although an exponential gradient can be produced using a pressure controlled pump, a linear gradient is often desired. Development of flow controlled UHPLC requires that check valves and a flow meter as well as a flow controlled pump work well under ultrahigh pressures. Tolley *et al.* reported the use of flow control in very high pressure liquid chromatography (VHPLC).[8] Their system was based on a commercial pump which was modified to operate at up to 1375 bar (20,000 psi). A computer-controlled low-pressure mixer was used to generate linear gradients. Protein digests were separated by gradient VHPLC at pressures as high as 13,500 psi, and detected using either a tandem mass spectrometer with electrospray ionization or a UV/visible detector. The results using VHPLC-MS/MS for protein identification were compared to those from nanoelectrospray-MS/MS. It was found that the VHPLC method gave more sequence information and higher signal-to-noise ratio than nanoelectrospray.

In addition, for UHPLC, sample introduction has been particularly challenging because of the difficulty in constructing a valve that satisfies the sealing requirements at ultrahigh pressures while concurrently limiting the internal volume to a minimum. Capillary LC requires extremely narrow sample plugs to minimize any sample volume contribution to peak broadening as discussed in Chapter I. At the beginning of the development of UHPLC, Jorgenson used a static-split injector, which could withstand pressures as high as 100,000 psi, and which could inject samples as small as 0.2 nL. This injector has proven to work very well under ultrahigh pressures. Using a static-split injector, the injected sample volume is determined by the injection pressure, injection time or time interval between valve opening and closing, and the resistance of the separation column.[3-6] There are many factors involved in an injection with the static-split injector, making it hard to use UHPLC for quantitative analysis due to poor injection reproducibility. There are several additional drawbacks of this injection technique. It consumes too much sample and takes several minutes to complete because sample loading must be performed under atmospheric pressure. Also, slow depressurization is required. When the injector was used for gradient UHPLC, the dwell volume (the volume between the inlets of the mixer and the column) was large.[4] Therefore, the separation column had to be first installed in the static-split injector for sample injection, and then taken off from the injector and connected to the outlet of the mixer for gradient elution.[4] These limitations have made the injection process itself the major limiting factor to use of gradient UHPLC.

Wu *et al.* evaluated an experimental pressure-balanced injection valve manufactured by Valco.[9] The injection valve allowed routine operation at pressures up to

15 kpsi. Compared to the static-split injector, this valve showed many advantages, such as much better reproducibility, short injection time, ease of operation and small amount of injected sample. Following that, another new experimental injection valve, a passive feedback switching valve, similar to the one evaluated by Wu *at al*., was routinely used for peptide mapping with UHPLC.[10] It was proven that this valve could be effectively used for 10 kpsi capillary LC separations with a lifetime exceeding 4 months and 200 switching cycles. The passive feedback switching valves made it possible to implement a high efficiency, multiple capillary LC system equipped with small particles (e.g., 3 μm) packed in long capillary columns (e.g., 85 cm). Successful use of pressure-balanced and passive feedback switching valves at ultrahigh pressure is an important step forward in the development of UHPLC for routine analysis. However, due to leakage of the switching valve at pressures higher than 17.5 kpsi, an injector that could withstand even higher pressures, e.g., 30-60 kpsi, was still desirable.

In this chapter, a novel injection assembly is described and evaluated. The injection assembly is composed of six small needle valves, each of which is electrically controlled. When the loop, filled with sample, is connected to the eluent stream for a short time by opening three valves and closing the three other valves at the same time, the sample is introduced into the separation column. Using this new injector, sample volumes as low as several pL could be introduced at a column inlet pressure of 25 kpsi. Because of the small dwell volume characteristic of this injector, simple gradient elution can be utilized in UHPLC.

V.2 Theory on Maximum Injection Volume

The maximum injection volume (V_{max}) that can be injected into a microcolumn can be expressed as[11,12]

$$V_{max} = \sigma K \pi \varepsilon d_c^2 L(k+1)/\sqrt{N} \qquad \text{V. 1}$$

where σ is the fractional loss of the column plate number caused by the injection, K is a constant describing the injection profile, L is the column length, k is the retention factor, and N is the theoretical plate number.

Generally, a typical value of 5% in volume dispersion (σ = 0.05) is acceptable. Assuming that the column porosity (ε) is 0.7, the injection profile is almost an ideal rectangular plug with K = 4, and the column reduced plate height is 2. Substituting $N = L/hd_p$ into equation V.1 gives

$$V_{max} = 0.4396 d_c^2 (k+1)\sqrt{Lhd_p} \qquad \text{V. 2}$$

Based on the above equation, the calculated maximum acceptable injection volumes for different capillary columns are listed in Table V.1.

It can be seen that for 30 and 50 μm i.d capillary columns, injection volumes are at the nanoliter level. For a 15 cm × 30 μm i.d column packed with 1.0 μm particles, the maximum injection volume is as small as 0.2 nL. For such a small required injection volume, it is difficult to use conventional injection valves, which can deliver minimum volumes of 20-25 nL. To solve this problem, dynamic split injection or timed-split injection, or both, must be used to decrease band broadening caused by large injection volume.[13]

Table V. 1. Maximum acceptable injection volumes for different capillary columns for a non-retained compound.

Column i.d. (μm)	Column length (cm)	V_{max} (nL)		
		d_p = 1 μm	d_p = 3 μm	d_p = 5 μm
50	15	0.60	1.0	1.4
	25	0.78	1.4	1.7
	40	0.98	1.7	2.2
30	15	0.22	0.37	0.49
	25	0.28	0.49	0.63
	40	0.35	0.61	0.79

V.3 Experimental

V.3.1 Materials and Chemicals

Nonporous 1.5 μm isohexylsilane modified (C_6) and octadecylsilane modified (C_{18}) silica particles (Kovasil MS-H) were obtained from Chemie Uetikon (Uetikon, Switzerland). Acetonitrile, hexane, acetone and water were HPLC grade as obtained from Fisher Scientific (Fair Lawn, NJ, USA). Fused silica capillary tubing was purchased from Polymicro Technologies (Phoenix, AZ, USA). Ovalbulmin, TPCK treated trypsin and barbitals were obtained from Sigma (St. Louis, MO). Trifluoroacetic acid (TFA) was acquired from Aldrich (Milwaukee, WI, USA). SFC-grade carbon dioxide and compressed nitrogen were obtained from Airgas (Salt Lake City, UT, USA). All buffers and solvents were filtered through Durapore® membrane filters (0.22 μm pores, Millipore, Bedford, MA, USA) before use. Similarly, samples were filtered through polytetrafluoroethylene (PTFE) syringe filters (0.2 μm pores, Chromacol, Trumbull, CT, USA). Zeflor™ filter membranes with 3.0 μm pore size were supplied by Gelman Science (Ann Arbor, MI, USA) and used to filter the particle slurry before packing.

V.3.2 Column Preparation

The high pressure packing system used to prepare columns for this study was described in Chapter III.

V.3.3 Valco Injection Valve Assembly

Figure V.1 shows the Valco injection valve assembly, comprised of six small needle valves, each of which is electrically controlled. The valve assembly can partially or completely inject the sample loaded into the sample loop by adjusting the injection time. In capillary LC, due to the small dimensions of the capillary columns as discussed in Section V.2, the injected sample volume must be minimized to decrease the band-broadening caused by injection. Therefore, partial injection was used for the isocratic elution mode. For partial injection, the injected sample volume was dependent on the injection pressure (mobile phase flow rate), injection time, and resistance of the separation column. The injection time was dependent on the time interval between valve open and close, which was electronically controlled by a computer. In addition, the splitter could decrease the sample injection volume and reduce any dead volume. The split ratio depended approximately on the ratio of the volumetric flow rates through the separation column and the splitter capillary column. Similar to a conventional switching valve, sample injection using the new valve assembly can be accomplished under the same pressure as needed for separation. Therefore, there is no depressurization involved in the injection process.

Using the new injection valve assembly for injection, the following steps were followed:

(1) The controller was set at the "load" position. At this position, needle valves 2, 3 and 5 were open and needle valves 1, 4 and 6 were closed (see Figure V.1A). The mobile phase entered the separation column via valve 2 and the small diameter tubing between valve 2 and one port of the tee, to which the separation column was connected.

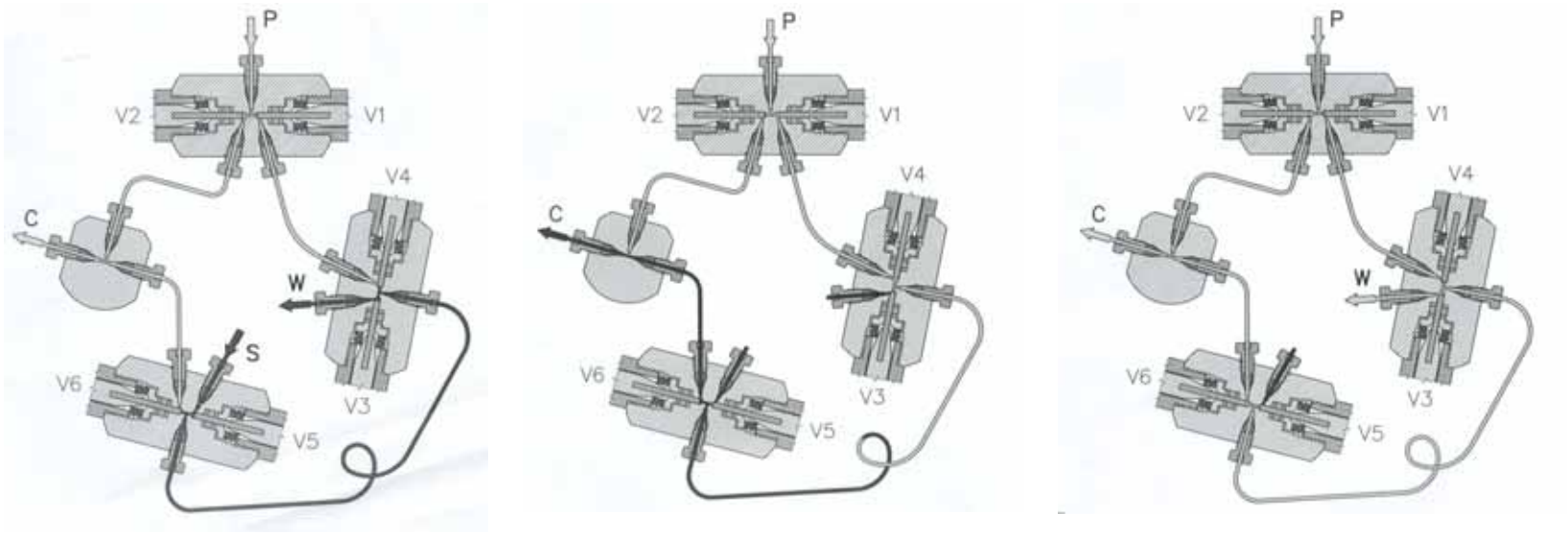

A B C

Figure V. 1. Schematic of the new injection valve assembly. (A) Sample loading; (B) Sample injection; (C) Sample flushing. P = pump; C = column; S = sample; W = waste; V1, 2, 3, 4, 5, 6 = valves 1, 2, 3, 4, 5, 6 (see text for details).

At the same time, the sample was loaded into the sample loop using a syringe as shown in Figure V.1A. The sample loop could be selected from 250 nL and 50 μL volumes.

(2) The sample in the sample loop was injected into the column by clicking the "injection" button on the controller, which closed valves 2, 3 and 5 and opened valves 1, 4 and 6, as shown in Figure V.1B, allowing the mobile phase to carry the sample into the separation column. After a defined time, the injection valve assembly was automatically switched back to the "load" position with valves 1, 4 and 6 closed and valves 2, 3 and 5 open. The injection time was controlled by the computer.

(3) The rest of the sample in the sample loop was purged away as shown in Figure V.1C. This step removed the rest of the sample, avoiding diffusion into the separation column during the separation. By clicking "flush", valves 1, 4 and 5 were closed and valves 2, 6 and 3 were opened, allowing the mobile phase to flow through the connection tubing between valve 2 and one port of the tee, the tubing between valve 6 and another port of the tee, the sample loop, and out of the waste port. After flushing for a defined injection time, the injection valve assembly was automatically switched back to the "load" position with valves 1, 4 and 6 closed and valves 2, 3 and 5 open. "Flushing" must be very fast to avoid any significant drop in the pressure in the system. Otherwise, a gap in the packed bed can be created. It was found that this "flushing" step could be accomplished before subsequent sample loading rather than immediately after each injection.

If the isocratic elution mode is desired for fast separation, a short injection time from 0.1 to 2.5 s should be selected to deliver a small injection volume. If the gradient

elution mode is desired, a large sample injection volume can be selected by adjusting the injection time from 1 to 10 min.

V.3.4 Ultrahigh Pressure Liquid Chromatographic System

A photograph of the gradient UHPLC system with new injection valve assembly is shown in Figure V.2. This system used the same pump (Model DSHF-302, Haskel, Burbank, CA) as previously described.[14] A high pressure three-way valve (Model 60-13HF2, HiP) was used to connect the pump outlet, a high pressure tee (Model 60-23HF2, HiP) and a high pressure two-way valve (Model 60-11HF2, HiP), which was used for pump depressurization. The other two ports of the high pressure tee were connected to a high precision pressure transducer (Model THE/4834-06TJG) and the new injection valve assembly, if the isocratic elution mode was used. For gradient elution, the port, which was connected to the new injection valve assembly in the isocratic elution mode, was coupled to a valve assembly (called the control valve assembly as shown in Figure V.2, Model 15-15AF1, HiP), which consisted of two valves and three flow paths. One valve (called the main valve) of the control valve assembly was used to control the main mobile phase stream from the pump to the solvent mixer, while the other valve (called the purge valve) was used to control the mobile phase flow from the pump to the vent.

When the exponential gradient mode was desired, after the whole system (solvent mixer, injector, connecting tubing and column) was filled with solvent A, the purge valve was opened to purge solvent A away and introduce solvent B into the pump, valves, and connecting tubing before the valve assembly. Before the purge valve was opened, the main valve was closed to disconnect the mixer, injector and column from the pumping system. By doing so, there was no need for slow depressurization of the system. The

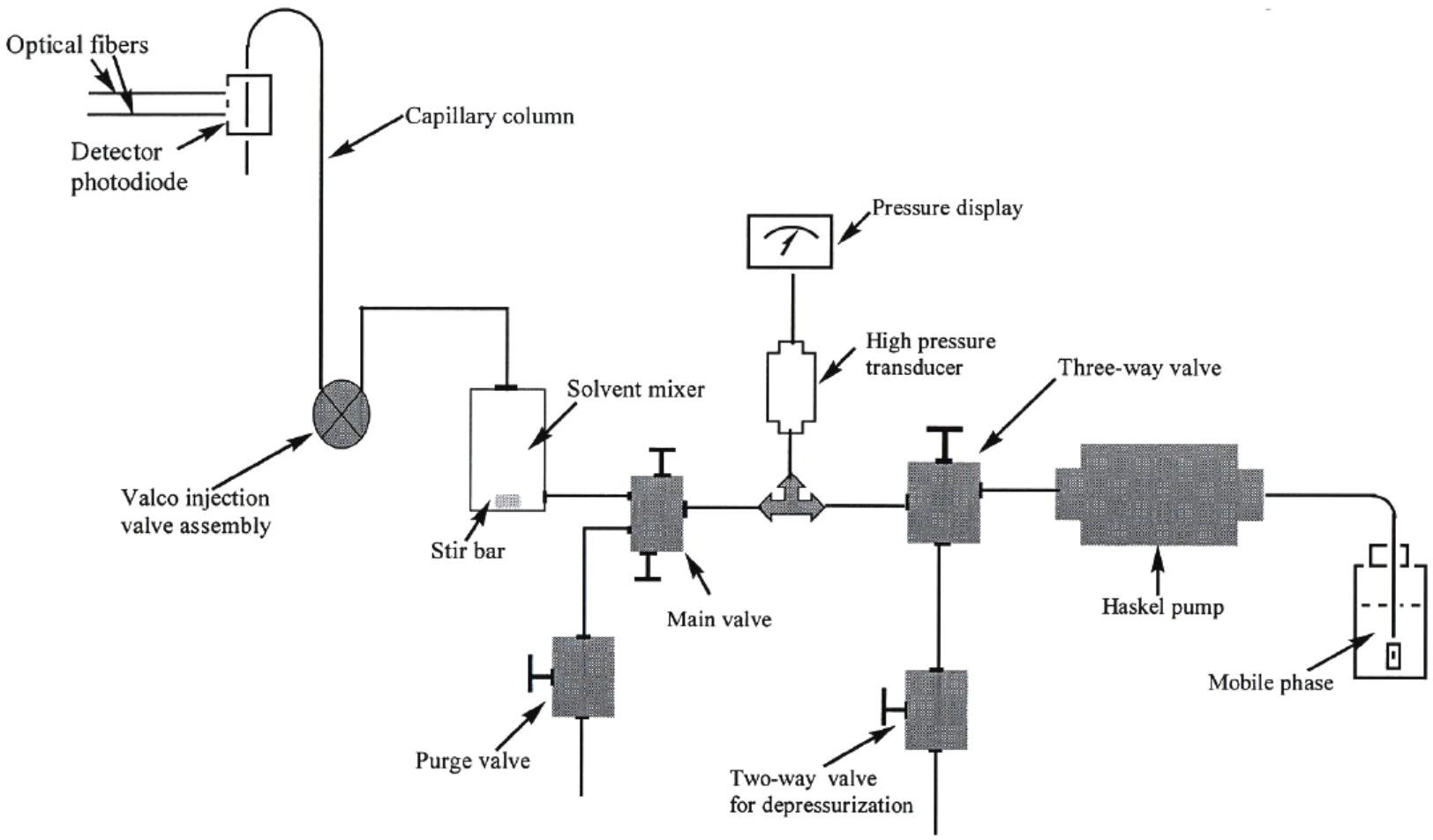

Figure V. 2. Schematic of gradient ultrahigh pressure capillary liquid chromatography system.

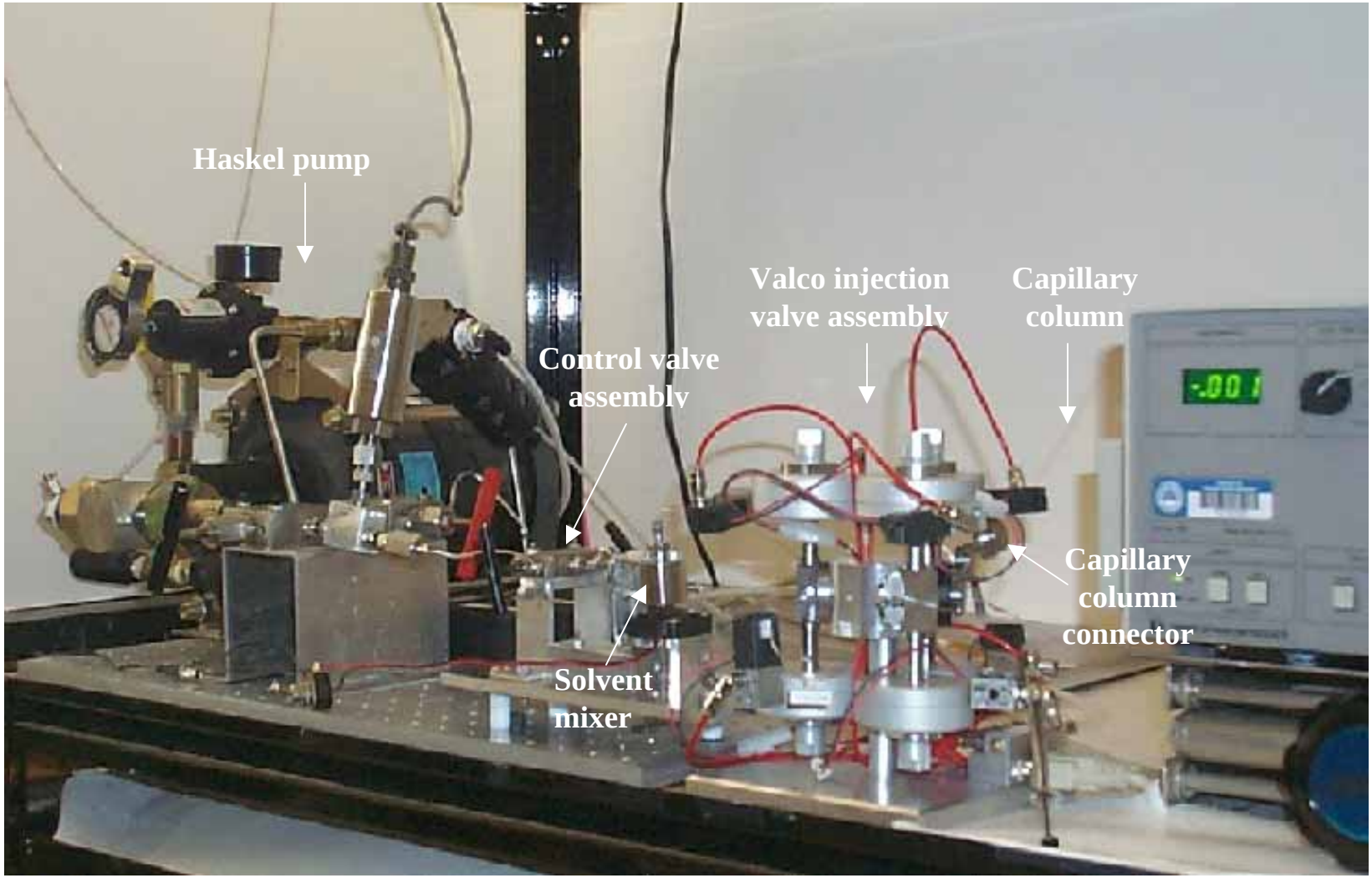

Figure V. 3. Gradient ultrahigh pressure capillary liquid chromatograph with new injection valve assembly.

solvent mixer (80 μL) containing a magnetic stir bar was used to mix the solvents before they entered the separation column via the new injection valve assembly. Stainless steel tubing (1/32" o.d.), which interconnected the control valve assembly and the mixer, and the mixer and the Valco injection valve assembly, had to be as short as possible to reduce gradient delay. Figure V. 3 shows a photograph of the UHPLC system as described above.

V.3.5 High Pressure Capillary Connector

In conventional capillary LC, the capillary column was connected to the injection valve via a Vespel/graphite (85/15) ferrule (Alltech, Deerfield, IL, USA) and a 1/16'' or 1/32" fitting as shown in Figure V.4A. This connection, however, could not be used up to 10 kpsi; otherwise, the capillary was ejected out of the valve (capillary projectile as described in Chapter II) under the ultrahigh pressure. A new design for the ultrahigh pressure capillary connector is shown in Figure V.4B. Two stainless steel fittings (1/32'') were soldered together as one piece. One fitting of this unit was used to connect the capillary column to the connection port of the injection valve in the same way as in Figure V.4A, while the other fitting was used to connect the capillary to a union via a ferrule. The union had a bore diameter of 425 μm, through which the capillary column was inserted. Deformation of the polymer ferrule produced a holding force on the capillary column. The conventional connection used one ferrule, therefore, producing a "one-point" holding force on the capillary. The fitting unit in Figure V.4B used two ferrules in opposite directions, producing "two-point" holding forces on the capillary. This fitting could hold much higher pressure than that in Figure V.4A. This fitting unit

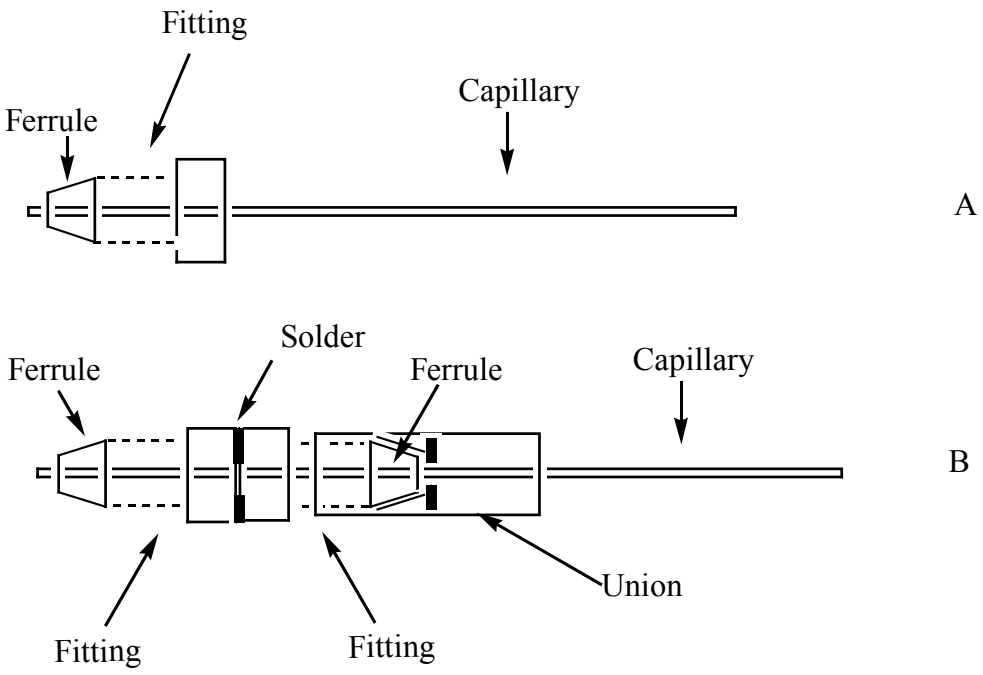

Figure V. 4. Schematics of two connector assemblies. (A) capillary connector for conventional capillary LC; (B) capillary connector for ultrahigh pressure capillary LC.

was successfully used to hold capillary columns at pressures as high as 30 kpsi without leaking or breaking.

V.4 Results and Discussion

V.4.1 Volume Injected

Using a static-split injector, a column efficiency as high as 500,000 plates m^{-1} was achieved.[3,5,6] From previous theoretical calculations, for 1.5 μm nonporous particles packed in a capillary column (33 cm × 29 μm i.d), the injection volume must be as small as 0.30 nL. Otherwise, band broadening caused by injection will be significant. When 800 Psi was used for injection, the flow rate in the column (33 cm × 29 μm i.d) was 0.025 nL s^{-1}, assuming a column porosity of 0.7.[15] Generally, 1-3 s were used for injection. Therefore, the injection volume should have been in the range of 25-75 pL. In order to achieve comparable column efficiency with the new injection valve assembly, the same small volume was required.

Initially, we attempted to use the new injection valve assembly to inject the sample directly into the separation column without splitting. However, peak tailing was very serious. Decreasing the injection volume by shortening the injection time did not improve the efficiency significantly. It was thought that low efficiency might be due to the dead volume in the connecting tubing between the tee and valve 6 (see Figure V.1B). The valve geometry required a minimum length of 3 cm tubing for connection, so it was necessary to use a splitter in the system to decrease the extracolumn band broadening caused by the tubing. When a splitter with split ratio of 200 was used, the column efficiency was increased significantly. The injected sample volumes were calculated

Table V. 2. Injection volumes at different pressures.

Inlet pressure (psi)	Flow rate ($\mu L\ s^{-1}$)	Injection time (s)	Injected amount (nL)
10	0.00123	0.5	0.003
15	0.00185	0.4	0.004
20	0.00238	0.3	0.004
22.5	0.00274	0.2	0.003

Conditions: 25 cm × 50 μm i.d. fused silica capillary column packed with 1.5 μm Kovasil MS-H nonporous particles; water (0.1% TFA)/acetonitrile (90:10, v/v); 215 nm UV detection; column porosity (ε) of 0.7; the injection time was defined in the program assuming no electronic delay; 200:1 split ratio, assuming the split ratio did not vary when the inlet pressure was changed.

from the injection time, eluent flow rate and split ratio.[15,16] The results are listed in Table V.2. It can be seen that very small sample amounts were injected using the new injection valve assembly. Compared to the theoretical calculations listed in Table V.1, these values are approximately 20 times smaller. Compared to the injection volume using a static-split injector, the values are 2-5 times smaller. Therefore, no significant band broadening should be caused by sample injection when the new injection valve assembly is used.

V.4.2 Reproducibility

Injection reproducibility is critical for quantitative analysis, especially when an external standard method is used. In this study, the reproducibilities of sample retention time, efficiency and peak area using the new injection valve assembly were investigated for different inlet pressures as listed in Table V.3. The repeatabilities of injection, reflected by relative standard deviation (RSD) of retention time, efficiency and peak area, were calculated. All RSD values were less than 3.1% and are comparable to those obtained with pressure-balanced valve.[10]

At the same time, standard calibration curves, which are necessary for quantitative analysis, were determined for different inlet pressures. For determination of the standard curve, a plot of peak area against concentration was used. The slope, the intercept and the correlation coefficient for four standards were determined as summarized in Table V.4. It can be seen that the relationships between peak areas and concentrations were linear within the studied concentration range. Therefore, this novel valve makes UHPLC possible for quantitative analysis.

Table V. 3. Reproducibilities of the new valve assembly.[a]

Pressure (kpsi)	Retention time (min) Mean ± S.D.[b,c]	RSD (%)	Efficiency (plates) Mean ± S.D.[b,c]	RSD (%)	Peak area Mean ± S.D.[b,c]	RSD (%)
10	4.66 ± 0.09	1.9	92,200 ± 230	0.25	38,200 ± 200	0.6
15	3.09 ± 0.03	1.0	75,000 ± 1,600	2.1	73,600 ± 2000	2.8
20	2.40 ± 0.01	0.5	48,000 ± 1,500	3.1	112,300 ± 3,200	2.9
22.5	2.09 ± 0.02	1.1	43,000 ± 1,300	3.0	145,500 ± 2,800	1.9
25	1.88 ± 0.02	1.1	38,000 ± 900	2.4	175,700 ± 2,500	1.4

[a]Conditions: 25 cm × 50 μm i.d. fused silica capillary column packed with 1.5 μm Kovasil MS-H nonporous particles; water (0.1% TFA)/acetonitrile (90:10, v/v); two columns were tested and 5 measurements for each column were made; hydroquinone was used as the test solute; 215 nm UV detection.

[b]Calculations were based on 95% confidence level.

[c]n=4.

Table V. 4. Calibration curves for the new injection valve assembly.[a]

Compound	10 kpsi		20 kpsi	
	Calibration curve	R^2	Calibration curve	R^2
Hydroquinone	y = 3323x + 1197	0.99	y = 9692x - 1536	0.99
Resorcinol	y = 7253x + 1919	0.99	y = 22628x - 5155.9	0.98
Catechol	y = 9268x + 1002	0.99	y = 29386x - 12822	0.99
4-Methylcatechol	y = 5958x + 4295	0.99	y = 21921x - 10894	0.99

[a]y is the peak area and x is the sample concentration (mg/mL); conditions are the same as in Table V.3.

V.4.3 Fast Separations Using Isocratic Elution

Using the new injection valve assembly, fast separations under isocratic conditions were achieved as shown in Figures V.4 and V.5. At 15 kpsi, it took approximately 6 min to separate five test compounds using a 25 cm × 50 μm i.d. fused silica capillary column packed with 1.5 μm Kovasil C_{18} bonded nonporous particles (see Figure V.5A). A column efficiency of 100,000 plates was obtained for the first two eluting peaks. This result is better than that obtained using the pressure-balanced valve and comparable to that using the static-split injection valve.[5,6,10] The efficiencies for the last three peaks, however, were not as good as for the first two. The last peak tailed seriously. When a 13 cm × 50 μm i.d. fused silica capillary column packed with 1.5 μm Kovasil C_6 bonded nonporous particles was used and the inlet pressure was increased to 25 kpsi, the separation time was shortened to 48 s, an approximate 7-fold reduction, compared to the separation at lower pressure (see Figure V.5B). Five peaks were still baseline separated.

Figure V.6 demonstrates the fast separation of seven barbital standards. Increasing the pressure from 10 kpsi to 25 kpsi allowed a 3-fold reduction in the separation time. It can be seen that the peaks were sharp (average efficiency is 120,000 plates m^{-1}) and symmetric (symmetric factor is 1.10 for the last eluting peak) for the 1 min separation.

V.4.4 Peptide Separation Using Gradient Elution

Homogenous mixing, small dwell volume and reproducible delivery of the mobile phase are critical to generate a proper gradient, especially for nanoliter flow rates in

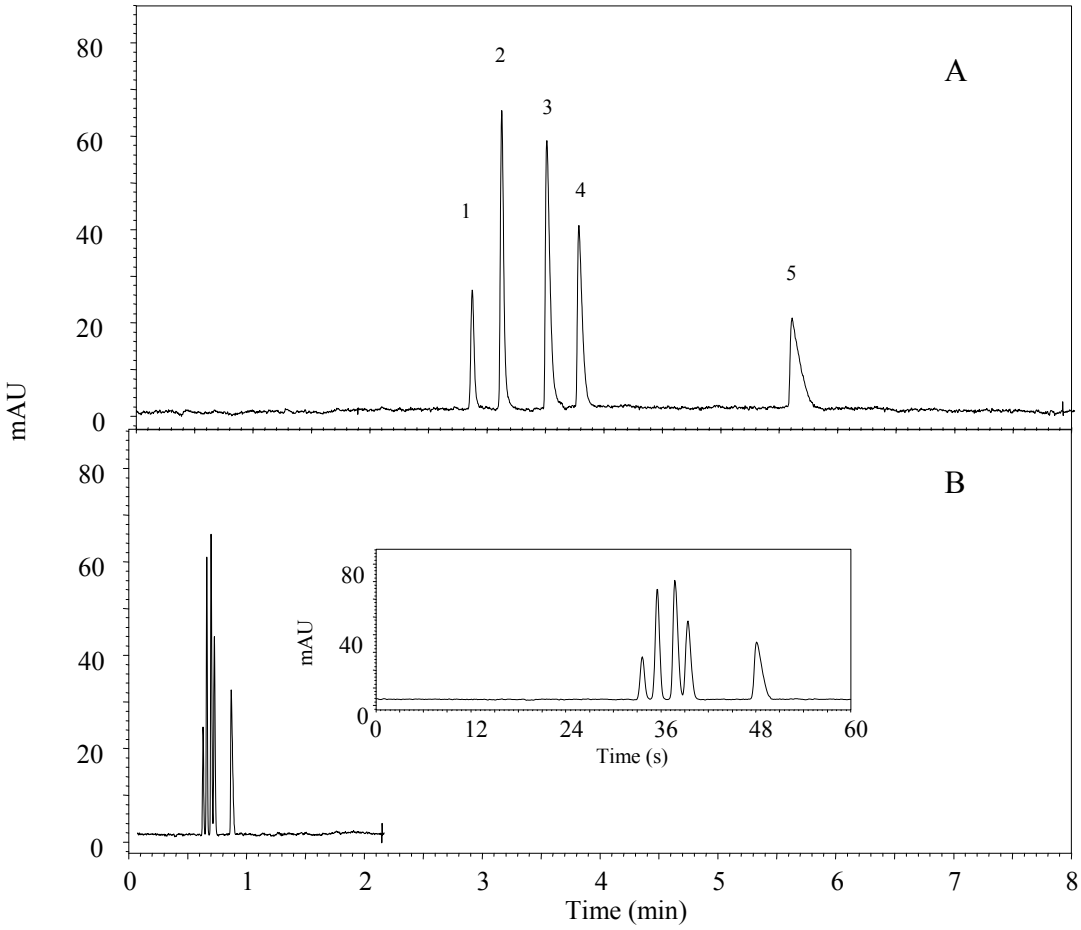

Figure V. 5. Chromatograms of test compounds. Conditions: (A) 25 cm × 50 μm i.d. fused silica capillary packed with 1.0 μm C_{18} bonded nonporous silica particles; water (0.1% TFA)/acetonitrile (90:10 , *v*/*v*); 215 nm UV detection; 15 kpsi inlet pressure; (B) 13 cm × 50 μm i.d. fused silica capillary packed with 1.0 μm C_6 bonded nonporous silica; 25 kpsi inlet pressure; other conditions are the same as in (A) Peak identifications: (1) uracil (2) hydroquinone (3) resorcinol (4) catechol (5) 4-methylcatechol.

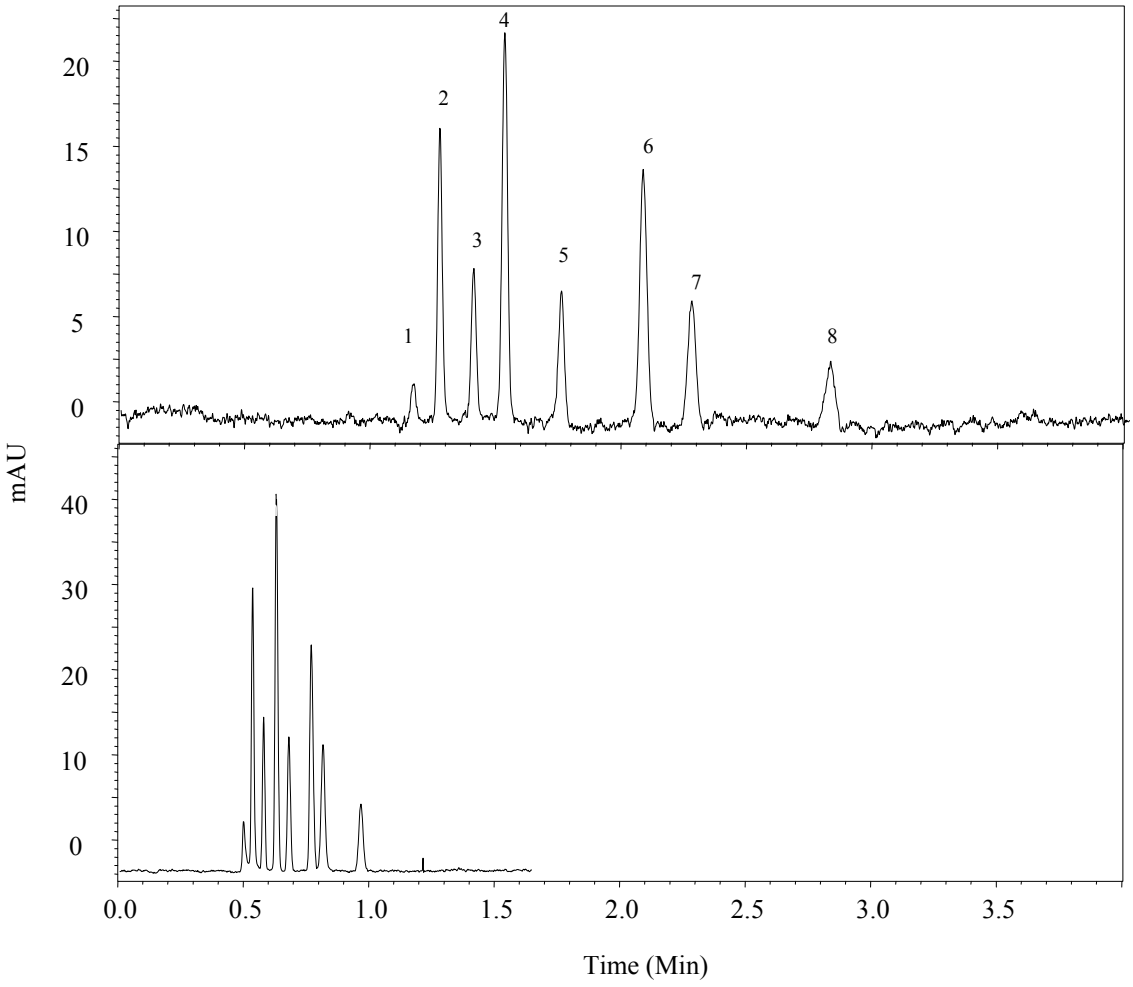

Figure V. 6. Chromatograms of barbitals. Conditions: (A) 13 cm × 50 μm i.d. fused silica capillary packed with 1.0 μm C_6 bonded nonporous silica particles; water (40 mM NaH_2PO_4, pH = 7.0)/acetonitrile (80:20, *v*/*v*), 215 nm UV detection; 10 kpsi inlet pressure; (B) water (40 mM NaH_2PO_4, pH = 7.0)/acetonitrile (75:25, *v*/*v*); 25 kpsi inlet pressure; other conditions are the same as in (A). Peak identifications: (1) uracil (2) allobarbital (3) barbital (4) phenobarbital (5) butalbital (6) hexabarbital (7) pentobarbital (8) secobarbital.

UHPLC. As described in the instrumentation section, an exponential gradient elution method was used in this study. A dwell volume as small as 8 μL was achieved by using short connecting tubing. Effective mixing was obtained by using a microstir bar in the mixer.

Figure V.7 illustrates a gradient profile at 10 kpsi. It can be seen that the system provided a gradient delay of only 6 min (measured from the separation column). At 100 min, the percentage of solvent B reached 82%, calculated from the experimental gradient profile. The same experiment was repeated three times and identical gradient profiles were obtained. Therefore, using this new injector, the UHPLC system can generate a reproducible gradient with short delay time.

Separations of an ovalbumin tryptic digest were conducted at pressures of 10 and 15 kpsi, respectively (see Figures V.8 and V.9). Compared to Figure V.8, a similar separation pattern was obtained in Figure V.9, however, the separation time was reduced by approximately 20 min. For these separations, it is difficult to measure the peak width for most of the peaks since they are not completely resolved. For the last eluting peaks where the baseline is relatively flat, the peak widths were approximately 6-9 s.

V.5 Conclusions

Compared to a static spit injector, a new Valco injection valve assembly provided many advantages such as much better reproducibility, shorter injection time, greater ease of operation and smaller injection sample volume. In addition, high column efficiency was preserved when using the new injection valve assembly. This novel injector can withstand pressures up to 30 kpsi, which are much higher than for the pressure balanced injection valves. With a newly designed capillary column connector, the injection valve

assembly was successfully used for both isocratic and gradient elution at ultrahigh pressures. The achievable injection reproducibilities allow the use of this valve for quantitative analysis.

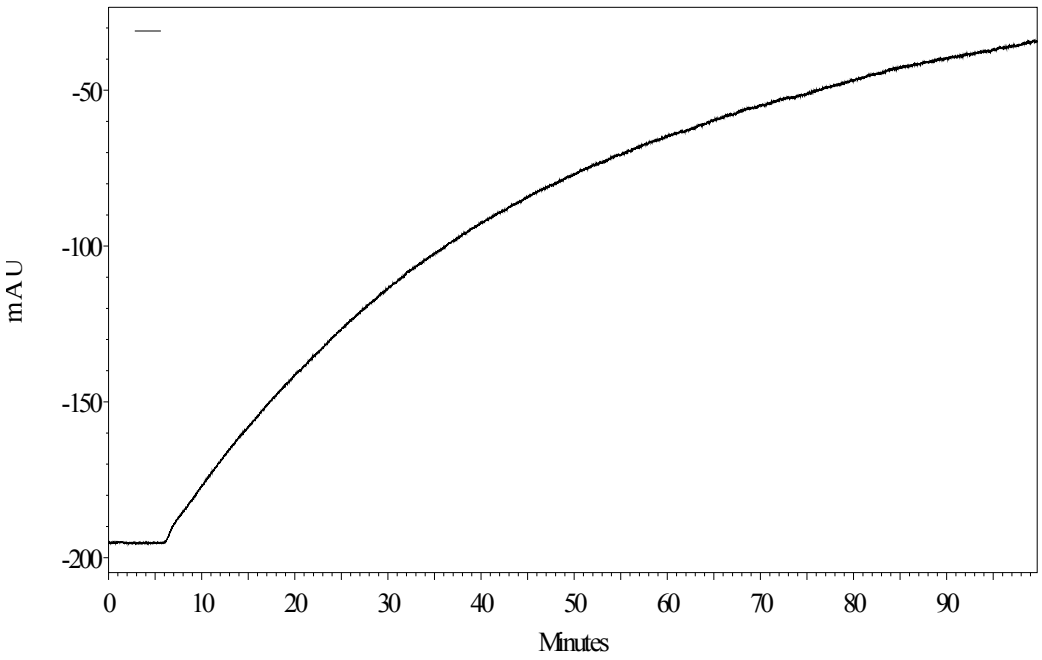

Figure V. 7. Experimental gradient profile at 10 kpsi. Conditions: acetonitrile/10% acetone (solvent A) in the mixer and 100% acetonitrile in the pump (solvent B); 8 μL min^{-1} pump flow rate; UV detection at 254 nm.

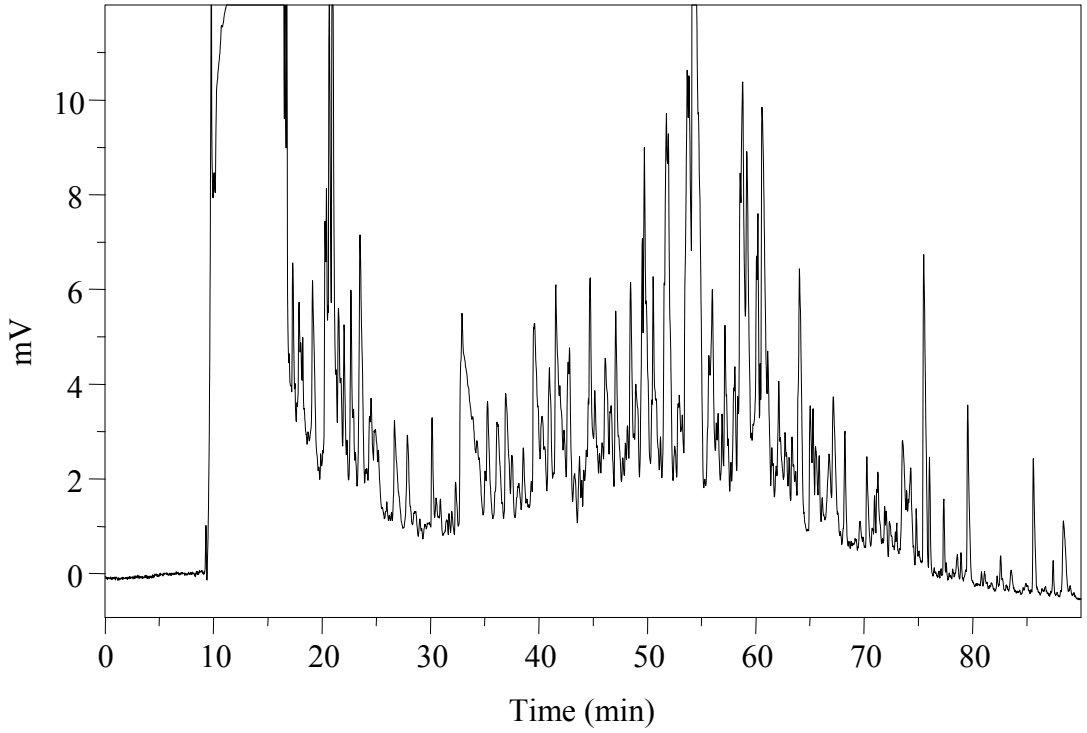

Figure V. 8. Chromatogram of an ovalbumin tryptic digest. Conditions: 35 cm × 100 μm i.d. fused silica capillary packed with 1.5 μm C_{18} bonded nonporous silica particles; mobile phase A: water (0.1% TFA); mobile phase B: acetonitrile/water (85:15, v/v, 0.1% TFA); exponential gradient from 100% mobile phase A to 82% mobile phase B in 100 min; trypsin-digested ovalbumin 2.5 mg mL^{-1}; 215 nm UV detection; 10 kpsi inlet pressure.

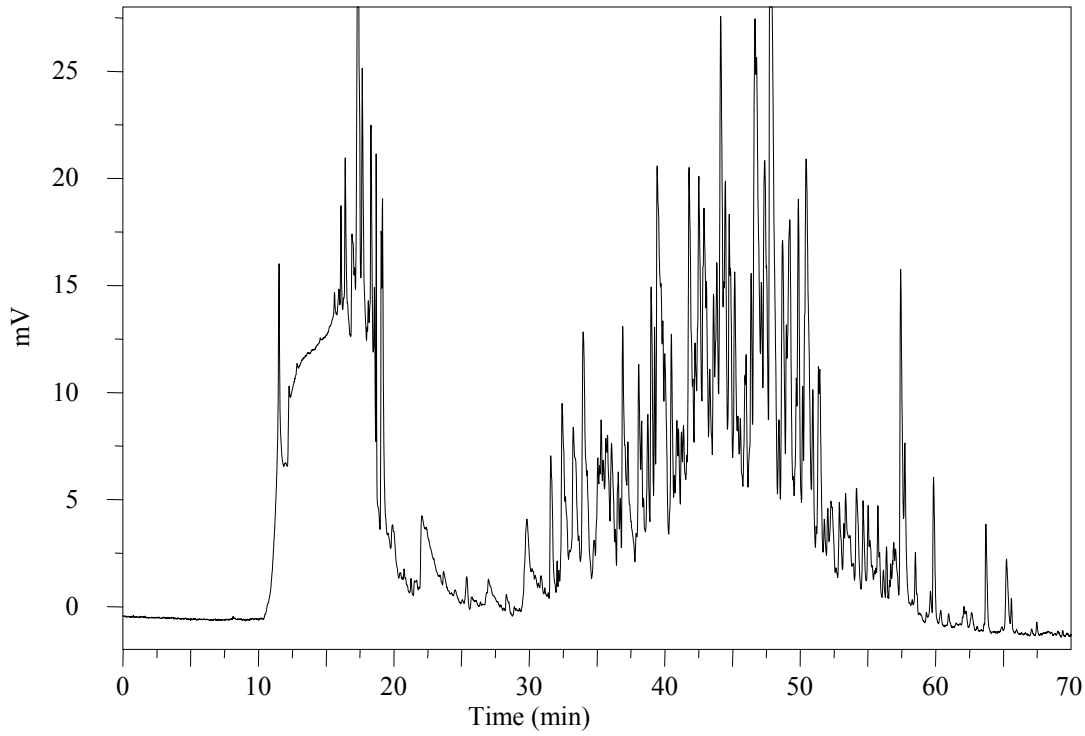

Figure V. 9. Chromatogram of an ovalbumin tryptic digest. Conditions: 15 kpsi inlet pressure; other conditions are the same as Figure V. 8.

V.6 References

1. Chen, H.; Horváth, Cs. J. Chromatogr. A 705 (1995) 3.
2. Halász, I.; Endele, R.; Asshauer, J. J. Chromatogr. 112 (1975) 37.
3. MacNair, J. E.; Lewis, K. C.; Jorgenson, J. W. Anal. Chem. 69 (1997) 983.
4. MacNair, J. E.; Patel, K. D.; Jorgenson, J. W. Anal. Chem. 71 (1999) 700.
5. Lippert, J. A.; Xin, B.; Wu, N.; Lee, M. L. J. Microcol. Sep. 11 (1999) 631.
6. Wu, N.; Collins, D. C.; Lippert, J. A.; Xiang, Y.; Lee, M. L. J. Microcol. Sep. 12 (2000) 462.
7. Xiang, Y.; Wu, N.; Lippert, J. A.; Lee, M. L. Chromatographia 55 (2002) 399.
8. Tolley, L.; Jorgenson, J. W.; Moseley, M. A. Anal. Chem. 73 (2001) 2985.
9. Wu, N.; Lippert, J. A.; Lee, M. L. J. Chromatogr. A. 911 (2001) 1.
10. Shen, Y.; Tolić, N.; Zhao, R.; Paša-Tolić, L.; Li, L.; Berger, S. J.; Harkewicz, R.; Anderson, G. A.; Belov, M. E.; Smith, R. D. Anal. Chem. 73 (2001) 3011.
11. Chervet, J.P.; Ursem, M. Anal. Chem. 68 (1996) 1507.
12. Vissers, J. P. C.; Claessens, H. A.; Cramers, C. A. J. Chromatogr. A. 779 (1997) 1.
13. Wu, N. Ph.D Dissertation, Brigham Young University, 2000.
14. Lippert J. A. Ph.D Dissertation, Brigham Young University, 1999.
15. Manz, A.; Simon, W. J. Chromatogr. 387 (1987) 187.
16. Claessens, H. A.; Burcinova, A.; Cramers, C. A. Mussche, P.; van Tilburg, C. C. E. J Microcol. Sep. 2 (1990) 132.

CHAPTER VI

ON-LINE PROTEIN DIGESTION AND ANALYSIS BY CAPILLARY LIQUID CHROMATOGRAPHY

VI.1 Introduction

Many of the challenges facing researchers in the fields of proteomics and biopharmaceuticals are related to the need to obtain as much information as possible on very limited samples. One of the most effective approaches for characterizing extremely small amounts of proteins and peptides is capillary liquid chromatography-mass spectrometry (LC-MS).[1-8]

In addition to the ability to work with minute sample sizes, use of capillary columns in LC can improve detection with concentration-sensitive detection devices as a result of reduced chromatographic dilution.[8-11] Because of the very small volumetric flow-rate, capillary LC can be easily coupled via nano-electrospray ionization (nano-ESI) to MS for the analysis of complex biological samples.

Most importantly, with complex proteins or protein mixtures, separation of protein digests using capillary LC before ESI-MS allows for much easier analysis and identification of proteins. LC techniques can help to remove matrix components, including salts and detergents in the sample that might depress the MS signal, and preconcentrate the protein fragments at the head of the separation column before separation. Samples that have been digested in basic solution can be made acidic by the mobile phase, producing positively charged fragment ions which are easier to detect by MS. This improves signal-to-noise ratios and results in simpler, easier to interpret mass spectra.[12-15]

Peptide profiling serves as a powerful tool for protein identification, structure elucidation, sequence determination and analysis of protein microheterogeniety, including post-translational modifications such as phosphorylation and glycosylation.[16,17] Traditionally, a protein of interest is digested by a proteolytic enzyme, most often trypsin, and the resultant peptides are extracted, desalted, preconcentrated and further separated by chromatography or analyzed directly by MS. This method generally requires a large excess of enzyme to maximize peptide recovery. However, a dissolved high concentration of trypsin in the protein mixture results in trypsin autodigestion with undesired formation of additional peptides. This may complicate the unambiguous assignment of the studied protein. It has been stated that it would be embarrassing to analyze the tryptic digest of a protein of unknown sequence when trypsin peptide fragments are also considered as part of the sample protein's sequence.[18]

Particles with immobilized trypsin can offer fewer trypsin autodigestion products, potentially higher enzyme stability, and much faster digestion because a higher amount of trypsin can be used without leading to autodigestion.[19,20] Also, automation with continuous flow through a packed reactor bed formed from immobilized particles is easier to perform. Recently, there has been increasing interest in protease microreactors. In 1995, Davis synthesized trypsin immobilized silica particles. These particles were slurry packed into 320 μm i.d. × 450 μm o.d. fused silica capillary columns at 2000 psi using Milli-Q water as the driving solvent. It was claimed that some microreactors prepared by this method displayed little variation in activity over a six-month period.[21] In 1997, Blackburn *et al.* prepared a capillary protease column by packing Poroszyme™ trypsin beads into 5 cm × 500 μm i.d. PEEK tubing. A protein sample was loaded into

this capillary column first, and then washed out using digest buffer. The protease reactor showed very good digestion efficiency at ambient temperature.[22] Recently, Wang *et al.* investigated the use of immobilized trypsin beads for protein digestion within a microfluidic chip.[23] A relatively large channel (800 μm wide, 150 μm deep and 15 mm long) was etched into the cover plate, which served as a protease reactor. Vacuum was used to pack the immobilized trypsin bead suspension into the reactor. After the protein sample was digested in this reactor, the digested peptides were separated by on-line microchip-CE. There is a trend to replace the protease beads with a protease monolith. Peterson *et al.* prepared protease microreactors in capillaries and on microchips by immobilizing trypsin on porous polymer monoliths of 2-vinyl-4,4-dimethylazlactone, ethylene dimethacrylate, and acrylamide or 2-hydroxyethyl methacrylate.[24] These microreactors have very low back pressure, enabling use of simple mechnical pumping to drive the protein solution through the reactor.

In this chapter, peptide separations on three different packing materials, including nonporous, porous and perfusion particles, are compared. Factors affecting protein digestion inside the protease microreactor are discussed.

VI.2 Experimental

VI.2.1 Materials and Chemicals

Porous (5/10 μm, 300 Å) bare silica particles were obtained from YMC (Wilmington, NC, USA), 3.0 μm nonporous octadecylsilane (C_{18}) modified silica particles were obtained from Micra (Northbrook, IL, USA), 3.0 μm porous (100 Å) C_{18} modified silica particles were from Alltech (Deerfield, IL, USA), and 3.0 μm porous

(1500 Å) C_{18} modified silica particles were from Poly LC (Columbia, MO, USA). Dithiothreitol, acetonitrile and water (HPLC-grade) were obtained from Fisher Scientific (Fair Lawn, NJ, USA). Fused silica capillary tubing was purchased from Polymicro Technologies (Phoenix, AZ, USA). All protein standards, aminopropyl triethoxysilane (APTES), glutaraldehyde, TPCK-treated trypsin and Nα-p-tosyl-$_L$-arginine methyl ester (TAME) were obtained from Sigma (St. Louis, MO, USA). Guanidine hydrochloride, iodoacetic acid, ammonium carbonate and trifluoroacetic acid (TFA) were purchased from Aldrich (Milwaukee, WI, USA). SFC-grade carbon dioxide was obtained from Airgas (Salt Lake City, UT, USA). All buffers and solvents were filtered through Durapore® membrane filters (0.22 μm pores) (Millipore, Bedford, MA, USA) before use. Similarly, samples were filtered through polytetrafluoroethylene (PTFE) syringe filters (0.2 μm pores, Chromacol, Trumbull, CT, USA).

VI.2.2 Protein Sample Preparations

β-Casein was directly dissolved in the digestion buffer (50 mM ammonium carbonate, pH = 8.6). Ovalbumin was denatured by mixing it with 6 M guanidine hydrochloride and heating at 90 °C for 1 h. Then the sample was cooled, reduced with 10 mM dithiothreitol at 37 °C for 4 h, and alkylated with 25 mM iodoacetic acid/NaOH at room temperature for 30 min in the dark. The denaturant, reduction, and alkylation reagents were removed using a 3 kDa molecular weight cutoff centrifugation filter (Pall, Ann Arbor, MI, USA). The protein samples were diluted to the desired concentration using 50 mM $(NH_4)_2CO_3$ (pH = 8.6). Then, this denatured, reduced, alkylated and desalted ovalbulmin sample was divided into two portions. One was digested

traditionally by adding TPCK-treated trypsin into the protein solution, and leaving it in a water bath for reaction at 37 °C overnight. The protein/trypsin ratio was 20. The digested protein solution and the rest of the undigested protein sample were both refrigerated at 4 °C for further use.

VI.2.3 Preparation of Protease Immobilized Silica Particles

Porous (5/10 μm, 300 Å) bare silica particles were first immersed in HCl/MeOH (v/v, 1:1) for 30 min at room temperature. Then the particles were rinsed thoroughly with distilled water before they were introduced into concentrated H_2SO_4 for 30 min. After the particles were rinsed thoroughly again with distilled water, they were boiled in water for 30 min and then dried. The dried particles were treated with 5% APTES (v/v) in water for 30 min and then washed thoroughly with distilled water and ethanol sequentially. After this, the particles were placed in a vacuum oven at 50 °C overnight. The particles were then immersed in a 2.5% glutaraldehyde solution (100 mM, pH 9.2 carbonate buffer) for 2 h. Then the particles were washed thoroughly with PBS buffer (pH 7.4, 40 mM) and immersed overnight in carbonate buffer (pH 9.2) containing 1.6 mg mL^{-1} TPCK treated trypsin. Finally, the modified particles were thoroughly rinsed using PBS buffer and then stored in a refrigerator.

VI.2.4 Column Preparation

A supercritical fluid method was used for capillary column packing as described previously.[25] Briefly, a Lee Scientific Model 600 SFC pump was used to drive supercritical fluid carbon dioxide through the column. One end of a fused silica capillary was connected to a Valco 1/16” union (Valco, Houston, TX, USA) with a piece of PEEK

tubing (Upchurch, Oak Harbor, WA, USA) and a stainless steel screen or frit (2 μm pore size) to retain the particles in the capillary, thus eliminating the need to make an initial frit. The other end of the capillary to be packed was connected to a modified Swagelok reducing union, which acted as the packing material reservoir and was connected to the SFC pump. An approximate amount of dry packing material was introduced into the packing reservoir. Both the column and the reservoir were placed in an ultrasonic bath (Branson Ultrasonic, Danbury, CT, USA) that was set at room temperature and turned on until the column was completely filled. The initial packing pressure was 1200 psi. Then, the pressure was programmed to 5000 psi at a rate of 225 psi min^{-1} to maintain a constant packing speed. The pressure was kept constant at 5000 psi for an additional 30 min conditioning after the column was packed. The column was then left to depressurize overnight. The frit-making process used here was the same as described in Chapter III.

VI.2.5 Preparation of Protease Microreactor

Protease microreactors were made by packing trypsin immobilized particles into 150 μm i.d. × 360 μm o.d. capillary columns. The same packing procedure as described previously was followed. First, a trypsin immobilized silica particle slurry (in PBS buffer) was loaded into the packing reservoir. Then supercritical carbon dioxide was used to drive the particles into the capillary column. The maximum pressure used was 1200 psi, instead of 5000 psi as described previously. The pressure was programmed from 400 psi to 1200 psi at a rate of 50 psi min^{-1} to maintain a constant packing speed. The packed column was placed in an ice bath and left overnight. After complete depressurization, the capillary was rinsed with water using a syringe pump.

The frits for these microreactors were made in a similar manner as for zirconia particles as described in Chapter III. Bare silica particles (5 μm) were first packed into a capillary column for approximately 3-5 cm before packing trypsin immobilized silica particles. Then the outlet frit was made by sintering the bare silica particles at a distance of 3 mm from the beginning of the trypsin immobilized particle bed while water was pumped through the column at a flow rate of 20 μL min^{-1} using a syringe pump. This process avoids loss of enzyme activity, which could occur when sintering trypsin immobilized particles at very high temperature to make the frit. In order to measure the activity of the microreactor, an on-column window was made using the same procedure as used to prepare a detection window. Reactors were stored in a refrigerator at 4 °C to prevent loss of activity of the enzyme.

VI.2.6 Measurement of Activity of the Protease Microreactor

The trypsin reactor activity was determined using the TAME assay.[26] The capillary reactor was connected to a 4-port injection valve. A syringe pump was used to drive water through the capillary reactor. TAME solution was loaded into the sample loop of the injection valve. When a stable baseline was obtained, the TAME sample was injected. The hydrolysis of TAME by trypsin produces Nα-p-tosyl-$_L$-arginine, which has strong absorption at 247 nm. Therefore, Nα-p-tosyl-$_L$-arginine can be determined on-column using a detector which was connected to the capillary reactor detection window.

VI.2.7 Instrumentation

Capillary liquid chromatography pumps and pump control software were from Micro-Tech Scientific (Sunnyvale, CA, USA). Mobile phases A and B delivered by the

pumps were combined in a micromixer with internal volume of 50 μL. A tee (1/32" o.d., 0.15 mm bore, Valco, Houston, TX, USA) was used to interconnect the micromixer outlet, a six-port injection valve (Rheodyne, Rohnert, CA, USA) and another tee (1/32", o.d., 0.50 mm bore, Valco), one port of which was connected to a splitter capillary, and the other port of which was connected to a purge valve (Rheodyne). The external sample loop was made from an open tubular capillary (30 μm i.d.). The sample loop volume was adjusted by changing the capillary length. Injection was automatically controlled with a computer. The injection volume could be adjusted by changing the injection time from 0.2 s to 99.9 min.

Harvard syringe pumps (South Natick, MA, USA) were used to drive the protein solution or wash solution through the microreactor. Plastic needle tubing was used to connect the Hamilton Gastight syringe (Hamilton, Reno, NV, USA) to the capillary microreactor.

VI.3 Results and Discussion

VI.3.1 Peptide Separation Using Different Packing Materials

The pore size of the silica particles is an important parameter in the separation of proteins or peptides. A thin porous layer on nonporous particles allows a much faster rate of mass transfer by eliminating most of the intraparticle diffusion in the support pores in porous particles. This feature makes nonporous particles an attractive choice for high speed and high efficiency protein or peptide separations.[27-30] The through pores in perfusion particles allow mobile phase flow through the particle, minimize the potential permanent retention of large polypeptides and poorly digested proteins within the surface

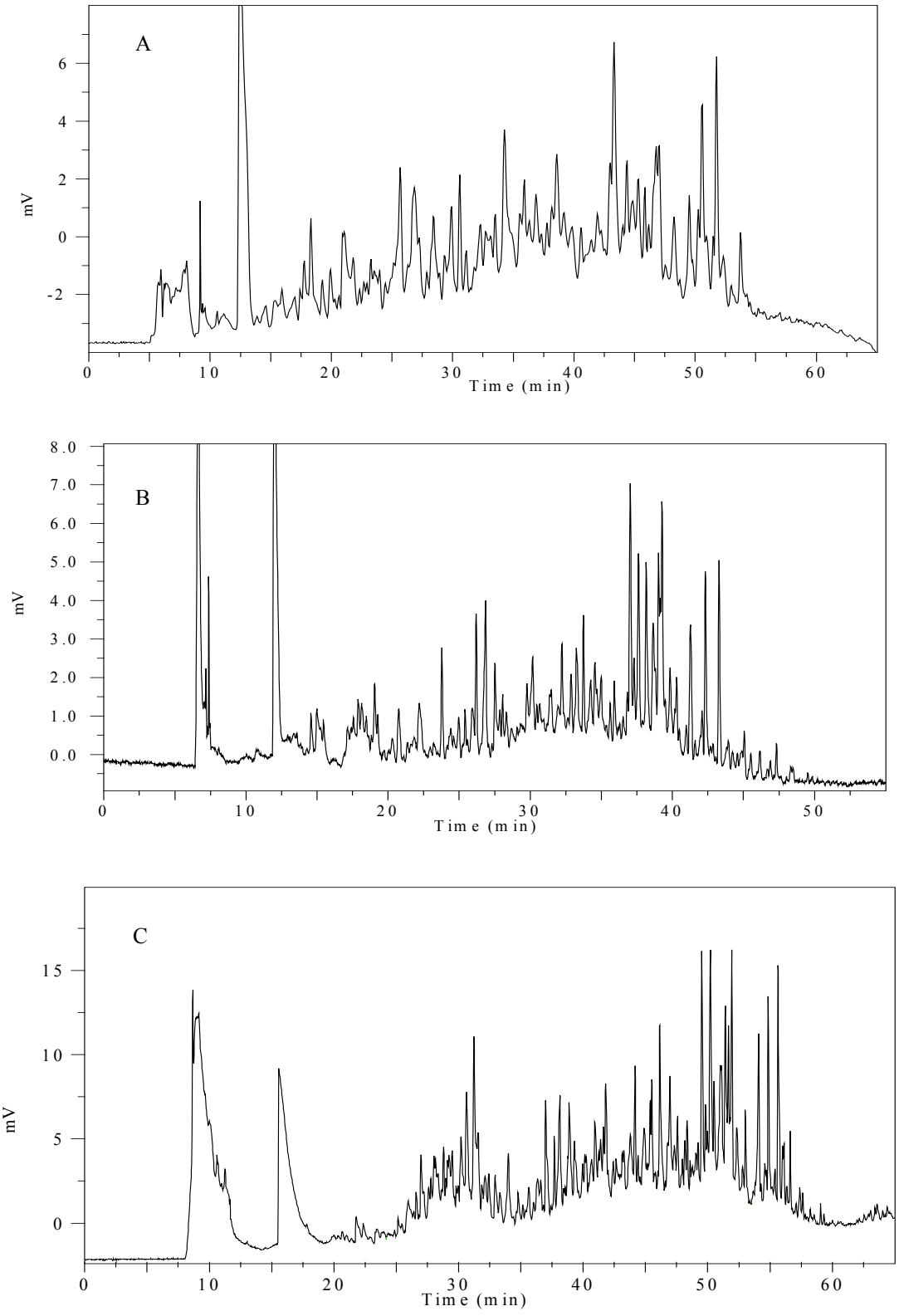
A
mV
6
4
2
0
-2
0
10
20
30
40
50
60
Time (min)
B
mV
8.0
7.0
6.0
5.0
4.0
3.0
2.0
1.0
0.0
0
10
20
30
40
50
Time (min)
C
mV
15
10
5
0
0
10
20
30
40
50
60
Time (min)

Figure VI. 1. Chromatograms of ovalbumin tryptic digests (traditional method) using different packing materials. Conditions: 33 cm × 100 μm i.d. fused silica capillary packed with 3 μm C_{18} bonded particles. (A) 100 Å pores; (B) nonporous; (C) 1500 Å pores; 5.3 μL min^{-1} total flow rate; 18:1 split ratio; 25 μL min^{-1} purge flow rate; 50 nL sample injection volume; 3 mg mL^{-1} sample concentration; gradient from 100% mobile phase A (H_2O, 0.1% TFA) to 75% mobile phase B (ACN, 0.1% TFA) in 45 min, then to 100% mobile phase A in 10 min and hold for 5 min; UV detection at 215 nm.

pores, and accelerate intraparticle mass transfer of macromolecules by one to two orders of magnitude.[31-33] This feature greatly facilitates high speed and high efficiency separation of proteins and peptides.

In this study, three different packing materials were evaluated for peptide separation as shown in Figure VI.1. Compared with the results obtained using 3 μm C_{18} bonded particles with 100 Å pore size (see Figure VI.1A), significant improvements in separation efficiency were observed with nonporous particles (see Figure VI.1B) and perfusion particles with 1500 Å pore size (see Figure VI.1C).

High sample loading capacity is critical for analysis of proteins and peptides. For a complex sample, such as proteins and peptides, which have a wide range of concentrations, low-abundance components can be better detected by increasing the sample loading capacity. Otherwise, sample overloading will degrade the separation quality.[5] The major limitation with nonporous particles is that they have approximately 100-fold lower surface area than porous particles and, therefore, have limited sample loading capacity. Compared to nonporous particles, perfusion particles have relatively large surface area. Furthermore, decreasing the pore size from 6000-8000 Å to 500-1500 Å can increase the surface area of perfusion particles by 30-40%.[32] Therefore, in this study, perfusion particles with 1500 Å pore size were used for peptide separations. It was observed that some small hydrophilic peptides were poorly retained on these hydrophobic columns and they eluted early, resulting in relatively broad peaks in the early part of the chromatograms.

Reproducible elution order for proteolytic polypeptides under reversed-phase LC conditions is important for high throughput proteome analysis. In this study, method

reproducibility was investigated as shown in Figure VI.2. It can be seen that similar elution patterns were achieved using a column packed with perfusion particles.

VI.3.2 Protease Reactor Activity

Immobilization involves a bimolecular reaction of the enzyme in solution with the functional groups on the particle surface. Increases in concentrations of enzyme in solution and of functional groups on the particle surface, or an increase in reaction time, could increase the enzyme loading in the microreactor. Increasing the surface area of the particles allows more functional groups to be attached to the particle surface. Reducing the particle size helps to increase the surface area, leading to higher loading of the enzyme. However, the pressure drop along the reactor is inversely proportional to the cube of the particle size.[34] Smaller particles lead to higher pressure drop, which makes it difficult to wash sample out of the reactor using a simple mechanical pump. In addition, a smaller pore size also helps to increase the surface area. However, pores that are too small retain large proteins and peptides inside the pores. Therefore, in this study, 5/10 μm particles with 300 Å pore size were used as substrate for enzyme loading. The reaction time also affects the enzyme loading. Overnight reaction was used in this study to avoid physical adsorption of the enzyme on the particle surface after exposing the silica particle to the enzyme solution for a long time.

A Lineweaver-Burk plot was plotted based on the TAME assay as shown in Figure VI.3. The Michaelis constant (K_m) and maximum velocity (v_{max}) used to characterize the activity of the enzyme were calculated. Their values were 227 μM and 8.80 μM min^{-1}, respectively. Compared to data in the literature,[23] these values are

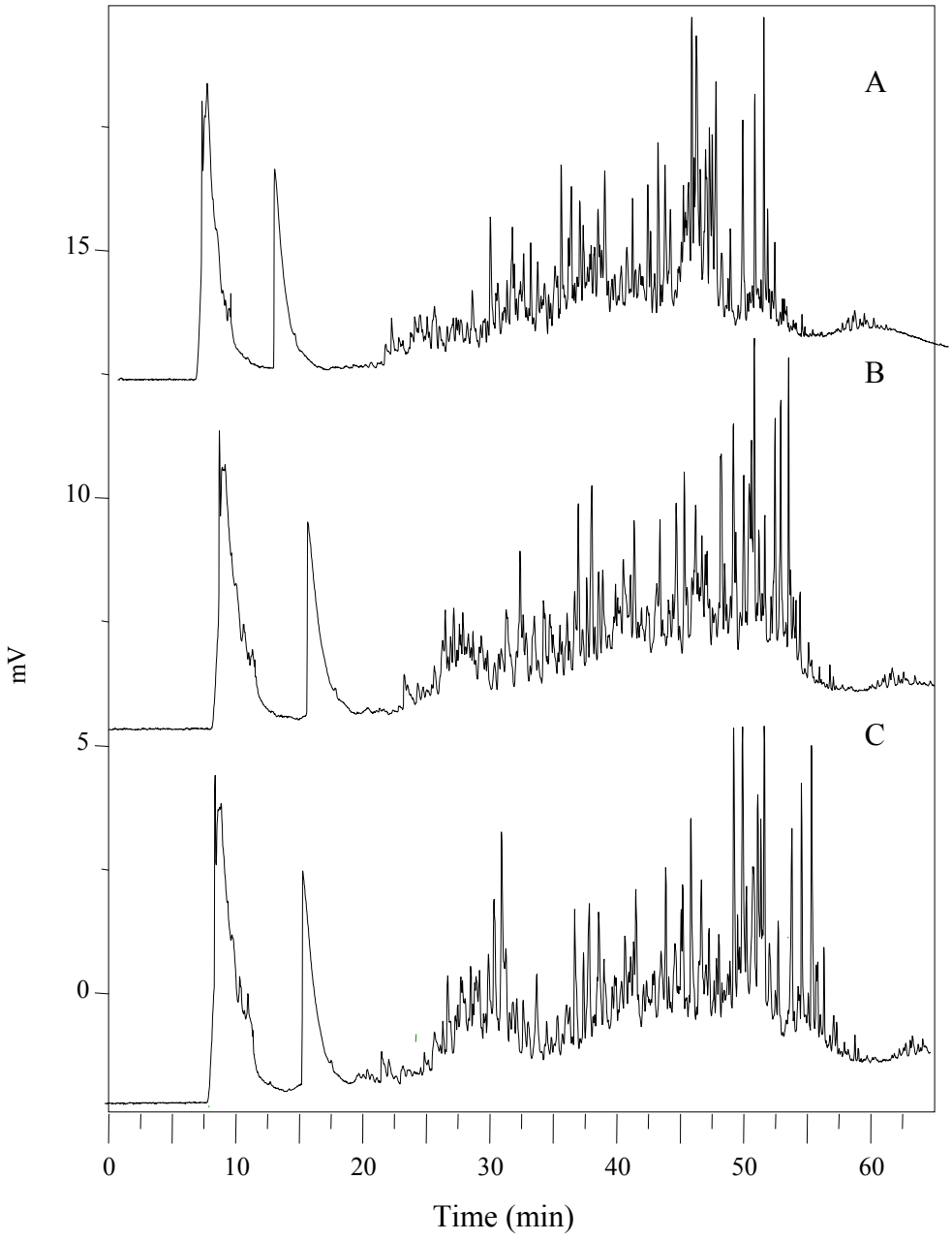

Figure VI. 2. Reproducibility of separations of ovalbumin tryptic digests. Conditions are the same as in Figure VI.1C: (A) run 1; (B) run 5; (C) run 9.

relatively high, which means that a relatively large amount of enzyme was attached to the particles. Higher enzyme loading allows more efficient protein digestion.

VI.3.3 Effects of Ovabulmin Concentration and Flow Rate on Digestion Using the Trypsin Immobilized Reactor

Because of the relatively small amount of protease in the capillary reactor, one concern is the completeness of protein digestion. There are several parameters, such as flow rate, protein concentration, and length and diameter of capillary reactor, that affect the completeness of protein digestion. When longer and larger diameter capillaries are used, a larger number of protease beads are packed in the reactor, resulting in more efficient protein digestion. However, it is known that the pressure drop along the column is proportional to the column length. A lower pressure drop is very important for this type of protease microreactor because it would be desirable to wash the protein sample through the column using a simple mechanical pumping system. Therefore, it is not reasonable to use a longer column to increase the digestion efficiency. In this study, microreactors of 15 cm in length were used. Column diameters of 200 μm i.d. × 365 μm o.d. and 325 μm i.d. × 420 μm o.d. were investigated in this study. It was found that these capillaries became very fragile after packing with protease beads. This may be due to the large changes in pressure applied to the relatively thin walls of the capillaries from compression and decompression of supercritical carbon dioxide fluid.

The effect of ovalbumin concentration on digestion in the protease microreactor was investigated. For this study, the ovalbulmin sample was driven through the microreactor and the digested protein was collected at the outlet. The collected sample was then analyzed by capillary LC and the results are shown in Figure VI.4. In Figure

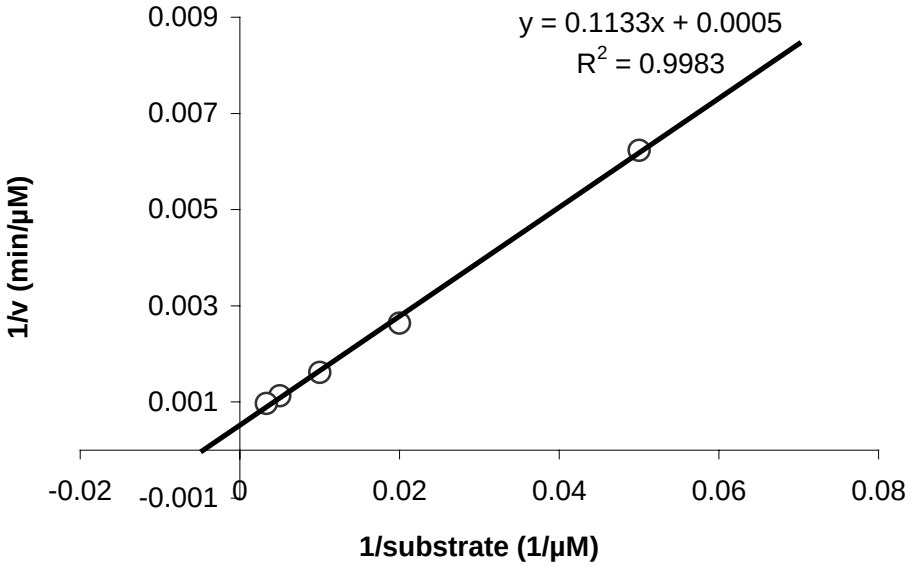

Figure VI. 3. Lineweaver-Burk plot for trypsin immobilized capillary reactor. Conditions: 20-300 µM TAME in 50 mM $(NH_4)_2CO_3$ (pH 8.6, 10 mM $CaCl_2$); detection at 247 nm; 0.5 µL min^{-1} flow rate.

VI.4A, there is a large peak at a retention time of 55 min. This intact ovalbumin represents a significant fraction of the protein still present in the digested sample. When the protein concentration was decreased from 1.5 mg mL^{-1} to 0.5 mg mL^{-1}, the nondigested protein peak (retention time of approximately 50 min) became smaller as shown in Figure VI.4B. When the protein concentration was decreased to 0.3 mg mL^{-1}, the nondigested protein peak almost disappeared. (see Figure VI.4C). The flow rate carrying the protein sample through the microreactor was 0.1 μL min^{-1}. The retention times for nondigested protein in Figures VI.4B and VI.4C are different from that in Figure VI.4A because the gradient elution and data recording programs were started several minutes after the sample had been injected in Figures VI.4B and VI.4C, while the programs were started at the same time as the sample has been injected in Figure VI.4A.

The effect of flow rate through the protease microreactor was investigated. For small proteins such as β-casein, there was no significant difference in chromatograms for flow rates of 0.1 μL min^{-1} and 1.0 μL min^{-1} (data not shown). Flow rates in this range had little effect on digestion of β-casein. Therefore, relatively high flow rates can be used for β-casein. For ovalbumin and bovine serum albumin, a lower flow rate, such as 0.1 μL min^{-1}, must be used for better digestion due to their relatively large sizes.

VI.3.4 Peptide Separation Using On-line Protein Digestion-Capillary Liquid Chromatography

The ultimate goal of this project was to establish an on-line protein digestion-capillary LC-MS system for peptide profiling. The complete design is shown

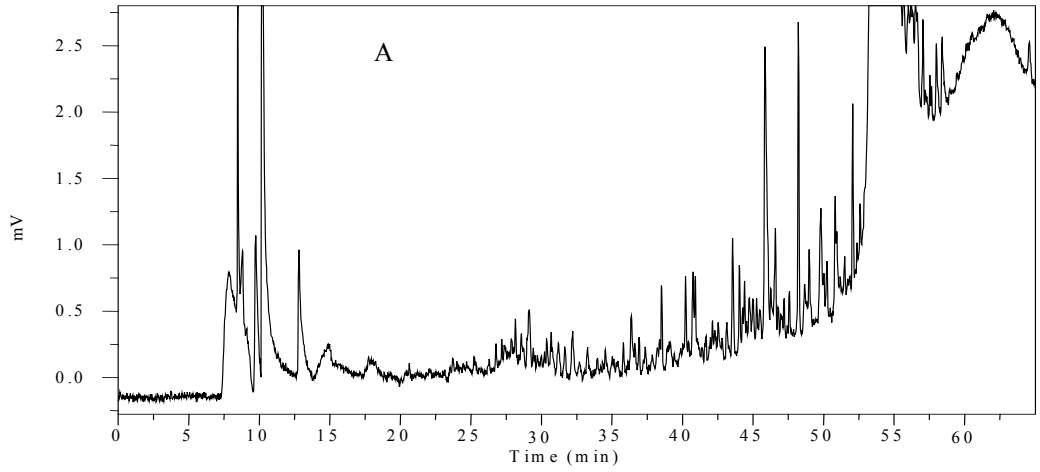
A
mV
2.5
2.0
1.5
1.0
0.5
0.0
0
5
10
15
20
25
30
35
40
45
50
55
60
Time (min)

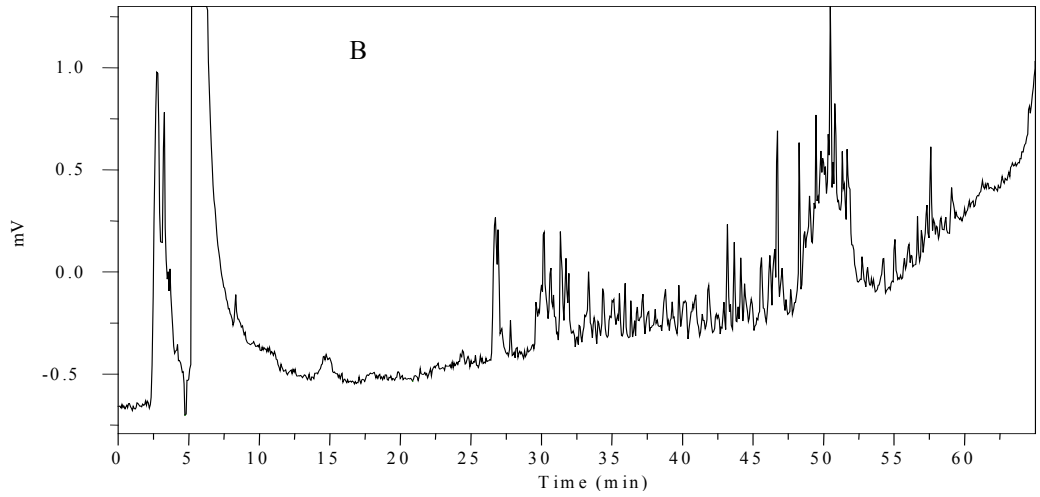
B
mV
1.0
0.5
0.0
-0.5
0
5
10
15
20
25
30
35
40
45
50
55
60
Time (min)

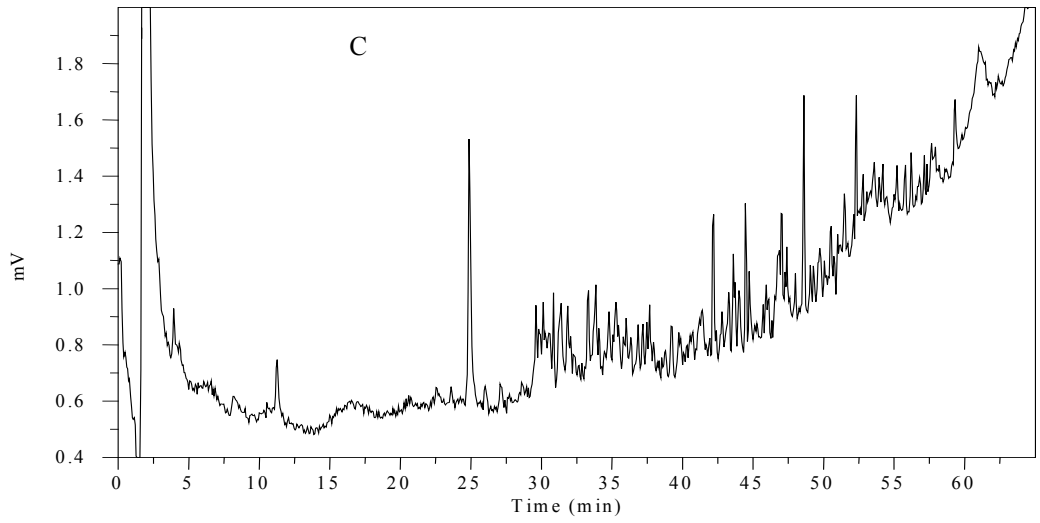
C
mV
1.8
1.6
1.4
1.2
1.0
0.8
0.6
0.4
0
5
10
15
20
25
30
35
40
45
50
55
60
Time (min)

Figure VI. 4. Chromatograms of ovalbumin digests from an immobilized trypsin capillary reactor for different ovalbumin concentrations. Conditions: separation column 33 cm × 100 μm i.d. fused silica capillary column packed with 3 μm diameter (1500 Å), C_{18} bonded stationary phase; microreactor 15 cm × 150 μm i.d. fused silica capillary column packed with 5/10 μm (300 Å) trypsin immobilized particles; 0.1 μL min^{-1} digest flow rate; (A) 1.5 mg mL^{-1} ovalbumin; gradient program initiated at the same time as the sample was injected; (B) 0.5 mg mL^{-1} ovalbumin; gradient program initiated 3 min after the sample was injected; (C) 0.2 mg mL^{-1} ovalbumin; gradient program initiated 6 min after the sample was injected; other conditions are the same as in Figure VI.2.

schematically in Figure VI.5. In Figure VI.5A, the protein sample was driven by a syringe pump (defined as syringe pump 1) through a protease microreactor, which was mounted onto the first valve. The digested sample exiting the microreactor entered the sample loop of the second valve. Simutaneously, the separation column, which was connected to the second valve, equilibrates. After the digested sample filled the sample loop, both valves were switched as shown in Figure VI.5B. By switching the second valve, the digested sample was injected into the separation column. After several min injection, the valve was switched back and gradient elution began as shown in Figure VI.5C. Switching valve 1 allows syringe pump 2 to carry the wash solution [(ACN/buffer (50 mM $(NH_4)_2CO_3$, pH = 8.6) (70:30, *v/v*)] through the microreactor for cleaning. After cleaning for 10 min, valve 1 was switched back to allow the next protein sample into the microreactor for digestion (shown in Figure VI.5C). The clean-up step helped to wash away autocatalytic peptides and/or hydrophobic peptides bound to the column from previous samples. The whole process, including protein digestion, loading, separation, microreactor clean-up, and separation column equilibration, was done with this set-up.

Ovalbumin and β-casein were digested and separated as shown in Figures VI.6 and VI.7. For on-line digestion of ovalbumin, instead of using valve 1, the protease microreactor was directly connected to the inlet port of the sample loop on valve 2. This design facilitated use of a heater to heat up the microreactor. The heater was similar to the one we used for elevated temperature UHPLC in Chapter III. The protease microreactor was thermostated at 37 °C for efficient digestion of ovalbumin.

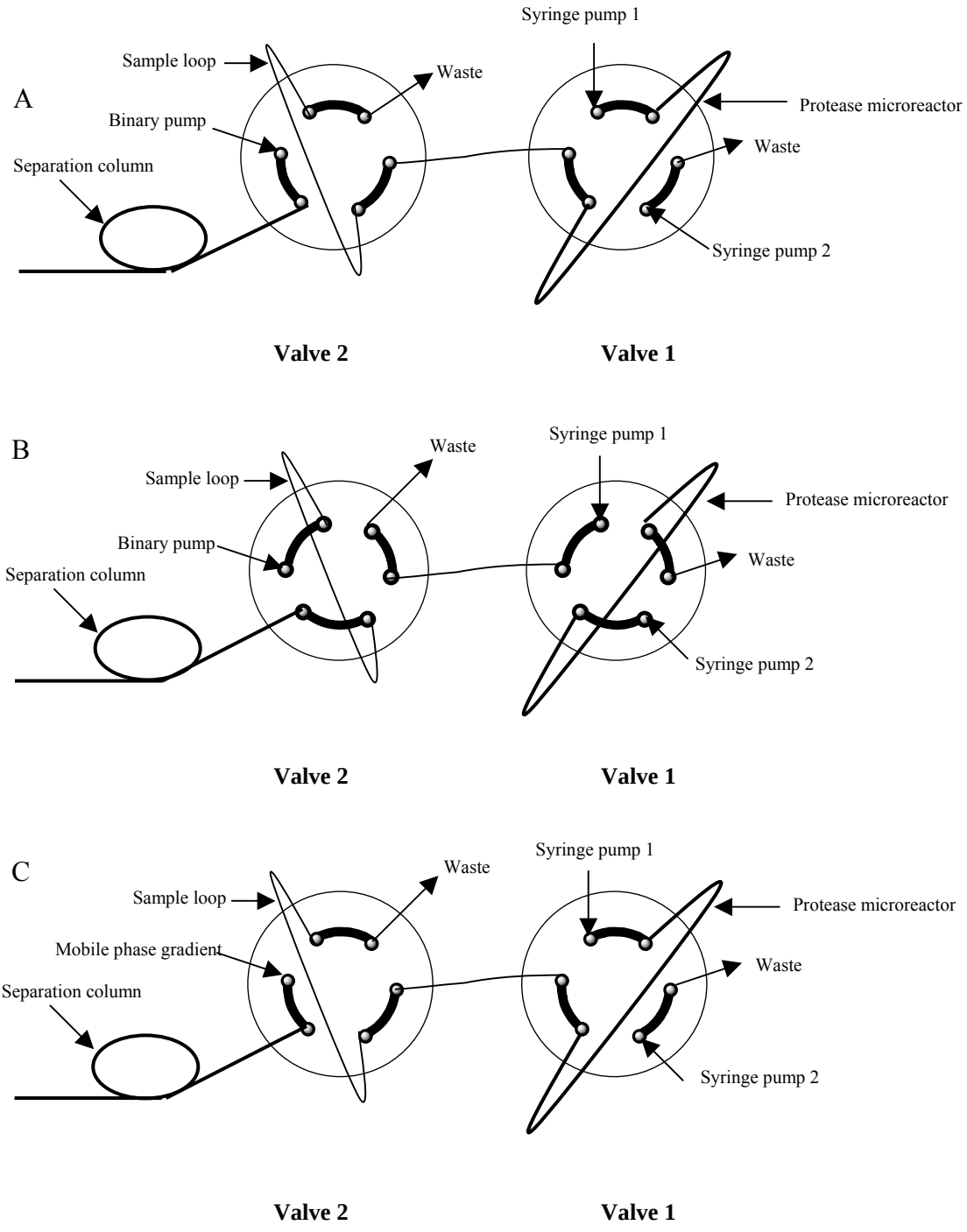

Figure VI. 5. Schematic diagrams showing the operation of an on-line protease microreactor coupled to capillary LC-MS (see text for details).

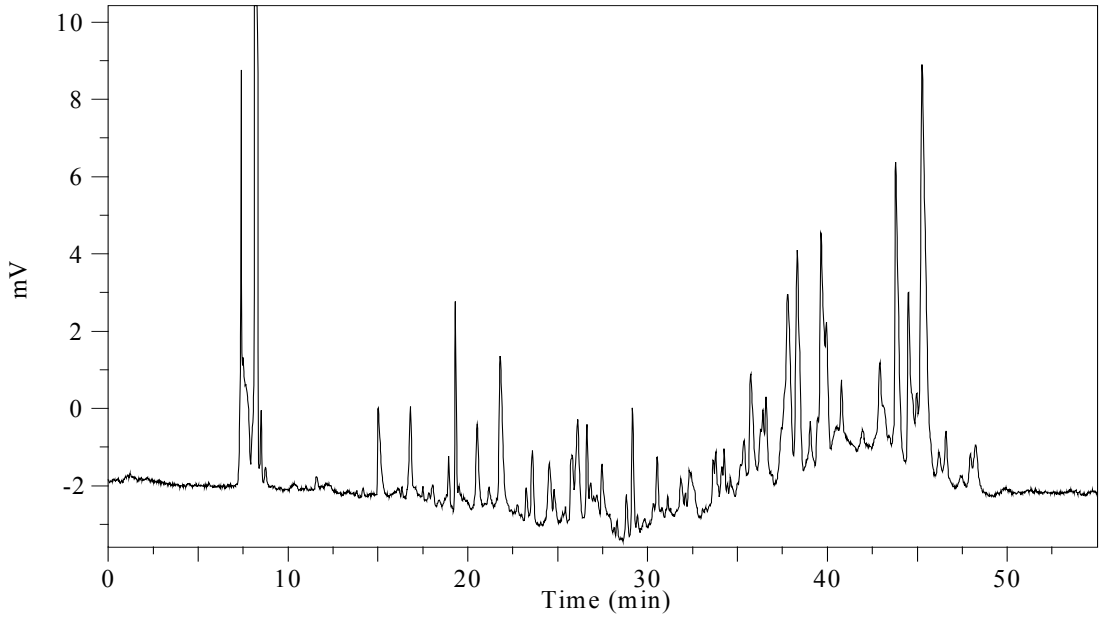

Figure VI. 6. Chromatogram of a β-casein digest from an on-line trypsin immobilized microreactor-capillary LC. Conditions: 150 nL sample injection volume; 1.5 mg mL^{-1} β-casein; 1.0 μL min^{-1} digest flow rate; other conditions are the same as in Figure VI.1C.

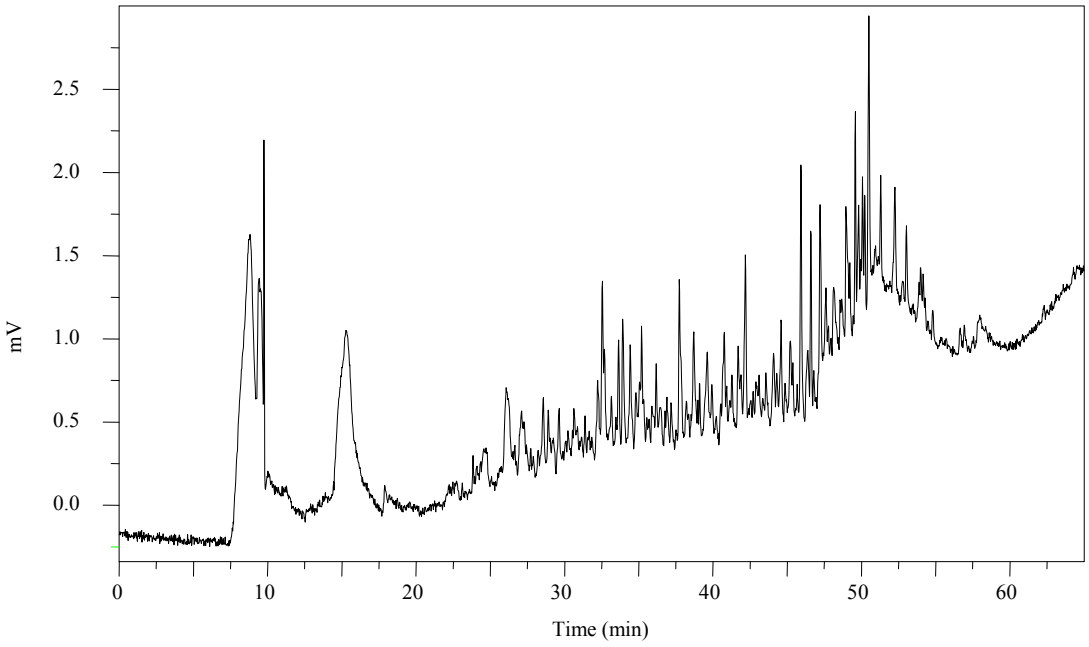

Figure VI. 7. Chromatogram of an ovalbumin digest from an on-line trypsin immobilized microreactor-capillary LC. Conditions: 150 nL sample injection volume; 0.5 mg mL^{-1} ovalbumin; 0.1 μL min^{-1} digest flow rate; 37 °C digest temperature; other conditions are the same as in Figure VI.1C.

VI.4 Conclusions

In this chapter, three particle types were investigated for the separation of peptides. It was found that, compared to conventional porous particles (100 Å), nonporous and perfusion particles (1500 Å) gave better efficiency for the separation of trypsin digested protein. Trypsin immobilized onto silica particles demonstrated good activity for protein digestion. Protein concentration, microreactor size (length and diameter) and flow rate significantly affect protein digestion in the trypsin immobilized microreactor. Finally, coupling the trypsin immobilized microreactor with capillary LC allowed on-line protein digestion and separation.

VI.5 References

1. Bihan, T. Le.; Pinto, D.; Figeys, D. Anal. Chem. 73 (2001) 1307.
2. Gatlin, C. L.; Eng, J. K.; Cross, S. T.; Detter, J. C.; Yates III, J. R. Anal. Chem. 72 (2000) 757.
3. Meiring, H. D.; van der Heeft, E.; ten Hove, G. J.; de Jong, A. P. J. M. J. Sep. Sci. 25 (2002) 557.
4. Shen, Y.; Tolić, N.; Zhao, R.; Paša-Tolić, L.; Li, L.; Berger, S. J.; Harkewicz, R.; Anderson, G. A.; Belov, M. E.; Smith, R. D. Anal. Chem. 73 (2001) 3011.
5. Shen, Y.; Zhao, R.; Belov, M. E.; Conrads, T. P.; Anderson, G. A.; Tang, K.; Paša-Tolić, L.; Veenstra, T. D.; Lipton, M. S.; Udseth, H.; Smith, R. D. Anal. Chem. 73 (2001) 1766.
6. Shen, Y.; Zhao, R.; Berger, S. J.; Anderson, G. A.; Rodriguez, N.; Smith, R. D. Anal. Chem. 74 (2002) 4235.
7. Shen, Y.; Moore, R. J.; Zhao, R.; Blonder, J.; Auberry, D. L.; Masselon, C.; Paša-Tolić L.; Hixson, K. K.; Auberry, K. J.; Smith, R. D. Anal. Chem. 75 (2003) 3596.
8. Shen, Y.; Tolić, N.; Masselon, C.; Paša-Tolić, L.; Camp, II, D. G.; Hixson, K. K.; Zhao, R.; Anderson, G. A.; Smith, R. D. Anal. Chem. 76 (2004) 144.
9. Martin, S. E.; Shabanowits, J.; Hunt, D. F.; Marto, J. A. Anal. Chem. 2000, 72, 4266.
10. Qunzer, T. L.; Emmett, M. R.; Hendrickson, C. L.; Kelly, P. H.; Marshall, A. G. Anal. Chem. 73 (2001) 1721.
11. Hixson, K. K.; Rodriguez, N.; Camp II, D. G.; Strittmatter, E. F.; Lipton, M. S.; Smith, R. D. Electrophoresis 23 (2002) 3234.
12. Lazar, I. M.; Ramsey, R. S.; Ramsey, J. M. Anal. Chem. 73 (2001) 1733.

13. Loo, J. A.; Udseth, H. R.; Smith, R. D. Rapid Commun. Mass Spectrum. 2 (1988) 207.

14. Manoori, B. A.; Volmer, D. A.; Boyd, R.K. Rapid Commun. Mass Spectrum. 11 (1997) 1120.

15. Konermann, L.; Douglas, D. J. J. Am. Soc. Mass Spectrum. 9 (1998) 1248.

16. Loo, J. A. Bioconjugate Chem. 6 (1995) 644.

17. Gevaert, K.; Vandekerckyear, J. Electrophoresis 21 (2000) 1145.

18. Aebersold, R. H.; Leavitt, J. Saavedra, R. A.; Hood, L. E.; Kent, S. B. H. Proc. Natl. Acad. Sci. USA 84 (1987) 69

19. Cobb, K. A; Novotny, M. Anal. Chem. 61 (1989) 2226.

20. Stachowiak, K.; Wilder, C.; Vesral, M. L.; Dyckes, D.F. J. Am. Chem. Soc. 110 (1988) 1758.

21. Davis, M. T.; Lee, T. D.; Ronk, M.; Hefta, S. A. Anal. Biochem. 224 (1995) 235.

22. Blackburn, R. K.; Anderegg, R. J. J. Am. Soc. Mass Spectrom. 8 (1997) 483.

23. Wang, C.; Oleschuk, R.; Ouchen, F.; Li, J.; Thibault, P.; Harrison, D. J. Rapid Commun. Mass Spectrom. 14 (2000) 1377.

24. Peterson, D. S.; Rohr, T.; Svec, F.; Frechet J. M. J. Anal. Chem. 74 (2002) 4081.

25. Malik, A.; Li, W.; Lee, M. L. J. Microcol. Sep. 5 (1993) 361.

26. Rick, W. Methods of Enzymatic Analysis; Bergmeyer, H. U., Ed.; Academic Press: New York, 1965; pp 807.

27. Jilge, G.; Janzen, R.; Giesche, H.; Unger, K. K.; Kinkel, J. N.; Hearn, M. T. W. J. Chromatogr. 397 (1987) 71.

28. Unger, K. K.; Jilge, G.; Kinkel, J. N.; Hearn, M. T. W. J. Chromatogr. 359 (1986) 61.

29. Unger, K. K.; Janzen, R.; Jilge, G. Chromatographia 24 (1987) 144.

30. Chen, H.; Horvath, C. J. Chromatogr. A 705 (1995) 3.

31. Fulton, S. P.; Afeyan, N. B.; Gordon, N. F.; Regnier, F. E. J. Chromatogr. 547 (1991) 452.

32. Paliwal, S. K.; de Frutos, M.; Regnier, F. E. Meth. Enzymol. 270 (1996) 133.

33. Regnier, F. E. Nature, 350 (1991) 634.

34. MacNair, J. E.; Lewis, K. C.; Jorgenson, J. W. Anal. Chem. 69 (1997) 983.

CHAPTER VII

RECOMMENDATIONS FOR FUTURE RESEARCH

VII.1 Effect of Ultrahigh Pressure on Protein Retention

The effect of pressure on chromatographic behavior has not usually been considered due to mobile phase noncompressibility. Actually, it has been found that pressure influences various behaviors of solute in solution, such as ionization equilibrium, size of solvated macromolecules, aggregation of macromolecules, and adsorption of both liquid and solute on adsorbent surfaces.[1] For example, protein-solvent interactions are energetically more favorable under pressures higher than atmosphere pressure.[2] The energies of protein-protein interactions increase with increasing pressure.[3] In addition, positional fluctuations of atoms decrease with an increase in pressure.[4] Therefore, dependence of retention factor on pressure within the column has been observed for almost all LC modes.[5] This dependency becomes significant for large molecules such as proteins. For example, pressure induced changes in partial molar volume for insulin and lysozyme were of the order of –100 mL mol^{-1} when the pressure was increased from 750 psi to 3000 psi.[6,7]

Unfortunately, little research has been carried out in the areas just described at pressures over 6000 psi. In this ultrahigh pressure range, the effect of pressure on retention of proteins might be significant.

VII.2 Construction of Flow Controlled UHPLC

Due to its superior resolving power, UHPLC has potential to be commercialized and intensively exploited in the future. Currently, UHPLC is still in its infancy and the

current instrumentation must be improved. The pressure controlled pumping system should eventually be replaced by flow controlled pumping. An Isco pump (Model 65 D, Isco, Lincoin, NE) introduced in Pittcon 2003 has the highest pressure rating of any flow controlled pump to date.[8] It is able to produce flow rates from 0.00001 mL min^{-1} to 25 mL min^{-1} at pressures up to 20,000 psi. Use of these pumps together with the new Valco injection valve assembly should provide a more convenient UHPLC gradient, which would be a major step forward in the commercialization of UHPLC.

VII.3 Temperature Programmed UHPLC and Elevated Temperature Gradient UHPLC

The current UHPLC system with new injection valve assembly allows the injector and capillary column to be heated easily and efficiently. This provides the possibility for work on temperature programming, which is widely used for eluting samples containing components of wide volatility in gas chromatography. The use of temperature programming in LC also offers advantages. For example, temperature programming could complement gradient elution, because it has been observed that the change in selectivity with changing temperature is different from changing the mobile phase composition for the separation of peptides.[9,10]

In addition, increasing the temperature reduces the mobile phase viscosity and enhances solute diffusion. Therefore, elevated temperature accelerates sorption/desorption kinetics of proteins or peptides, leading to higher separation efficiency.

VII.4 References

1. Macko, T.; Berek, D. J. Liq. Chrom. & Rel. Technol. 24 (2001) 1275.

2. Hillson, N.; Onuchic, J.N.; Garcia, A. E. Proc. Natl. Acad. Sci. USAQ 96 (1999) 14848.

3. Paci, E.; Biochim. Biophys. Acta 1595 (2002) 185.

4. Liu, X.; Szabelski, P.; Kacmarski, K.; Zhou, D.; Guiochon, G. J. Chromatogr. A 988 (2003) 205.

5. Macko, T.; Berek, D. J. Liq. Chrom. & Rel. Technol. 24 (2001) 1275.

6. Szabelski, P.; Cavazzini, A.; Kaczmarski, K.; Liu, X.; Van Horn, J.; Guiochon, G. J. Chromatogr. A 950 (2002) 41.

7. Liu X.; Zhou D.; Szabelski, P.; Guiochon, G.; Anal. Chem. 75 (2003) 3999.

8. www.isco.com

9. Chen, H.; Horvath, Cs. J. Chromatogr. A 705 (1995) 3.

10. Greibrokk, T.; Andersen, T. J. Sep. Sci. 24 (2001) 899.